LIMBURGS UNIVERSITAIR CENTRUM

FACULTEIT WETENSCHAPPEN

RANDOM WALKS IN ONE DIMENSION : NEW RESULTS AND APPLICATIONS

Ina Claes

1991

Promotor : Prof. dr. C. Van den Broeck

Proefschrift voorgelegd tot het behalen van de graad van doctor in de wetenschappen.

BIJSTELLING

Trainingsalgoritmes, die voor het perceptron geformuleerd werden, kunnen veralgemeend en met succes toegepast worden op een "niet-lineair multineuron" perceptron. De bekomen veralgemeningscurven liggen dicht bij een ondergrens, toepasbaar op het "random search" algoritme. Deze ondergrens kan bepaald worden op basis van de a priori waarschijnlijkheidsverdeling die het perceptron karakteriseert vooraleer training heeft plaats gevonden.

Thanks ...

I am indebted to my family, my friends and my colleagues at the LUC for their support and friendship, each one of them contributing in their own way not only to the realization of this work, but also to making the past few years pleasant ones and worthwhile remembering. Some of these people I would like to mention in particular.

I am very grateful to Chris Van den Broeck for offering me the opportunity to work with him and for his continuous help and advice in solving the problems encountered along the way.

I also would like to thank Martine Machiels and Viviane Mebis for typing parts of this dissertation, and Kristien Bauwens and Marina Lens for carefully reading it and trying to localize the many typographical errors.

I also acknowledge support from the Program on Inter University Attraction Poles of the Belgian government.

Contents

Chapter 1

Introduction

The random walk is one of the paradigms of statistical physics, but it is also a very practical concept that has found applications in a wide variety of fields. Since the gambler's ruin problem can be formulated as a random walk problem (how many time steps does it take before the gambler exhausts his capital), one can argue that the concept of a random walk goes back as far as the seventeenth century, when the vivid interest in gambling led to the formulation of probability theory [1]. However, we have to wait until the beginning of the twentieth century for the first explicit formulation of a random walk problem. In 1905, Pearson [2] inquired on the solution of the following problem :

> A man starts from a point O and walks l yards in a straight line, he then turns through any angle whatever and walks another l yards in a second straight line. He repeats this process n times. I require the probability that after these n stretches he is at a distance between r and $r + dr$ from his origin O.

Although this was the first time a random walk problem was formulated, other stochastic models had already been treated, be it in a more disguised form. In fact, Pearson's problem had been solved a few years earlier by Lord Rayleigh [3], albeit in a very different context, while Bachelier [4], a student of Poincaré,

presented in 1900 a random walk model for the behaviour of prices of items traded in the stock exchange. The real breakthrough of random walk models was provided by the pioneering work of Einstein on Brownian motion [5]. Over the next decade, this theory was developped and extended by several other authors, among which Kluyver [6], Markov [7], Smoluchowsky [8], Wiener [9] and Ornstein and Uhlenbeck [10]. In 1921, Pólya [11] introduced another class of important random walk models, namely the lattice random walks : he studied the probability of return to the origin of a random walker on periodic lattices. Since the first random walk models for polymer chains by Kuhn and Grün [12,13] and the work of Montroll and his co-workers on lattice random walks in the fifties [14], random walk theory has become very popular and has found a vast range of applications in different fields such as solid state physics, chemical kinetics, biology and astronomy. Excellent reviews on random walk theory that cover both the state of the art and its applications can be found e.g. in the book by Barber and Ninham [15] and in the review articles by Weiss and Rubin [16] and Haus and Kehr [17], while an inspiring account of the early history of random walks is given by Montroll and Shlesinger in "The wonderful world of random walks" [1].

Random walk theory continues to be, even today, a field of very active and exciting research. Our purpose here will be to add a few new technical results, in particular for the case of one-dimensional random walks, and to add some further applications to the long list of existing ones.

In chapter 2, we will review the techniques that can be used to calculate the Green's function of a random walk. We present a few "tricks", and derive some new explicit results for the Green's function of a one-dimensional random walk.

We then proceed with two applications of random walks in the field of polymer physics. In the model we consider in chapter 3, a polymer chain is described as a random walk with persistence. We give a complete analytic treatment of the model, and derive expressions for quantities of interest such as the moments of the end-to-end distance of the polymer. These results were published in [18]. In chapter 4, we investigate the orientational relaxation in the so-called reptation model for polymers. This model was introduced by de Gennes and Edwards to describe the dynamics of entangled polymers. We derive compact,

analytic results for the variables that are observed in experiments, notably the stationary anisotropy. These results have been published in [19].
Random walks have successfully been used to describe one of the basic transport processes in nature : Fickian diffusion. Another basic transport process is pure convection. An interesting situation arises when one combines these two processes, for example when Brownian particles are suspended in a fluid in non-uniform flow. This problem is known in the literature under the name of Taylor diffusion [20]. In chapter 5, we consider another variant of the Taylor dispersion problem, namely the dispersion of particles in spatially periodic flows. Our main contribution is to show that the quantity of interest for these processes, the effective dispersion coefficient, can be expressed in terms of the Green's function of the random walk inside the unit cell.
Finally, we discuss a new, interesting phenomenon of stochastic resonance for particles suspended in an oscillating flow in chapter 6. We find that the interplay between the frequencies that characterize a stochastic process, e.g. a random walk, and the frequency of the oscillating flow, can lead to a resonance phenomenon, reminiscent of that encountered in classical mechanics. The difference is that here, the resonance is characterized by a strong increase of an effective diffusion coefficient rather than that of an amplitude of oscillation. These results have been published in [21].

Some people have dedicated their entire lifetime to the study of random walks. Indeed, there seems to be no end to the surprises that one encounters on the random walk track. We hope that our results, however modest, will have contributed a few new surprises.

Chapter 2

The Green's function

One of the central quantities in random walk problems is the probability distribution $P(m, m_0; t)$ for the random walker to be in site m, given that he started from m_0 at $t = 0$. For a Markovian random walk, this distribution is the solution of the Master equation

$$\partial_t P(m, m_0; t) = \sum_{m'} \left[W_{mm'} P(m', m_0; t) - W_{m'm} P(m, m_0; t) \right] \tag{2.1}$$

with $W_{m'm}$ the transition probability to go from site m to site m', $W_{mm} = 0$ and with initial condition

$$P(m, m_0; t = 0) = \delta_{mm_0}. \tag{2.2}$$

To simplify the notations, we introduce the transition matrix $\mathbf{T}$:

$$\partial_t P(m, m_0; t) = \sum_{m'} T_{mm'} P(m', m_0; t) \tag{2.3}$$

where the nondiagonal elements $T_{mm'}$ are identical to $W_{mm'}$, and the diagonal elements T_{mm} contain the contributions to the jump rate of particles that leave

state m :

$$T_{mm} = -\sum_{m'} W_{m'm}. \tag{2.4}$$

A standard method to solve the Master equation is to take the Laplace transform of both sides. The Laplace transform $G^C_{mm_0}(s)$ of $P(m, m_0; t)$

$$G^C_{mm_0}(s) = \int_0^\infty P(m, m_0; t) e^{-st} dt \tag{2.5}$$

is then the solution of

$$-\delta_{mm_0} + sG^C_{mm_0}(s) = \sum_{m'} T_{mm'} G^C_{m'm_0}(s). \tag{2.6}$$

Rearranging the terms, $G^C_{mm_0}(s)$ can be expressed as

$$G^C_{mm_0}(s) = \left(\frac{1}{s\mathbf{1} - \mathbf{T}}\right)_{mm_0}. \tag{2.7}$$

$G^C_{mm_0}(s)$ is the so-called Green's function of the random walk. In principle, once the Green's function for a particular random walk is known, the probability distribution describing the position of the particle can be obtained from it by inverting the Laplace transform. Unfortunately, this proves to be very difficult, if not impossible in many cases. However, even if Laplace inversion turns out to be difficult, the Green's function itself remains a key result, because it is directly related to other quantities of practical interest, such as the moments of the displacement, the span of the random walk and the first passage time distribution.

In section 2.1 we review various calculation techniques and results for the Green's function. We start with the representation of the Green's function in terms of the eigenvectors of the transition matrix $\mathbf{T}$, and the properties of these eigenvalues and eigenvectors. We then proceed with the calculation of closed form expressions for translationally invariant one-dimensional random walks, and with an example of the derivation of the small s expansion in a case where no closed form expression is available. In the last part of section

2.1, we give the Green's function for a continuous time random walk with nonexponential waiting times. All the results presented here, are given for further use in the following chapters. Finally, in section 2.2, we illustrate the relation between the Green's function on one hand, and the first passage time distribution, the span of the random walk and the probability of return to the origin on the other hand.

2.1 Calculation of the Green's function

2.1.1 Eigenfunction expansion

Consider the Markovian random walk on a discrete set of states introduced above. We saw that the Green's function $G^C_{mm_0}(s)$ is given by Eq. (2.7). A standard method to calculate $G^C_{mm_0}(s)$ is to invert $(s\mathbf{1} - \mathbf{T})$ by using the expansion in eigenvectors of the matrix $\mathbf{T}$:

$$G^C_{mm_0}(s) = \left(\frac{1}{s\mathbf{1} - \mathbf{T}}\right)_{mm_0} = \sum_\alpha X_{m\alpha} \frac{1}{s - \lambda_\alpha} Y_{\alpha m_0}, \tag{2.8}$$

provided a complete set of eigenvalues λ_α and right eigenvectors $\mathbf{X}_\alpha$ exists. The disadvantage of this procedure is that the Green's function is expressed in terms of a series, rather than in a compact form. However, sometimes the series can be resummed, as we will see in the example given below, or a compact result can be derived using a more ingenious method described in the next subsection. For the remainder of this subsection, we will concentrate on the properties of the transition matrix $\mathbf{T}$ and its eigenvalues and eigenvectors.

The conservation of probability implies that

$$\sum_m T_{mm'} = 0. \tag{2.9}$$

Therefore, the vector $\mathbf{Y_0} = (1, \cdots, 1)$ is a left eigenvector with eigenvalue $\lambda_0 = 0$. The corresponding normalized right eigenvector is, by definition, the

stationary distribution $\mathbf{P}^{st}$:

$$X_{m0} = P_m^{st}. \tag{2.10}$$

We will assume that the system under consideration is not decomposable. Therefore, the matrix $\mathbf{T}$ is irreducible and the stationary solution $\mathbf{P}^{st}$ is unique. We will also make the rather strong assumption that the detailed balance condition holds (this will anyway be the case for most situations considered in this work), i.e. that the transitions between each pair of stationary states m and m' are balanced or that there exists no net flux in the system

$$T_{mm'} P_{m'}^{st} = T_{m'm} P_m^{st}. \tag{2.11}$$

Under these conditions, one easily verifies that the matrix $\mathbf{V}$ with elements

$$V_{mm'} = \frac{1}{\sqrt{P_m^{st}}} \, T_{mm'} \, \sqrt{P_{m'}^{st}} \tag{2.12}$$

is symmetric. Consequently, it has a complete set of eigenvalues λ_α and eigenvectors $\tilde{\mathbf{X}}_\alpha$ and, moreover, the left and right eigenvectors are the same. We conclude that

$$\sum_{m,m'} \tilde{X}_{m\alpha} V_{mm'} \tilde{X}_{m'\beta} = \lambda_\alpha \delta_{\alpha\beta} \tag{2.13}$$

or

$$\sum_{m,m'} \frac{\tilde{X}_{m\alpha}}{\sqrt{P_m^{st}}} T_{mm'} \sqrt{P_{m'}^{st}} \tilde{X}_{m'\beta} = \lambda_\alpha \delta_{\alpha\beta}. \tag{2.14}$$

Thus the right and left eigenvectors $\mathbf{X}_\alpha$ and $\mathbf{Y}_\alpha$ of the matrix $\mathbf{T}$ are given by

$$X_{m\alpha} = \sqrt{P_m^{st}} \tilde{X}_{m\alpha} \tag{2.15}$$

$$Y_{\alpha m} = \frac{\tilde{X}_{m\alpha}}{\sqrt{P_m^{st}}}. \tag{2.16}$$

They have the following properties, as can easily be checked :

$$X_{m\alpha} = Y_{\alpha m} P_m^{st} \tag{2.17}$$

$$\sum_{\alpha} X_{m\alpha} Y_{\alpha m'} = \delta_{mm'} \tag{2.18}$$

$$\sum_{m} X_{\alpha m} Y_{m\beta} = \delta_{\alpha\beta}. \tag{2.19}$$

Because the matrix $\mathbf{V}$ is symmetric, we know that the eigenvalues λ_α are real. A further specification of the region to which the eigenvalues are restricted is provided by the Geršgorin theorem [22]. This theorem states that the eigenvalues of a general $n \times n$ complex matrix $\mathbf{C}$ are located in the union of N disks, each with origin C_{mm} and radius $\rho_m = \sum_{m' \neq m} |C_{mm'}|$. This implies for our case, due to the special form of the transition matrix $\mathbf{T}$ (cf. Eq. (2.9)), that the eigenvalues λ_α are negative and bounded as follows :

$$-2 \max_{\mathbf{m}} |T_{mm}| \leq \lambda_\alpha \leq 0. \tag{2.20}$$

As an example, we will use this method to solve the unbiased random walk on a line of N sites with periodic boundary conditions. The eigenvalues and eigenvectors are the solution of the following set of equations :

$$\begin{aligned} -2kX_{1\alpha} + kX_{2\alpha} + kX_{N\alpha} &= \lambda_\alpha X_{1\alpha} \\ kX_{i-1,\alpha} - 2kX_{i\alpha} + kX_{i+1,\alpha} &= \lambda_\alpha X_{i\alpha} \\ kX_{1\alpha} + kX_{N-1,\alpha} - 2kX_{N\alpha} &= \lambda_\alpha X_{N\alpha}. \end{aligned} \tag{2.21}$$

The N eigenvalues λ_α can be found by Fourier expansion

$$\lambda_\alpha = -2k\left(1 - \cos\frac{2\alpha\pi}{N}\right) \qquad \alpha \in [0, N-1]. \tag{2.22}$$

Since in this case, the matrix $\mathbf{T}$ is symmetric, its left and right eigenvectors are the same :

$$\alpha = 0 \qquad X_{m0} = \frac{1}{\sqrt{N}} \tag{2.23}$$

$$\alpha \neq 0 \qquad X_{m\alpha} = \sqrt{\frac{2}{N}} \cos\frac{2m\alpha\pi}{N}. \tag{2.24}$$

The Green's function for this random walk is thus given by

$$G^C_{mm_0} = \frac{1}{Ns} + \frac{2}{N}\sum_{\alpha=1}^{N-1}\left[\frac{\cos\frac{2m\alpha\pi}{N}\cos\frac{2m_0\alpha\pi}{N}}{s + 2k(1-\cos\frac{2\alpha\pi}{N})}\right]. \tag{2.25}$$

Introducing the variable $\xi_0^C = \xi_0^C(s)$ as

$$\cosh\xi_0^C = 1 + \frac{s}{2k} \tag{2.26}$$

in the denominator of Eq. (2.25), we can rewrite the Green's function as :

$$G^C_{mm_0} = \frac{1}{Ns} + \frac{1}{2kN}\sum_{\alpha=1}^{N-1}\left[\frac{\cos\left[\frac{2(m-m_0)\alpha\pi}{N}\right] - \cos\left[\frac{2(m+m_0)\alpha\pi}{N}\right]}{\cosh\xi_0^C - \cos\frac{\alpha\pi}{N}}\right]. \tag{2.27}$$

For this particular situation, the expression Eq. (2.27) can be resummed using the following summation formula [23,24] :

$$\sum_{\alpha=1}^{\left[\frac{N-1}{2}\right]} \frac{\cos\frac{2\pi\alpha m}{N}}{\cosh\xi_0^C - \cos\frac{2\pi\alpha}{N}} \tag{2.28}$$

$$= \frac{\cosh(\xi_0^C\left(\frac{N}{2} - m + N\left[\frac{m}{N}\right]\right))}{\sinh\xi_0^C\sinh\left(\frac{N\xi_0^C}{2}\right)} - \frac{1}{4\sinh^2\left(\frac{\xi_0^C}{2}\right)} - \frac{(-1)^m\left(1+(-1)^N\right)}{8\cosh^2\left(\frac{\xi_0^C}{2}\right)},$$

where $[a/b]$ is the largest integer in (a/b). After some algebra, we finally obtain the following closed form result for the Green's function $G^C_{mm_0}(s)$

$$G^C_{mm_0}(s) = \frac{\cosh\left(\xi_0^C(m_> - m_< - \frac{N}{2})\right)}{2k \sinh \xi_0^C \sinh\left(\frac{N\xi_0^C}{2}\right)} \tag{2.29}$$

with

$$m_> = \max(m, m_0) \tag{2.30}$$

$$m_< = \min(m, m_0).$$

In the next section, we will review the cases for which a compact form of the Green's function can be obtained.

2.1.2 Closed form expressions

The expression of the Green's function in terms of the eigenvector expansion is no doubt useful, but it would be preferable to obtain a closed form expression without first having to calculate the eigenvalues and eigenvectors of the transition matrix. We will present here two methods to obtain such results for one-dimensional nearest neighbour random walks which posses translational symmetry. The first method, which could be called "guided guesswork", was given by Mazo [25]. The idea is to work back from the known compact result for the Green's function of the diffusion process, which is the continuum version of the random walk problem under consideration (in appendix 7.A a brief comment is given on the relation between discrete random walks and diffusive motion). We will illustrate the calculation for a unbiased random walk on an infinite one-dimensional lattice. The Green's function for the diffusive process obeys the following equation

$$(s - D\partial_x^2)G^C(x, x_0; s) = \delta(x - x_0), \tag{2.31}$$

with $G^C(x, x_0; s)$ the Laplace transform of the probability $P(x, x_0; t)$ for the particle to arrive at x at time t, given that it started from x_0 at $t = 0$. The solution can easily be calculated (or found in the literature, see e.g. [26]) :

$$G^C(x, x_0; s) = \frac{e^{-\sqrt{\frac{s}{D}}|x-x_0|}}{2\sqrt{sD}}. \tag{2.32}$$

The problem that arises now is that there is no unique way of going back from $G^C(x, x_0; s)$ to the discrete version $G^C_{mm_0}(s)$. Indeed, in the continuum limit where the lattice spacing a goes to zero, not only expressions such as am (with m the label of the site on the infinite lattice) give x, but also $a(m+\text{constant})$ reduce to x in this limit (for any fixed value of the constant). Hence the Green's function for the random walk problem will have the same basic dependence on $|m - m_0|$, but the proportionality constants in Eq. (2.32) may differ. We will therefore try the following expression for $G^C_{mm_0}(s)$:

$$G^C_{mm_0}(s) = A(s)e^{-\xi_0^C|m-m_0|}. \tag{2.33}$$

The factors $A(s)$ and ξ_0^C are determined from the equation for $G^C_{mm_0}(s)$

$$-k\ G^C_{m-1,m_0}(s) + (1+2k)\ G^C_{mm_0}(s) - k\ G^C_{m+1,m_0}(s) = \delta_{mm_0}. \tag{2.34}$$

First consider $m > m_0$ (the case $m < m_0$ follows by symmetry) :

$$-ke^{\xi_0^C} + (s+2k) - ke^{-\xi_0^C} = 0. \tag{2.35}$$

This condition implies that we have to choose ξ_0^C according to

$$\cosh \xi_0^C = 1 + \frac{s}{2k}. \tag{2.36}$$

If, on the other hand, $m = m_0$, Eq. (2.34) reduces to

$$-2kA(s)e^{-\xi_0^C} + (s+2k)A(s) = 1. \tag{2.37}$$

Therefore

$$A(s) = \frac{1}{2k \sinh \xi_0^C}. \tag{2.38}$$

This fully specifies the Green's function :

$$G^C_{mm_0}(s) = \frac{e^{-\xi_0^C |m-m_0|}}{2k \sinh \xi_0^C}. \tag{2.39}$$

We now turn to a second, more ingenious, systematic method to obtain closed form expressions for the Green's function. Consider the slightly more complicated case of a biased nearest neighbour random walk on an infinite one-dimensional lattice with transition rates $k^{\pm} = k(1 \mp g)$. The Green's function for this situation is the solution of

$$-k(1+g)G^C_{m-1,m_0}(s)+(s+2k)G^C_{mm_0}(s)-k(1-g)G^C_{m+1,m_0}(s) = \delta_{mm_0}. \tag{2.40}$$

Defining the complex variable ξ^C as

$$\cosh \xi^C = \frac{1 + \frac{s}{2k}}{\sqrt{1-g^2}} \tag{2.41}$$

with $Re\xi^C > 0$, Eq. (2.40) can be rewritten as

$$\begin{aligned} -(1+g)\, G^C_{m-1,m_0}(s) \;+\; & (e^{\xi^C} + e^{-\xi^C})\sqrt{1-g^2}\, G^C_{mm_0}(s) \\ & - \;(1-g)\, G^C_{m+1,m_0}(s) = \frac{\delta_{mm_0}}{k} \end{aligned} \tag{2.42}$$

or

$$\begin{aligned} & G^C_{m+1,m_0}(s) - e^{\xi^C}\sqrt{f} G^C_{mm_0}(s) \\ & = e^{-\xi^C}\sqrt{f}\left(G^C_{mm_0}(s) - e^{\xi^C}\sqrt{f} G^C_{m-1,m_0}(s)\right) - \frac{\delta_{mm_0}}{k(1-g)} \end{aligned} \tag{2.43}$$

where we introduced f as

$$f = \frac{1+g}{1-g}. \tag{2.44}$$

We will first consider the case $m > m_0$. By iteration of Eq. (2.43) one finds (taking into account that $G^C_{mm_0}(s) \to 0$ for $m \to \pm\infty$, and that the factor $e^{-(m-m_0)\xi^C}$ does not diverge)

$$G^C_{m+1,m_0}(s) - e^{\xi^C}\sqrt{f}G^C_{mm_0}(s) = -\frac{e^{-(m-m_0)\xi^C} f^{\frac{m-m_0}{2}}}{k(1-g)}. \tag{2.45}$$

After a second iteration, $G^C_{mm_0}(s)$ can be expressed as

$$\begin{aligned} G^C_{mm_0}(s) &= e^{(m-m_0)\xi^C} f^{\frac{m-m_0}{2}} G^C_{m_0m_0}(s) \\ &\quad - \frac{e^{-(m-m_0-1)\xi^C} f^{\frac{m-m_0-1}{2}}}{k(1-g)} \sum_{j=0}^{m-m_0-1} e^{2j\xi^C}. \end{aligned} \tag{2.46}$$

Carrying out the sum in the last term on the r.h.s., Eq. (2.46) reduces to

$$G^C_{mm_0}(s) = e^{|m-m_0|\xi^C} f^{\frac{m-m_0}{2}} G^C_{m_0m_0}(s) - \frac{f^{\frac{m-m_0-1}{2}}}{k(1-g)} \frac{\sinh|m-m_0|\xi^C}{\sinh\xi^C}, \tag{2.47}$$

where we included the result for $m < m_0$. Since $G^C_{mm_0}(s) \to 0$ for $m \to \pm\infty$ we can derive from Eq. (2.47) the expression for $G^C_{m_0m_0}(s)$, so that we finally obtain the following compact result for the Green's function :

$$G^C_{mm_0}(s) = \frac{f^{\frac{m-m_0-1}{2}} e^{-|m-m_0|\xi^C}}{2k(1-g)\sinh\xi^C}. \tag{2.48}$$

Until now, we have limited ourselves to unrestricted random walks. One-dimensional random walks in the presence of reflecting or absorbing boundaries can be delt with either by using the methods given above, or by the method of images, also called reflection principle [27,28,29]. This technique uses the fact that the probability distribution for the random walk in the presence of

boundaries can be expressed in terms of the probability ditribution for the random walk on the infinite lattice. For example, for an unbiased random walk with one reflecting boundary in the origin, we have the following relation between $P_0(m, m_0; t)$ (reflecting barrier in 0) and $P(m, m_0; t)$ (infinite lattice)

$$P_0(m, m_0; t) = P(m, m_0; t) + P(m, -m_0 + 1; t). \tag{2.49}$$

The same relation is valid for the Laplace transform, and thus one finds by combining Eqs. (2.48) (with the bias g equal to zero) and (2.49) :

$$G^C_{mm_0}(s) = \frac{e^{-m_> \xi_0^C}(e^{\xi_0^C} - 1)\cosh(m_< - \frac{1}{2})\xi_0^C}{s \cosh \frac{\xi_0^C}{2}} \tag{2.50}$$

with

$$m_> = \max(m, m_0)$$

$$m_< = \min(m, m_0)$$

In the table on pages 17-20 we have listed the results for the Green's functions for discrete time step random walks, random walks with a continuous time variable as well as for diffusive processes with various sets of boundary conditions (some of them can be found in the literature, cf. [24,25,30,31]). The following notations are used

- for a biased random walk

$$f = \frac{1+g}{1-g} \tag{2.51}$$

$$\beta = \frac{1}{2} \ln f \tag{2.52}$$

  - with discrete time variable

$$\cosh \xi^D = \frac{1 + \frac{1-z}{2z\alpha}}{\sqrt{1-g^2}} \tag{2.53}$$

– with continuous time variable :

$$\cosh \xi^C = \frac{1 + \frac{s}{2k}}{\sqrt{1 - g^2}} \tag{2.54}$$

$$\frac{1}{\lambda} = \frac{1}{2D}\sqrt{4sD + v^2} \tag{2.55}$$

- for an unbiased random walk ($g = 0$)

$$\cosh \xi_0^D = 1 + \frac{1 - z}{2z\alpha} \tag{2.56}$$

$$\cosh \xi_0^C = 1 + \frac{s}{2k} \tag{2.57}$$

We finally would like to mention that the cases for which a closed form expression for the Green's function can be obtained are not limited to the nearest neighbour transitions we considered in this section. In refs. [32,33] e.g., results for the Green's function for a one-dimensional symmetric random walk with exponentially distributed step lengths and various boundary conditions have been calculated using the eigenfunction expansion.

Infinite lattice		
	biased	unbiased
$G^D_{mm0}(z) =$	$\dfrac{f^{(m-m_0-1)/2} e^{-\xi^D(m_> - m_<)}}{2z\alpha(1-g)\sinh\xi^D}$	$\dfrac{e^{-\xi^D_0(m_> - m_<)}}{2z\alpha\sinh\xi^D_0}$
$G^C_{mm0}(s) =$	$\dfrac{f^{(m-m_0-1)/2} e^{-\xi^C(m_> - m_<)}}{2k(1-g)\sinh\xi^C}$	$\dfrac{e^{-\xi^C_0(m_> - m_<)}}{2k\sinh\xi^C_0}$
$G(x, x_0; s) =$	$\dfrac{\lambda\, e^{(x-x_0)\frac{v}{2D}}\, e^{-\frac{(x_> - x_<)}{\lambda}}}{2D}$	$\dfrac{e^{-\sqrt{\frac{s}{D}}(x_> - x_<)}}{2\sqrt{sD}}$
Reflecting boundaries in 0 and $N+1$		
	biased	unbiased
$G^D_{mm_0}(z) =$	$\dfrac{f^{(m-m_0-1)/2}}{(1-z)\sinh\xi^D\sinh(N\xi^D)}\left[\sinh[(N-m_>+1)\xi^D] - \sqrt{f}\sinh[(N-m_>)\xi^D]\right]$ $\times\left[\sqrt{f}\sinh(m_<\xi^D) - \sinh[(m_<-1)\xi^D]\right]$	$\dfrac{\cosh[\xi^D_0(N+\frac{1}{2}-m_>)]\cosh[\xi^D_0(m_<-\frac{1}{2})]}{z\alpha\sinh\xi^D_0\sinh(N\xi^D_0)}$
$G^C_{mm_0}(s) =$	$\dfrac{f^{(m-m_0-1)/2}}{s\sinh\xi^C\sinh(N\xi^C)}\left[\sinh[(N-m_>+1)\xi^C] - \sqrt{f}\sinh[(N-m_>)\xi^C]\right]$ $\times\left[\sqrt{f}\sinh(m_<\xi^C) - \sinh[(m_<-1)\xi^C]\right]$	$\dfrac{\cosh[\xi^C_0(N+\frac{1}{2}-m_>)]\cosh[\xi^C_0(m_<-\frac{1}{2})]}{k\sinh\xi^C_0\sinh(N\xi^C_0)}$
$G(x, x_0; s) =$	$\dfrac{\lambda\, e^{(x-x_0)\frac{v}{2D}}}{2D\sinh\frac{L}{\lambda}}\left[\dfrac{v^2+2sD}{2sD}\cosh\left(\dfrac{L-x_>-x_<}{\lambda}\right) + \cosh\left(\dfrac{L-x_>+x_<}{\lambda}\right)\right.$ $\left. - \dfrac{v}{\lambda s}\sinh\left(\dfrac{L-x_>-x_<}{\lambda}\right)\right]$	$\dfrac{\cosh[\sqrt{\frac{s}{D}}(L-x_>)]\cosh(\sqrt{\frac{s}{D}}x_<)}{\sqrt{sD}\sinh(L\sqrt{\frac{s}{D}})}$

Half infinite line with reflecting boundary in 0		
	biased	unbiased
$G^D_{mm0}(z) =$	$f^{(m-m_0-1)/2}\frac{e^{-m_>\xi^D}}{(1-z)}\frac{(e^{\xi^D}-\sqrt{f})}{\sinh\xi^D}\left[\sqrt{f}\sinh(m_<\xi^D)\sinh[(m_<-1)\xi^D]\right]$	$\frac{e^{-m_>\xi^D}(e^{\xi^D}-1)\cosh[\xi_0^D(m_<-\frac{1}{2})]}{(1-z)\cosh\frac{\xi_0^D}{2}}$
$G^C_{mm0}(s) =$	$f^{(m-m_0-1)/2}e^{-m_>\xi^C}\frac{(e^{\xi^C}-\sqrt{f})}{s\sinh\xi^C}\left[\sqrt{f}\sinh(m_<\xi^C)-\sinh[(m_<-1)\xi^C]\right]$	$\frac{e^{-m_>\xi_0^C}(e^{\xi_0^C}-1)\cosh[(m_<-\frac{1}{2})\xi_0^C]}{s\cosh\frac{\xi_0^C}{2}}$
$G(x,x_0;s) =$	$e^{(x-x_0)\frac{v}{2D}}\ e^{-\frac{x_>}{\lambda}}(\frac{1}{s}-\frac{\lambda v}{2Ds})(\frac{v}{2D}\sinh\frac{x_<}{\lambda}+\frac{1}{\lambda}\cosh\frac{x_<}{\lambda})$	$\frac{e^{-x_>\sqrt{\frac{1}{D}}}}{\sqrt{sD}}\cosh(x_<\sqrt{\frac{s}{D}})$
Absorbing boundaries in 0 and $N+1$		
	biased	unbiased
$G^D_{mm0}(z) =$	$\frac{f^{(m-m_0-1)/2}\sinh(m_<\xi^D)\sinh[(N+1-m_>)\xi^D]}{z\alpha(1-g)\sinh\xi^D\sinh[(N+1)\xi^D]}$	$\frac{\sinh(m_<\xi_0^D)\sinh[(N+1-m_>)\xi_0^D]}{z\alpha\sinh\xi_0^D\sinh[(N+1)\xi_0^D)]}$
$G^C_{mm0}(s) =$	$\frac{f^{(m-m_0-1)/2}\sinh(m_<\xi^C)\sinh[(N+1-m_>)\xi^C]}{k(1-g)\sinh\xi^C\sinh[(N+1)\xi^C]}$	$\frac{\sinh(m_<\xi_0^C)\sinh[(N+1-m_>)\xi_0^C]}{k\sinh\xi_0^C\sinh[(N+1)\xi_0^C]}$
$G(x,x_0;s) =$	$\frac{\lambda\ e^{(x-x_0)\frac{v}{2D}}\sinh\frac{x_<}{\lambda}\sinh\left(\frac{L-x_>}{\lambda}\right)}{D\sinh\frac{L}{\lambda}}$	$\frac{\sinh(x_<\sqrt{\frac{s}{D}})\sinh[(L-x_>)\sqrt{\frac{s}{D}}]}{\sqrt{sD}\sinh(L\sqrt{\frac{s}{D}})}$

Half infinite line with absorbing boundary in 0		
	biased	unbiased
$G^D_{mm0}(z) =$	$\dfrac{f^{(m-m_0-1)/2} e^{-m_> \xi^D} \sinh(m_< \xi^D)}{z\alpha(1-g)\sinh \xi^D}$	$\dfrac{e^{-m_> \xi^D_0} \sinh(m_< \xi^D_0)}{z\alpha \sinh \xi^D_0}$
$G^C_{mm0}(s) =$	$\dfrac{f^{(m-m_0-1)/2} e^{-m_> \xi^C} \sinh(m_< \xi^C)}{k(1-g)\sinh \xi^C}$	$\dfrac{e^{-m_> \xi^C_0} \sinh(m_< \xi^C_0)}{k \sinh \xi^C_0}$
$G(x, x_0; s) =$	$\dfrac{\lambda\, e^{(x-x_0)\frac{v}{2D}}\, e^{-\frac{x_>}{\lambda}} \sinh \dfrac{x_<}{\lambda}}{D}$	$\dfrac{e^{-x_> \sqrt{\frac{s}{D}}} \sinh(x_< \sqrt{\dfrac{s}{D}})}{\sqrt{sD}}$
Reflecting boundary in 0 and absorbing boundary in $N+1$		
	biased	unbiased
$G^D_{mm0}(z) =$	$\dfrac{f^{(m-m_0-1)/2} \sinh[(N+1-m_>)\xi^D][\sqrt{f}\sinh(m_< \xi^D) - \sinh[(m_<-1)\xi^D]]}{z\alpha(1-g)\sinh \xi^D[\sqrt{f}\sinh[(N+1)\xi^D] - \sinh(N\xi^D)]}$	$\dfrac{\sinh[(N+1-m_>)\xi^D_0]\cosh[(m_< - \frac{1}{2})\xi^D_0]}{z\alpha \sinh \xi^D_0 \cosh[(N+\frac{1}{2})\xi^D_0]}$
$G^C_{mm0}(s) =$	$\dfrac{f^{(m-m_0-1)/2} \sinh[(N+1-m_>)\xi^C][\sqrt{f}\sinh[m_< \xi^C] - \sinh[(m_<-1)\xi^C]]}{k(1-g)\sinh \xi^C[\sqrt{f}\sinh[(N+1)\xi^C] - \sinh(N\xi^C)]}$	$\dfrac{\sinh[(N+1-m_>)\xi^C_0]\cosh[(m_< - \frac{1}{2})\xi^C_0]}{k \sinh \xi^C_0 \cosh[(N+\frac{1}{2})\xi^C_0]}$
$G(x, x_0; s) =$	$\dfrac{\lambda\, e^{(x-x_0)\frac{v}{2D}}}{D} \sinh\left(\dfrac{L-x_>}{\lambda}\right) \dfrac{[\frac{v\lambda}{2D}\sinh\frac{x_<}{\lambda} + \cosh\frac{x_<}{\lambda}]}{[\frac{v\lambda}{2D}\sinh\frac{L}{\lambda} + \cosh\frac{L}{\lambda}]}$	$\dfrac{\sinh[(L-x_>)\sqrt{\frac{s}{D}}]\cosh(x_<\sqrt{\frac{s}{D}})}{\sqrt{sD}\cosh(L\sqrt{\frac{s}{D}})}$

Periodic boundaries		
	biased	unbiased
$G^D_{mm0}(z) =$	$f^{(m-m_0-1)/2}\left[\frac{\sinh[\xi^D(N-m_>+m_<)]-\sinh(N\beta)\sinh[\xi^D(m-m_0)]}{2z\alpha(1-g)\sinh\xi^D[\cosh(N\xi^D)-\cosh(N\beta)]}\right.$ $\left.\underline{+\cosh(N\beta)\sinh[\xi^D(m_>-m_<)]}\right]$	$\frac{\cosh[\xi^D_0(m_>-m_<-\frac{N}{2})]}{2z\alpha\sinh\xi^D_0\sinh(\frac{N}{2}\xi^D_0)}$
$G^C_{mm0}(s) =$	$f^{(m-m_0-1)/2}\left[\frac{\sinh[\xi^C(N-m_>+m_<)]-\sinh(N\beta)\sinh[\xi^C(m-m_0)]}{2k(1-g)\sinh\xi^C[\cosh(N\xi^C)-\cosh(N\beta)]}\right.$ $\left.\underline{+\cosh(N\beta)\sinh[\xi^C(m_>-m_<)]}\right]$	$\frac{\cosh[\xi^C_0(m_>-m_<-\frac{N}{2})]}{2k\sinh\xi^C_0\sinh(\frac{N}{2}\xi^D_0)}$
$G(x,x_0;s) =$	$-\frac{\lambda\, e^{(x-x_0)\frac{v}{2D}}}{2D\left[\cosh(\frac{Lv}{2D})-\cosh\frac{L}{\lambda}\right]}\left[\sinh(\frac{L-x_>+x_<}{\lambda})\right.$ $\left.+\sinh\left(\frac{x_0-x}{\lambda}\right)\sinh\left(\frac{Lv}{2D}\right)+\sinh\left(\frac{x_>-x_<}{\lambda}\right)\cosh\left(\frac{Lv}{2D}\right)\right]$	$\frac{\cosh[\sqrt{\frac{s}{D}}(x_>-x_<-\frac{L}{2})]}{2\sqrt{sD}\sinh(\sqrt{\frac{s}{D}}\frac{L}{2})}$

2.1.3 Small s expansion

Even though one may not be able to calculate the complete Green's function, it is in some cases possible to obtain an analytic expression for its small s expansion, without knowing the explicit form of the eigenvectors. We will illustrate this method for a one-dimensional, nearest neighbour random walk with general transition probabilities $k_i^{\pm}$ on a strip of N sites with reflecting boundary conditions. The Green's function is expanded around $s = 0$ by first separating out the singular contribution corresponding to the eigenvalue zero :

$$\begin{aligned} G^C_{mm_0}(s) &= \frac{P^{st}_m}{s} + \sum_{\alpha \neq 0} X_{m\alpha} \frac{1}{s - \lambda_\alpha} Y_{\alpha m_0} \\ &= \frac{P^{st}_m}{s} - \frac{1}{s} \sum_{n=1}^{\infty} s^n G^{*n}_{mm_0}, \end{aligned} \tag{2.58}$$

with the terms $\mathbf{G}^{*n}$ defined as

$$G^{*n}_{mm_0} = \sum_{\alpha \neq 0} X_{m\alpha} \frac{1}{(\lambda_\alpha)^n} Y_{\alpha m_0}. \tag{2.59}$$

We will limit ourselves here to the calculation of the first two terms, $\mathbf{P}^{st}$ and $\mathbf{G}^{*1}$, which we will use later in chapter 5.

For this particular situation, the stationary distribution $\mathbf{P}^{st}$ obeys the detailed balance condition. We have ($\forall\ m\ \epsilon\ [1, N-1]$) :

$$k^+_m P^{st}_m = k^-_{m+1} P^{st}_{m+1}. \tag{2.60}$$

From this set of $N-1$ equations, combined with the normalization condition

$$\sum_{m=1}^{N} P^{st}_m = 1, \tag{2.61}$$

we find the following solution for P_m^{st} :

$$P_m^{st} = \frac{1}{\mathcal{N}} \, k_1^+ \, \cdots \, k_{m-1}^+ \, k_{m+1}^- \cdots \, k_N^- . \tag{2.62}$$

The normalization factor $\mathcal{N}$ is given by

$$\mathcal{N}^{-1} = k_2^- \, \cdots \, k_N^- + k_1^+ \, k_3^- \cdots \, k_N^- + \cdots + k_1^+ \cdots \, k_{N-1}^+ . \tag{2.63}$$

We will now proceed with the derivation of $\mathbf{G}^{*1}$. The right eigenvectors $\mathbf{X}_\alpha$, $\alpha \neq 0$, are the solution of the following set of equations :

$$-k_1^+ X_{1\alpha} + k_2^- X_{2\alpha} = \lambda_\alpha X_{1\alpha} \tag{2.64}$$

$$k_{m_0-1}^+ X_{m_0-1,\alpha} - (k_{m_0}^- + k_{m_0}^+) X_{m_0\alpha} + k_{m_0+1}^- X_{m_0+1,\alpha} = \lambda_\alpha X_{m_0\alpha} \tag{2.65}$$

$$k_{N-1}^+ X_{N-1,\alpha} - k_N^- X_{N\alpha} = \lambda_\alpha X_{N\alpha} . \tag{2.66}$$

Using the relationship between left and right eigenvectors (Eq. (2.17)) and rearranging the terms, this can be written as

$$k_2^- P_2^{st} Y_{\alpha 2} - k_1^+ P_1^{st} Y_{\alpha 1} = \lambda_\alpha P_1^{st} Y_{\alpha 1} \tag{2.67}$$

$$\begin{aligned} & k_{m_0+1}^- P_{m_0+1}^{st} Y_{\alpha,m_0+1} - k_{m_0}^+ P_{m_0}^{st} Y_{\alpha m_0} \\ & = k_{m_0}^- P_{m_0}^{st} Y_{\alpha m_0} - k_{m_0-1}^+ P_{m_0-1}^{st} Y_{\alpha,m_0-1} + \lambda_\alpha P_{m_0}^{st} Y_{\alpha m_0} \end{aligned} \tag{2.68}$$

$$k_N^- P_N^{st} Y_{\alpha N} - k_{N-1}^+ P_{N-1}^{st} Y_{\alpha,N-1} = -\lambda_\alpha P_N^{st} Y_{\alpha N} . \tag{2.69}$$

By iteration, this set of equations can be replaced by

$$Y_{\alpha m_0} - Y_{\alpha,m_0-1} = \lambda_\alpha \sum_{k=1}^{m_0-1} \frac{Y_{\alpha k} P_k^{st}}{k_{m_0-1}^+ P_{m_0-1}^{st}} , \tag{2.70}$$

where we also used the detailed balance condition (Eq. (2.60)). Multiplying

with $X_{m\alpha}/\lambda_\alpha$ and summing over α yield the recursion relation for $\mathbf{G}^{*1}$:

$$G^{*1}_{mm_0} = G^{*1}_{m,m_0-1} + \sum_{k=1}^{m_0-1} \frac{(\delta_{mk} - P^{st}_m)P^{st}_k}{k^+_{m_0-1}P^{st}_{m_0-1}} \tag{2.71}$$

or

$$G^{*1}_{mm_0} = G^{*1}_{m1} + \sum_{r=1}^{m_0-1}\sum_{k=1}^{r} \frac{(\delta_{mk} - P^{st}_m)P^{st}_k}{k^+_r P^{st}_r}. \tag{2.72}$$

The last step in our calculation will be the determination of G^{*1}_{m1}. Since

$$\sum_{l=1}^{N} G^{*1}_{ml}P^{st}_l = \sum_{l=1}^{N} \frac{X_{m\alpha}Y_{\alpha l}X_{l0}}{\lambda_\alpha} = 0, \tag{2.73}$$

we find for G^{*1}_{m1}

$$G^{*1}_{m1} = -\sum_{l=2}^{N} P^{st}_l \sum_{r=1}^{l-1}\sum_{k=1}^{r} \frac{(\delta_{mk} - P^{st}_m)P^{st}_k}{k^+_r P^{st}_r}. \tag{2.74}$$

So that the result for $G^{*1}_{mm_0}$ finally reduces to the following compact form

$$\begin{aligned} G^{*1}_{mm_0} &= \sum_{l=2}^{N}\sum_{r=1}^{l-1}\sum_{k=1}^{r} P^{st}_m \frac{(\delta_{mk} - P^{st}_k)(\delta_{m_0 l} - P^{st}_l)}{k^+_r P^{st}_r} \\ &= -\sum_{r=1}^{N-1}\sum_{l=1}^{r}\sum_{k=1}^{r} P^{st}_m \frac{(\delta_{mk} - P^{st}_k)(\delta_{m_0 l} - P^{st}_l)}{k^+_r P^{st}_r}. \end{aligned} \tag{2.75}$$

The last equality is obtained by reversing the summation order of r and l. The expressions for the higher order terms $\mathbf{G}^{*n}$ in the expansion of the Green's function can be obtained by an analogous, but increasingly tedious, computation.

2.1.4 Continuous time random walks

In the previous sections we have considered random walks where the time intervals between two jumps are uncorrelated, i.e. the walker jumps to another state at completely random points in time (cf. Eq. (2.3)). A natural generalization is to consider walks where the time interval between successive jumps is drawn from a distribution $\psi(t)$, also called the waiting time distribution [34]-[36]. This type of processes are usually referred to as continuous time random walks. For these problems, it is important to correctly specify the initial condition, because the moment that we start monitoring the motion of the particle does not necessarily coincide with a point in time where a transition took place. Therefore, the time interval prior to the first transition of the particle is not given by the waiting time distribution $\psi(t)$, but rather by a first waiting time distribution $\psi_0(t)$. If we assume stationarity in the sense that the starting time is picked at random, the following relation between $\psi_0(t)$ and $\psi(t)$ can be derived (see e.g. [27] or [37]) :

$$\psi_0(t) = \frac{\int_t^\infty \psi(t')dt'}{\int_0^\infty t'\psi(t')dt'} = \frac{\int_t^\infty \psi(t')dt'}{<\tau>}, \tag{2.76}$$

or after Laplace transformation

$$\tilde{\psi_0}(s) = \frac{1-\tilde{\psi}(s)}{s<\tau>}. \tag{2.77}$$

The only situation in which $\psi_0(t)$ and $\psi(t)$ are identical is when the waiting time is exponentially distributed :

$$\psi(t) = ke^{-kt}. \tag{2.78}$$

This is also the only case in which the walk is Markovian and can be described by a Master equation [38]. To study the non-Markovian effects, we consider the simplest case of a symmetric two-state random walk (symmetric in the sense that the waiting time density $\psi(t)$ is identical for the two states). If the

walker is to arrive at state two at time t, starting from state one at $t = 0$, it has to switch an odd number of times between the two states. $P(2|1;t)$ can thus be expressed as

$$P(2|1;t) = P(1|2;t) = \sum_{\substack{n=1 \\ \text{odd}}}^{\infty} \int_0^t \psi_0(\tau_1)d\tau_1 \int_0^{t-\tau_1} \psi(\tau_2)d\tau_2$$

$$\times \int_0^{t-\tau_1-\tau_2} \psi(\tau_3)d\tau_3 \cdots \left(1 - \int_0^{t-\tau_1-\tau_2-\cdots-\tau_n} \psi(\tau_{n+1})d\tau_{n+1}\right), \quad (2.79)$$

where the last factor states that step $n+1$ is taken after time t. Similarly, a walker can only return to its initial state after an even number of steps :

$$P(1|1;t) = P(2|2;t) = \sum_{\substack{n=1 \\ \text{even}}}^{\infty} \int_0^t \psi_0(\tau_1)d\tau_1 \int_0^{t-\tau_1} \psi(\tau_2)d\tau_2$$

$$\times \int_0^{t-\tau_1-\tau_2} \psi(\tau_3)d\tau_3 \cdots \left(1 - \int_0^{t-\tau_1-\cdots-\tau_n} \psi(\tau_{n+1})d\tau_{n+1}\right). \quad (2.80)$$

By Laplace transformation and carrying out the sums over n, we find for the Green's function $\mathbf{G}^C(s)$

$$G_{11}^C(s) = G_{22}^C(s) = \frac{1}{s} - \frac{\tilde{\psi}_0(s)}{s(1+\tilde{\psi}(s))} \quad (2.81)$$

$$G_{12}^C(s) = G_{21}^C(s) = \frac{\tilde{\psi}_0(s)}{s(1+\tilde{\psi}(s))}. \quad (2.82)$$

We will use these results in chapter 6 to derive the effective diffusion coefficient for a two-state model for particles suspended in a flow with an oscillating velocity field.

The procedure described above (but involving considerably more effort) can also be used to calculate the Green's function for a one-dimensional nearest neighbour random walk on an infinite lattice. For the symmetric case, the

Green's function is given by [39] :

$$G^C_{mm_0}(s) = \frac{1}{s}\left(1 - \frac{\tilde{\psi_0}(s)}{\tilde{\psi}(s)}\right)\delta_{mm_0} + \frac{1}{s}\frac{\tilde{\psi_0}(s)}{\tilde{\psi}(s)}\tanh\frac{\xi}{2}e^{-|m-m_0|\xi} \tag{2.83}$$

with

$$\cosh\xi = \frac{1}{\tilde{\psi}(s)}. \tag{2.84}$$

In the case of an exponential waiting time distribution, this reduces to the result for the infinite lattice we obtained earlier (cf. Eq. (2.39)).

The more complicated problem of a random walk on a semi-infinite or finite chain with reflecting or absorbing boundaries can be related to the random walk on the infinite lattice using the method of images already mentioned in section 2.1.2. Consider for instance a walker on a semi-infinite lattice with an absorbing boundary in site m. In order for the walker to survive at time t, it can never have reached the the barrier in m prior to t. Therefore $P_{\overline{m}}(m', m_0; t)$ (with an absorbing barrier) is equal to $P(m', m_0; t)$, provided we substract all the paths that have crossed the barrier m. This is equivalent (for a symmetric random walk) to the substraction of all the walks that have reached the "reflection" $2m - m'$ of m' on the infinite lattice. We thus have

$$P_{\overline{m}}(m', 0; t) = P(m', m_0; t) - P(2m - m', m_0; t). \tag{2.85}$$

Substituting the result Eq.(2.83) for the infinite lattice into the Laplace transform of Eq. (2.85) thus yields the desired result for the Green's function of a random walk in the presence of an absorbing boundary. Similar calculations can be performed to obtain the Green's function for symmetric as well as biased continuous time random walks with different kinds of boundaries [29].

2.2 First passage times and related quantities

One of the important quantitities that can be derived from the Green's function is the probability $Q(\mathbf{m}, \mathbf{m_0}; t)$ that the walker arrives at site $\mathbf{m}$ for the first time (starting from $\mathbf{m_0}$) at time t, also called the first passage time distribution. For a Markovian random walk, it can be related to the probability distribution $P(\mathbf{m}, \mathbf{m_0}; t)$ as follows. Consider a random walk on an infinite d-dimensional lattice. In order for the random walk to reach site $\mathbf{m}$, it has to pass through there for the first time at an earlier time t' and then return to $\mathbf{m}$ in the remaining time interval $t - t'$:

$$P(\mathbf{m}, \mathbf{m_0}; t) = \int_0^t Q(\mathbf{m}, \mathbf{m_0}; t') P(\mathbf{m}, \mathbf{m}; t - t') dt' \tag{2.86}$$

or after Laplace transformation :

$$\tilde{Q}(\mathbf{m}, \mathbf{m_0}; s) = \frac{G^C_{\mathbf{m}\mathbf{m_0}}(s)}{G^C_{\mathbf{m}\mathbf{m}}(s)}. \tag{2.87}$$

For a one-dimensional nearest neighbour random walk, the following stronger result due to Siegert [40] holds true :

$$\tilde{Q}(m, m_0; s) = \frac{G^C_{m_1 m}(s)}{G^C_{m_1 m_0}(s)} \qquad \text{for} \qquad m_0 < m \leq m_1 \tag{2.88}$$

Hence, using the closed form expressions for the Green's function of one-dimensional nearest neighbour random walks given in section 2.1.2, we can derive the result for the generating function of the first passage time distribution. For instance, for a biased random walk with a reflecting boundary in the origin we have [30]

$$\tilde{Q}(m, m_0; s) = f^{(m-m_0)/2} \left[\frac{\sqrt{f} \sinh(m_0 + 1)\xi^C - \sinh m_0 \xi^C}{\sqrt{f} \sinh(m + 1)\xi^C - \sinh m \xi^C} \right]. \tag{2.89}$$

The moments of the first passage time $< t^r >$ are determined by the small s behaviour of $\tilde{Q}(m, m_0; s)$:

$$< t^r >= (-1)^r \frac{\partial^r}{\partial s} \tilde{Q}(m, m_0; s) \mid_{s=0} . \tag{2.90}$$

From Eq. (2.89) we thus find for the mean first passage time $< t >$

$$< t >= \frac{1}{2k} \frac{f+1}{f-1} \left[(m - m_0) - \left(\frac{f^m - f^{m_0}}{f-1} \right) \right] \qquad \text{for } 0 \leq m_0 < m. \tag{2.91}$$

The Siegert eguation (2.88) is not valid for non-Markov processes such as the continuous time random walk with waiting times between consecutive jumps we considered earlier. For these cases, another approach has to be used to derive the first passage time distribution. This can be done as follows. For a walker on a one-dimensional infinite chain, the problem of the first passage to a point m, starting from m_0 ($m_0 < m$) is equivalent to the problem of a random walk with an absorbing barrier in m [41]. If the particle is in state m', somewhere in the interval $]-\infty, m[$, at time t, then at the slightly later time $t + dt$ two things can happen : the particle can survive, and therefore never have reached the absorbing barrier, or it can make a first passage to the barrier. We thus have

$$\sum_{m'=-\infty}^{m-1} P_{\overline{m}}(m', m_0; t) = \sum_{m'=-\infty}^{m-1} P_{\overline{m}}(m', m_0; t + dt) + Q(m, m_0; t)dt, \tag{2.92}$$

with $P_{\overline{m}}(m', m_0; t)$ the probability distribution in the presence of an absorbing boundary in m. We can rewrite Eq. (2.92) as

$$Q(m, m_0; t) = -\frac{d}{dt} \sum_{m'=-\infty}^{m-1} P_{\overline{m}}(m', m_0; t). \tag{2.93}$$

The distribution $P_{\overline{m}}(m', m_0; t)$ can be obtained from $P(m', m_0; t)$ for an infinite lattice using the method of images, described earlier

$$P_{\overline{m}}(m', m_0; t) = P(m', m_0; t) - P(2m - m', m_0; t). \tag{2.94}$$

In Laplace transform language, the generating function for the first passage time distribution can thus be expressed in terms of the Green's function for the random walk on an infinite lattice :

$$\tilde{Q}(m, m_0; s) = 1 + s \sum_{m'=-\infty}^{m-1} \left[G^C_{2m-m', m_0}(s) - G^C_{m', m_0}(s) \right]. \qquad (2.95)$$

Substituting the result of Eq. (2.83), we find for the first passage time distribution for a symmetric continuous time random walk on an infinite line [39]

$$\tilde{Q}(m, m_0; s) = \frac{\tilde{\psi}_0(s)}{\tilde{\psi}(s)} e^{-|m-m_0|\xi} \qquad (2.96)$$

with

$$\cosh \xi = \frac{1}{\tilde{\psi}(s)}. \qquad (2.97)$$

Another important quantity in the study of random walk problems is the probability of return to the origin. Consider a discrete time step random walk on a d-dimensional infinite lattice. The equivalent of Eq. (2.86) for this system reads (we choose the origin as the starting point of the random walks) :

$$P(\mathbf{m}, 0; n) = \sum_{j=1}^{n} Q(\mathbf{m}, 0; j) P(\mathbf{m}, \mathbf{m}; n-j) \qquad for\ n > 0. \qquad (2.98)$$

Introducing $\tilde{Q}(\mathbf{m}, 0; z)$, the generating function for the first passage time distribution :

$$\tilde{Q}(\mathbf{m}, 0; z) = \sum_{n=0}^{\infty} z^n Q(\mathbf{m}, 0; n), \qquad (2.99)$$

Eq. (2.98) can be rewritten as

$$\tilde{Q}(\mathbf{m}, 0; z) = \frac{1}{\tilde{G}(0, 0; z)} \left[\tilde{G}(\mathbf{m}, 0; z) - \delta_{\mathbf{m}0} \right]. \qquad (2.100)$$

Since $\widetilde{Q}(\mathbf{m}, 0; z = 1)$ is the probability that the random walker ever reaches the point $\mathbf{m}$, i.e. in any number of steps, we can derive from this the probability that the walker returns to the origin :

$$\widetilde{Q}(\mathbf{0}, \mathbf{0}; z = 1) = 1 - \frac{1}{\widetilde{G}(\mathbf{0}, \mathbf{0}; z = 1)}. \tag{2.101}$$

For nearest neighbour random walks on infinite one- and two-dimensional cubic lattices, $\widetilde{G}(\mathbf{0}, \mathbf{0}; z)$ diverges as z goes to one [42] and thus the particle is certain to return to the origin [11], while in three (or more) dimensions there exists a finite escape probability. The average number of steps required to return to the origin

$$< \tau >= \sum_{n=1}^{\infty} nQ(\mathbf{0}, \mathbf{0}; n) = \left. \frac{\partial \widetilde{Q}(\mathbf{0}, \mathbf{0}; z)}{\partial z} \right|_{z=1}, \tag{2.102}$$

is not only infinite in three (or more) dimensions as expected, but also in one and two dimensions [27]. On a finite d-dimensional lattice with periodic boundaries however, the number of steps required to return to the origin is equal to the number of lattice points [42] :

$$< \tau >= N^d. \tag{2.103}$$

We close this section with a last example of a quantity that can be expressed in terms of the Green's function, namely the average number of distinct lattice points visited after n steps, also called the span of the random walk, which we will denote by S_n. To calculate S_n, we note that

$$S_n = \sum_{\mathbf{m}} F_n(\mathbf{m}), \tag{2.104}$$

where $F_n(\mathbf{m})$ is the probability that, after n steps, the walker has visited site $\mathbf{m}$ at least once :

$$F_n(\mathbf{m}) = \sum_{j=1}^{n} Q(\mathbf{m}, \mathbf{0}; j). \tag{2.105}$$

Combining these last two equations, the generating function $\widetilde{S}(z)$ of the number of distinct sites visited can thus be expressed in terms of the Green's function as [42]

$$\widetilde{S}(z) = \frac{1}{(1-z)^2} \frac{1}{\widetilde{G}(\mathbf{0},\mathbf{0};z)}. \tag{2.106}$$

2.3 Conclusion

In this chapter we have reviewed results for the Green's function of a random walk. In some cases, such as one-dimensional translationally invariant nearest neighbour random walks, closed form expressions can be derived, while in other, more complicated situations (cf. section 2.1.3), one can only compute the small s expansion. We also discussed how some quantities can be directly related to the Green's function, with as most important example the first passage time distribution. In the following chapters, we will present other physical problems in which such a direct relation can be established.

Chapter 3

Random walk with persistence

In the context of random walk models for polymer chains, one is interested in properties such as the moments $< R^{2\ell} >$ of the end-to-end distance $\mathbf{R}$ (for $\ell \geq 2$) and the probability density $P(\mathbf{R}, n)$ [43,44]. In this chapter, such analytic results will be derived for a random walk with persistence.

In the free flight model a polymer is represented as a chain of n segments $\mathbf{r}_k$ $(k = 1, \ldots, n)$, each with a constant length $\mid \mathbf{r}_k \mid = b$, but with a random orientation. The end-to-end distance

$$\mathbf{R}(n) = \sum_{k=1}^{n} \mathbf{r}_k, \tag{3.1}$$

being the sum of uncorrelated random variables $\mathbf{r}_k$, is a Markov process. We now consider a model with persistence in which the k th segment $\mathbf{r}_k$ $(k = 2, \ldots, n)$ has the same direction as the segment $\mathbf{r}_{k-1}$ with probability p, and has a random orientation otherwise (probability $1 - p$). In this case, $\mathbf{r}_k$ itself is a Markov process and therefore $\mathbf{R}(n)$ alone is no longer Markovian. This complication can be dealt with by considering the pair of variables $(\mathbf{R}(n), \mathbf{r}_n)$ which again defines a Markov process.

In the free flight model, subsequent segments are uncorrelated, and the correlation length is therefore equal to b. In the model with persistence, the correlation length is defined as

$$a = \frac{b}{1-p} = n_c b \tag{3.2}$$

The free flight model corresponds to the particular case $p = 0$. For a polymer length much larger than a, we expect the end-to-end distance to be close to Gaussian. We will study this approach to the Gaussian regime on the basis of exact results for $< R^2(n) >$, $< R^4(n) >$ and $< R^6(n) >$.

In section 3.1, we present the analytic result for the fourier transform of the Green's function $G(\mathbf{R}, z)$ for a random walk with persistence

$$F(\mathbf{k}, z) = \int d\mathbf{R}\; e^{i\mathbf{k}.\mathbf{R}} G(\mathbf{R}, z), \tag{3.3}$$

with

$$G(\mathbf{R}, z) = \sum_{n=0}^{\infty} z^n P(\mathbf{R}, n), \tag{3.4}$$

the Laplace transform of the probability distribution for the end-to-end distance. From this result, we will derive in section 3.2 the expressions for the moments of the end-to-end distance $< R^2(n) >$, $< R^4(n) >$ and $< R^6(n) >$ and study their convergence to the Gaussian limit. In section 3.3, we discuss the continuum limit of the random walk with persistence.

3.1 Random walk with persistence

Both for the sake of generality and for conceptual simplicity, we will consider, instead of a continuum of possible orientation $\Omega(\theta, \phi)$ of the segments $\mathbf{r}_k$, a finite number of orientations Ω_j, $j = 1, \ldots, N$, in a general space. For example, Ω_j may correspond to a number of allowed polar angles in a two-dimensional space, or it may refer to the orientation of a vector in a many-

dimensional space. A continuum of orientations, such as appropriate for the polymer problem in three dimensions, will be obtained by taking a suitable limit.

At each step, an orientation is chosen. With a probability p, it is equal to the previous orientation, while it is any of the $N-1$ remaining orientations with probability $(1-p)/(N-1)$. Associated to each orientation we have a segment vector $\mathbf{b}_j$. The quantity of interest is the probability density for the end-to-end distance $\mathbf{R}$ as a function of the number of segments n. As discussed in the introduction, $\mathbf{R}(n)$ is not a Markov process, but a Markov process is obtained by including in the description the orientation j of the last segment. The probability density $P(\mathbf{R}, j, n)$ to arrive at an end-to-end vector $\mathbf{R}$ after n segments, with j being the orientation of the last segment, obeys the following Master Equation :

$$P(\mathbf{R}, j, n) = pP(\mathbf{R} - \mathbf{b}_j, j, n-1) + \sum_{j' \neq j} \frac{1-p}{N-1} P(\mathbf{R} - \mathbf{b}_j, j', n-1). \quad (3.5)$$

We will suppose that for the first segment all orientations are equally likely

$$P(\mathbf{R}, j, 0) = N^{-1}\delta(\mathbf{R}). \quad (3.6)$$

The exact solution of Eq. (3.5) can easily be obtained by Fourier-"Laplace" inversion. For the transform of the end-to-end probability density $P(\mathbf{R}, n)$:

$$F(\mathbf{k}, z) = \sum_{n=0}^{\infty} z^n \int d\mathbf{R}\; e^{i\mathbf{k}.\mathbf{R}} P(\mathbf{R}, n) \quad (3.7)$$

with

$$P(\mathbf{R}, n) = \sum_{j=1}^{N} P(\mathbf{R}, j, n), \quad (3.8)$$

we find from Eq. (3.5) :

$$F(\mathbf{k},z)=\frac{(\frac{1}{N}-\frac{1-p}{N-1})\sum(\mathbf{k},z)}{1-\frac{1-p}{N-1}\sum(\mathbf{k},z)} \tag{3.9}$$

with

$$\sum(\mathbf{k},z)=\sum_{j=1}^{N}[1-(p-\frac{1-p}{N-1})z\ e^{i\mathbf{k}.\mathbf{b}_j}]^{-1}. \tag{3.10}$$

Even though the inverse transformation leading to $P(\mathbf{R},n)$ cannot be performed, this result allows one to investigate various limits and particular cases.

Let us now apply Eq. (3.9) to the problem of a polymer chain in three dimensions. In order to obtain a continuum of possible orientations Ω for the segments, we have to take the limit where N goes to infinity. This leads to the following correspondences :

$$\begin{aligned} N &\longleftrightarrow N\to\infty \\ j &\longleftrightarrow \Omega=(\theta,\phi) \\ \mathbf{b}_j &\longleftrightarrow \mathbf{b}(\Omega)=(b\sin\theta\cos\phi, b\sin\theta\sin\phi,\cos\theta) \\ \frac{1}{N}\sum_{j=1}^{N} &\longleftrightarrow \frac{1}{4\pi}\int_0^{2\pi}d\phi\int_0^{\pi}d\theta\sin\theta. \end{aligned} \tag{3.11}$$

Applying this limit procedure, we obtain from Eqs. (3.9) and (3.10) :

$$F(\mathbf{k},z)=\frac{pkb+2p\mathrm{Arctan}[\frac{1+pz}{1-pz}\tan(\frac{kb}{2})]}{(p+1)kb+2(p-1)\mathrm{Arctan}[\frac{1+pz}{1-pz}\tan(\frac{kb}{2})]}. \tag{3.12}$$

Note that $F(\mathbf{k},z)$ is a function of $k=\mid\mathbf{k}\mid$, as was to be expected on the basis of spatial isotropy. Since the dependence of $F(\mathbf{k},z)$ on the variables k and z is still rather complicated, the inversion of the Fourier-Laplace transform

does not seem to be obvious. However, we can derive from Eq. (3.12) the expression for the moments of the end-to-end distance, as we will see in the next section.

3.2 Moments of the end-to-end distance

By expanding $F(\mathbf{k}, z)$ about $\mathbf{k} = 0$, we find

$$F(\mathbf{k}, z) = \sum_{\ell=0}^{\infty} A_{2\ell}(z) k^{2\ell} \tag{3.13}$$

and, by comparison with Eq. (3.7)

$$A_{2\ell}(z) = \frac{-1^{\ell}}{(2\ell+1)!} \sum_{n=0}^{\infty} z^n < R^{2\ell}(n) > . \tag{3.14}$$

Hence such an expansion allows one to obtain explicit results for the moments of the end-to-end distance.
This procedure quickly becomes tedious as ℓ increases, but can be handled by a symbolic manipulator. We obtain (see appendix 7.B)

$$< R^2(n) > = b^2 \left[n \frac{1+p}{1-p} - 2pb^2 \frac{1-p^n}{(1-p)^2} \right] \tag{3.15}$$

$$\begin{aligned} < R^4(n) > = b^4 \Bigg[& \frac{5}{3} n^2 \frac{(1+p)^2}{(1-p)^2} + \frac{16}{3} n^2 \frac{p^{n+1}}{(1-p)^2} + 4np^{n+1} \frac{(1+p)}{(1-p)^3} \\ & + \frac{8}{3} p \frac{(1-p^n)}{(1-p)^4} (p^2+p+1) - \frac{2}{3} n \frac{(1+p)}{(1-p)^3} (p^2+10p+1) \Bigg] \end{aligned} \tag{3.16}$$

$$
\begin{aligned}
< R^6(n) > \;=\; b^6 \Bigg[& \frac{88}{9} n^4 \frac{p^{n+1}}{(1-p)^2} + \frac{35}{9} n^3 \frac{(1+p)^3}{(1-p)^3} + \frac{128}{9} n^3 p^{n+1} \frac{(1+p)}{(1-p)^3} \\
& - \frac{2}{9} n^2 \frac{p^{n+1}}{(1-p)^4} (35p^2 - 58p + 35) - \frac{14}{3} n^2 \frac{(1+p)^2}{(1-p)^4} (p^2 + 5p + 1) \\
& - \frac{4}{9} n p^{n+1} \frac{(1+p)}{(1-p)^5} (29p^2 + 62p + 29) \qquad (3.17) \\
& + \frac{4}{9} n \frac{(1+p)}{(1-p)^5} (4p^4 + 63p^3 + 46p^2 + 63p + 4) \\
& - \frac{32}{3} p \frac{(1-p^n)}{(1-p)^6} (p^4 + p^3 + p^2 + p + 1) \Bigg] .
\end{aligned}
$$

The result Eq. (3.15) is in agreement with the general result for the second moment of the end-to-end distance of a random walk with "first order correlation" (see [45]). Approximate results for $< R^4(n) >$ and $< R^6(n) >$ have been obtained by computer simulation in reference [46]. All the results in tabel II of this paper agree within the simulation error with the analytic results Eqs. (3.16) and (3.17)[1].

In the limit $p \to 0$, the results Eqs. (3.15) - (3.17) reduce to those for the free flight model [43,44] :

$$< R^2(n) >_{FF} \;=\; nb^2 \qquad (3.18)$$

$$< R^4(n) >_{FF} \;=\; [\frac{5}{3} n(n-1) + n] b^4 \qquad (3.19)$$

$$< R^6(n) >_{FF} \;=\; [\frac{35}{9} n(n-1)(n-2) + 7n(n-1) + n] b^6 . \qquad (3.20)$$

On the other hand, for large n, or more precisely for n much larger than n_c (cf. Eq. (3.2)), $\mathbf{R}$ converges to a Gaussian random variable with the following

[1] There seems to be something systematically wrong with the results of table I in [46].

relations between the moments :

$$< R^4(n) >_G = \frac{5}{3} < R^2(n) >_G^2 \tag{3.21}$$

$$< R^6(n) >_G = \frac{35}{9} < R^2(n) >_G^3 \tag{3.22}$$

In order to investigate the convergence to the Gaussian limit, we have plotted the ratio's $< R^4 > /(5/3 < R^2 >^2)$ and $< R^6 > /(35/9 < R^2 >^3)$ as a function of $\frac{n}{n_c} = \frac{L}{a}$ for several values of p in Figs 3.1 and 3.2 ($L = nb$).

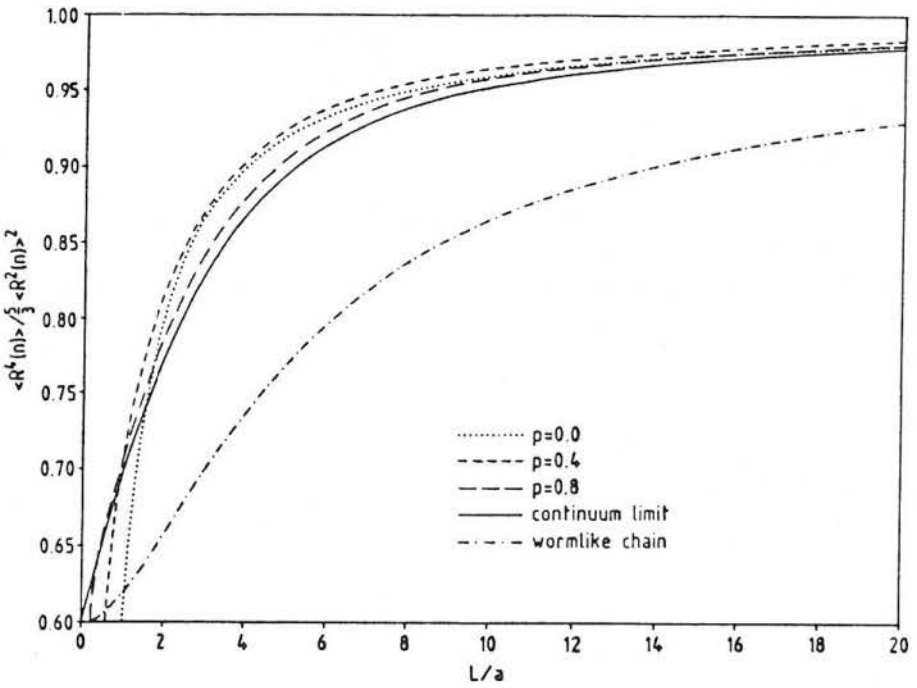

Figure 3.1: Convergence of the fourth moment of the end-to-end distance to the Gaussian limit, as a function of L/a.

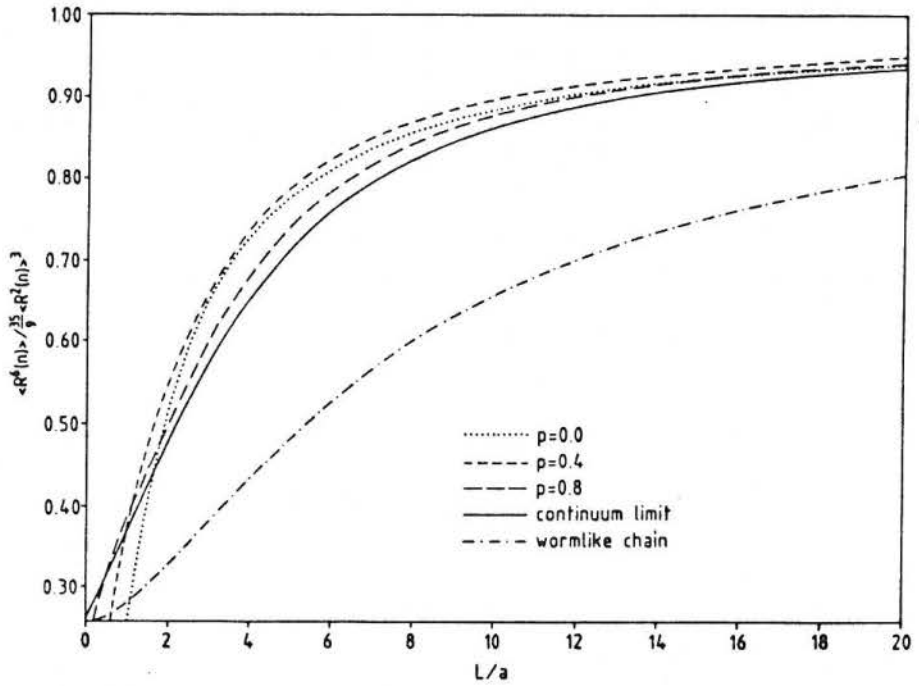

Figure 3.2: Convergence of the sixth moment of the end-to-end distance to the Gaussian limit, as a function of L/a.

Another quantity of interest in polymer statistics, which arises when evaluating hydrodynamic interactions between the polymer heads, is the average $< R^{-1}(n) >$. In the Gaussian limit, one has :

$$< \frac{1}{R(n)} >_G = \sqrt{\frac{6}{\pi < R^2(n) >}}. \tag{3.23}$$

To calculate corrections to this limit, one can expand the probability $P(\mathbf{R}, n)$ in a series of Hermite polynomials as follows ($\mu^2 = \frac{3R^2}{< R^2 >}$)

$$\begin{aligned} P(\mathbf{R}, n) &= \left[\frac{3}{2\pi < R^2 >}\right]^{3/2} e^{-\frac{\mu^2}{2}} \left[1 + \frac{1}{3!}(< \mu^2 > -3)\frac{H_3(\mu)}{\mu}\right. \\ &+ \left. \frac{1}{5!}(< \mu^4 > -10 < \mu^2 > +15)\frac{H_5(\mu)}{\mu} + \frac{1}{7!}(< \mu^6 > -21 < \mu^4 >\right. \end{aligned}$$

$$+ \quad 105 < \mu^2 > -105)\frac{H_7(\mu)}{\mu} + \ldots \Big] . \tag{3.24}$$

To evaluate the coefficients of H_3, H_5 and H_7, the expressions Eqs. (3.15) - (3.17) can be used. A typical probability profile is plotted in Fig. 3.3.

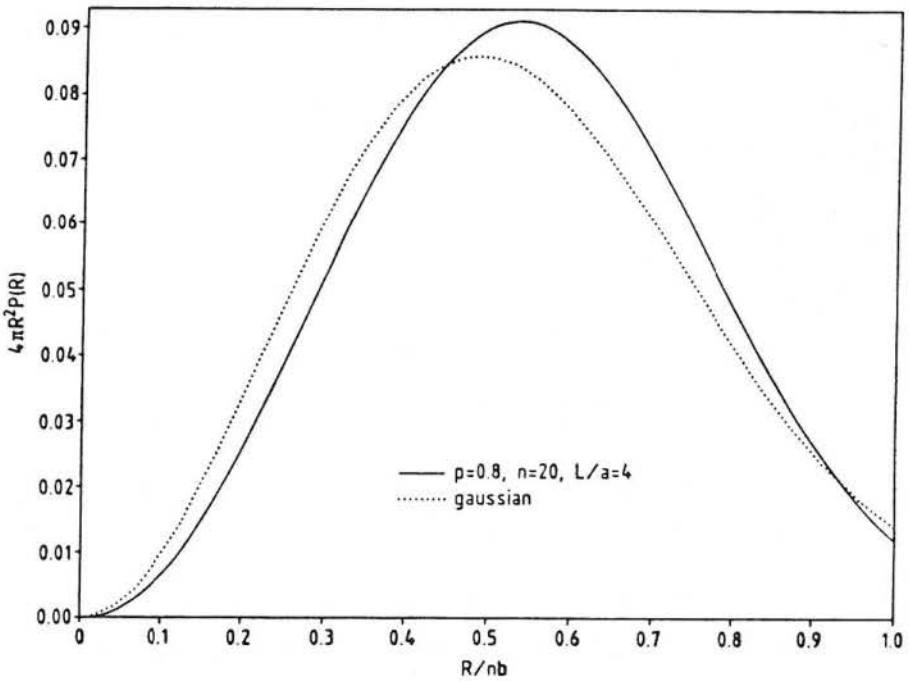

Figure 3.3: Radial probability distribution, obtained by the expansion in Hermite polynomials, as a function of R/nb.

The corresponding expansion for $< R^{-1}(n) >$ reads [43]

$$< \frac{1}{R(n)} >= \sqrt{\frac{6}{\pi < R^2 >}} \left[\frac{63}{80} \frac{< R^4 >}{< R^2 >^2} - \frac{9}{112} \frac{< R^6 >}{< R^2 >^3} \right] . \tag{3.25}$$

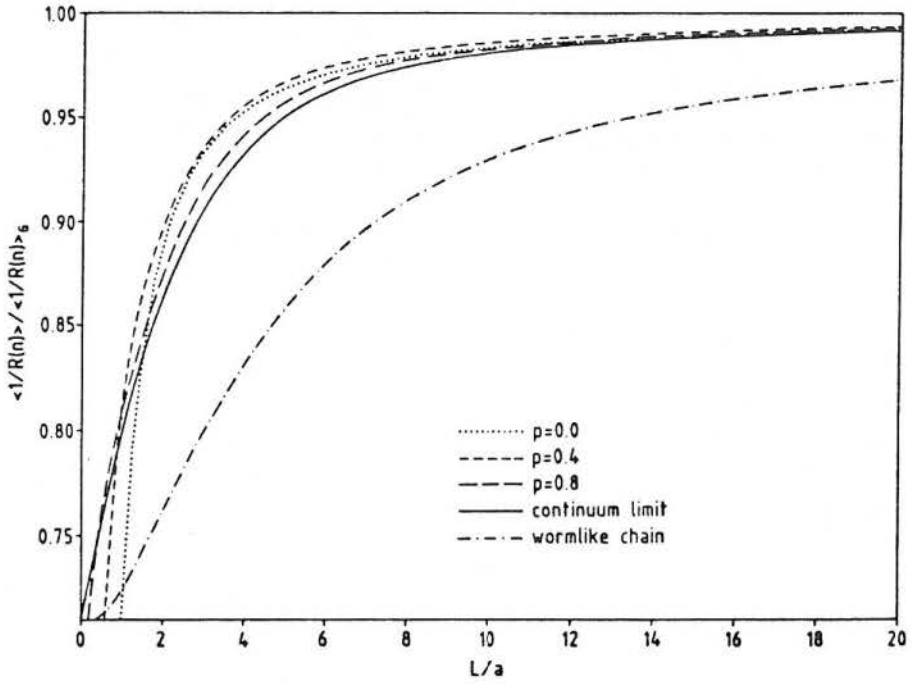

Figure 3.4: Convergence of the average inverse end-to-end distance to the Gaussian limit, as a function of L/a.

This result is plotted in Fig. 3.4 for different values of p. The agreement with the numerical results of reference [46] is, as could be expected, not so good, because the series expansion of the probability density $P(\mathbf{R}, n)$ in Hermite polynomials does not converge rapidly enough.

3.3 The continuum limit

A polymer model in polymer statistics, for which analytic results can be obtained, is the so-called worm-like chain. It can be looked upon as the continuum limit of the free rotation model in which the bond angle θ_0 is converging to 180^o while, at the same time, the length b of each segment is going to zero and the number of segments to infinity, with both $nb = L$ and $b/(1 + \cos\theta_0)$ kept constant. An analogous limit can be formulated for the

persistent random walk model :

$$\begin{array}{lll} n \to \infty & & nb = L \\ p \to 1 & \text{with} & \dfrac{b}{1-p} = a \\ b \to 0 & & \end{array} \qquad \text{constant.} \tag{3.26}$$

The evolution equation for the probability density $P(\mathbf{R}, i, L)$ becomes

$$\frac{\partial}{\partial L} P(\mathbf{R}, j, L) = \frac{1}{a(N-1)} \sum_{j' \neq j} P(\mathbf{R}, j', L) - \frac{1}{a} P(\mathbf{R}, j, L)$$

$$-\mathbf{u}_j \cdot \frac{\partial}{\partial \mathbf{R}} P(\mathbf{R}, j, L) \tag{3.27}$$

with

$$\mathbf{u}_j = \lim_{b \to 0} \frac{\mathbf{b}_j}{b}. \tag{3.28}$$

This equation can be solved by Fourier-Laplace transformation. Introducing

$$F(\mathbf{k}, s) = \int_0^\infty dL e^{-sL} \int d\mathbf{R}\ e^{i\mathbf{k}.\mathbf{R}} P(\mathbf{R}, L) \tag{3.29}$$

with

$$P(\mathbf{R}, L) = \sum_{j=1}^{N} P(\mathbf{R}, j, L), \tag{3.30}$$

one finds for the Laplace transform of the Green's function

$$F(\mathbf{k}, s) = \frac{a \text{Arctan} \dfrac{ak}{1+as}}{ak - \text{Arctan} \dfrac{ak}{1+as}}. \tag{3.31}$$

This result can also be obtained from Eq. (3.12). The moments of the end-to-end distance read

$$< R^2(L) > = 2a^2 \left[\frac{L}{a} - 1 + e^{-\frac{L}{a}} \right] \tag{3.32}$$

$$< R^4(L) > = 4a^4 \left[\frac{5}{3} \left(\frac{L}{a} \right)^2 - 4\frac{L}{a} + 2 + \left[\frac{4}{3} \left(\frac{L}{a} \right)^2 + 2\frac{L}{a} - 2 \right] e^{-\frac{L}{a}} \right] \tag{3.33}$$

$$< R^6(L) > = 8a^6 \left[\frac{35}{9} \left(\frac{L}{a} \right)^3 - \frac{147}{9} \left(\frac{L}{a} \right)^2 + 20\frac{L}{a} - \frac{20}{3} + \left[\frac{11}{9} \left(\frac{L}{a} \right)^4 + \frac{32}{9} \left(\frac{L}{a} \right)^3 - \frac{1}{3} \left(\frac{L}{a} \right)^2 - \frac{40}{3}\frac{L}{a} + \frac{30}{3} \right] e^{-\frac{L}{a}} \right]. \tag{3.34}$$

The ratio's $< R^4 > /(5/3 < R^2 >^2)$, $< R^6 > /(35/9 < R^2 >^3)$ and $< \frac{1}{R} > / < \frac{1}{R} >_G$ for the present continuum model have also been included in Figs 3.1, 3.2 and 3.4, as well as the corresponding results for the worm-like chain.

3.4 Conclusion

In this chapter, we have shown that random walk with persistence can, to a certain extend, be treated analytically by calculating the Fourier transform of the Green's function. Although the inverse Fourier-Laplace transform of the end-to-end distribution can not be performed, it is still possible to obtain the moments by expansion around $k = 0$. Apart from its intrinsic interest, the model can thus be used to test the validity of approximation schemes or to check numerical calculations. From Figs. 3.1, 3.2 and 3.4, it follows that the approach to the Gaussian form is rather insensitive to the value of p, provided that the length $L = nb$ of the polymer is expressed in terms of the correlation length a. Finally, we note that the present model differs strikingly from the worm-like chain.

Chapter 4

Orientational relaxation in the reptation model

In order to describe the dynamical behaviour of entangled polymers, de Gennes [47] and Edwards [48] introduced the so-called reptation model. In this model, the confinement of a given polymer by its surrounding neighbours is taken into account by supposing that the polymer can only glide along its own axis. Several quantities of experimental interest were calculated for this model, as e.g. exemplified by the Doi-Edwards papers [49]. In most of these calculations, a limit is taken in which the polymer is represented as a continuous chain. This is a good approximation since most polymers consist of a very large number of segments. On the other hand, the range of validity of the reptation model can also be studied in computer experiments (see e.g. [50,51]). In this case, the number of segments is usually small, and a comparison with theoretical results for the discrete chain rather than for the continuous chain would be preferable.

A given configuration of the polymer chain is characterized by the set of orientations $\alpha = \{\alpha_j | j = 1, \ldots, M\}$ of its M segments (see Fig. 4.1).

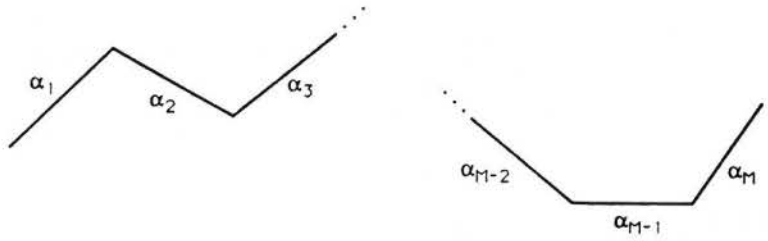

Figure 4.1: A configuration of a polymer chain is characterized by the set of orientations α_j.

The configuration, and hence the orientational ordering, changes due to the reptation process. The chain moves one segment step either forward or backward in such a way that each segment takes the orientation of the one it replaces (i.e. the orientation of segment i becomes that of segment $i+1$, if the chain moves in that direction), while the orientation of the top segment is chosen from the equilibrium distribution.

The question at hand is how fast a given segment of the polymer chain loses the memory of its initial orientation, i.e. how fast it relaxes to the equilibrium form. It is of interest to obtain the dependence of this relaxation on the position of the segment inside the chain, and on the chain length. We will derive the analytic result for the (Laplace transformed) probability density that a segment i has a given orientation at time t, for a general initial configuration of all the segments (Eq. (4.18)). This result includes other results from the literature as particular cases.

Orientational relaxation can be experimentally studied by e.g. fluorescence polarization spectroscopy [52]- [54]. In these experiments, one (or more) segment of the polymer is a fluorescent probe which can be excited by an incoming light beam with the right polarization. The excited state has a finite lifetime and the probe will eventually de-excite with the emission of a polarized photon. If the emission and absorption dipoles coincide, the randomnisation of the polarization of the emitted photon relative to the incident one, essentially reflects the orientational relaxation that has taken place meanwhile. As a result of the destructive interference between photons emitted by different probes, the intensity of the emitted light will decrease. In experiments con-

ducted under continuous illumination, one measures the so-called stationary anisotropy defined by

$$r_s = \frac{I_{\parallel} - I_{\perp}}{I_{\parallel} + 2I_{\perp}}. \tag{4.1}$$

Here $I_{\parallel}$ and $I_{\perp}$ are the emitted intensities with a polarization respectively parallel and perpendicular to that of the incoming beam. The latter will be chosen along the z axis, which in this case is also the symmetry axis of the sample. r_s can be expressed in terms of stochastic properties of the azimuthal angle θ of the probe as follows [55] (we choose absorption and emission dipoles along the axis of the probe) :

$$r_s = \frac{\int_0^{\infty} \frac{2}{\tau} e^{-t/\tau} \ll P_2(\cos\theta_0) P_2(\cos\theta_t) \gg dt}{1 + 2 < P_2(\cos\theta_0) >} + \frac{< P_2(\cos\theta_0) >}{1 + 2 < P_2(\cos\theta_0) >} \tag{4.2}$$

with τ the average lifetime (time before de-excitation) of the probe. The single brackets refer to an average over the azimuthal angle θ_0 with the steady state probability profile, while the double brackets indicate that the additional dynamical average has to be performed with the conditional probability $P(\theta_t, t \mid \theta_0, t = 0)$ to go from the value θ_0 at time $t = 0$ to the value θ_t at time t. The evaluation of this last quantity is the hardest part. Fortunately however, the stationary anisotropy is expressed in terms of the Laplace transform of $P(\theta_t, t \mid \theta_0, t = 0)$, for which we have been able to obtain the analytic result (cf. Eq. (4.41)).

Finally, there has been recent experimental and theoretical interest for orientational relaxation in anisotropic systems (see e.g. [56,57]). In this case, a nonisotropic equilibrium distribution prevails, being induced for instance by stretching, compression or the application of an electric field. We include this possibility by carrying out all the calculations for the case of a general orientational equilibrium distribution P^{eq} which need not be isotropic. This allows to identify explicitly the dependence of, for instance, the stationary anisotropy r_s on the equilibrium averages of the second and fourth Legendre polynomials.

The organization of this chapter is as follows. In section 4.1 we introduce

the equations describing orientational relaxation in the reptation model and show how they can be solved thanks to the knowledge of the Green's function for a random walk on a finite lattice. In section 4.2, these results are applied to the calculation of the stationary anisotropy as a function of the number M of segments of the polymer, the position $j \in \{1, 2, \ldots M\}$ of the probe in the polymer chain for a general form of the equilibrium orientational distribution function P^{eq}.

4.1 Orientational relaxation in the reptation model

A given configuration of the polymer chain is characterized by the set of orientations $\boldsymbol{\alpha} = \{\alpha_j \mid j = 1, \ldots, M\}$ (see Fig. 4.1). Each of these orientations can either be taken from a set of discrete values (for example in lattice models for which only a finite number of orientations are allowed) or from a continuum of values.

As explained in the introduction, the chain moves one segment step either forward or backward, each with a probability kdt during a small time interval dt, in such a way that each segment takes the orientation of the one it replaces. The orientation of the end segments is chosen from the equilibrium distribution P^{eq}. The probability that the configuration remains unchanged during the time interval dt is equal to $(1 - 2kdt)$. The time evolution of the probability distribution $P(\boldsymbol{\alpha}, t)$ is governed by the following Master equation $(\boldsymbol{\alpha} = \{\alpha_1, \ldots, \alpha_M\})$:

$$\begin{aligned} \partial_t P(\boldsymbol{\alpha}, t) &= kP^{eq}(\alpha_M) \sum_{\alpha'} P(\{\alpha', \alpha_1, \ldots, \alpha_{M-1}\}, t) \\ &+ kP^{eq}(\alpha_1) \sum_{\alpha'} P(\{\alpha_2, \ldots, \alpha_M, \alpha'\}, t) - 2kP(\boldsymbol{\alpha}, t). \end{aligned} \quad (4.3)$$

To study orientational relaxation, it will be sufficient to calculate the reduced

probability $P_j(\alpha_j, t)$

$$P_j(\alpha_j, t) = \sum_{\alpha_1} \cdots \sum_{\alpha_{j-1}} \sum_{\alpha_{j+1}} \cdots \sum_{\alpha_M} P(\alpha, t). \tag{4.4}$$

In the following, we will drop the subscript j in the orientation variable α_j. By summation of Eq. (4.3) over the orientations of all the segments but one, we find

$$\partial_t P_j(\alpha, t) = kP_{j-1}(\alpha, t) - 2kP_j(\alpha, t) + kP_{j+1}(\alpha, t) \tag{4.5}$$

for $1 < j < M$, and :

$$\partial_t P_1(\alpha, t) = -2kP_1(\alpha, t) + kP_2(\alpha, t) + kP^{eq}(\alpha) \tag{4.6}$$

$$\partial_t P_M(\alpha, t) = kP_{M-1}(\alpha, t) - 2kP_M(\alpha, t) + kP^{eq}(\alpha) \tag{4.7}$$

for the end segments.
We now consider the Laplace transform

$$\widetilde{P}_j(\alpha, s) = \int_0^\infty e^{-st} P_j(\alpha, t) dt. \tag{4.8}$$

Furthermore, we introduce the following vector notation :

$$\widetilde{\mathbf{P}}(\alpha, \mathbf{s}) = \begin{pmatrix} \widetilde{P}_1(\alpha, s) \\ \vdots \\ \widetilde{P}_M(\alpha, s) \end{pmatrix} \tag{4.9}$$

$$\mathbf{S}(\alpha) = \begin{pmatrix} \frac{k}{s}P^{eq}(\alpha) \\ 0 \\ \vdots \\ 0 \\ \frac{k}{s}P^{eq}(\alpha) \end{pmatrix} \tag{4.10}$$

$$\mathbf{T} = \begin{pmatrix} -2k & k & 0 & \dots & & & 0 \\ k & -2k & k & 0 & & \dots & \vdots \\ 0 & & & \ddots & & & 0 \\ & & & & k & -2k & k \\ 0 & \dots & & & 0 & k & -2k \end{pmatrix}. \tag{4.11}$$

Eqs. (4.5)–(4.7) can now be rewritten as

$$s\widetilde{\mathbf{P}}(\alpha, s) - \widetilde{\mathbf{P}}(\alpha, t=0) = \mathbf{T}\ \widetilde{\mathbf{P}}(\alpha, s) + \mathbf{S}(\alpha). \tag{4.12}$$

We conclude that :

$$\widetilde{\mathbf{P}}(\alpha, s) = \frac{1}{s\mathbf{1} - \mathbf{T}}\ [\mathbf{S}(\alpha) + \mathbf{P}(\alpha, t=0)]. \tag{4.13}$$

The matrix $\mathbf{T}$ is identical to the transition matrix for a symmetric nearest neighbour random walk with constant transition rates k and with absorbing boundary conditions (at $j = 0$ and $j = M + 1$). Hence the calculation of the (Laplace transformed) probability density that the segment i has orientation α is reduced to the calculation of the Green's function $(s\mathbf{1} - \mathbf{T})^{-1}$ (see section 2.1.2). We thus obtain :

$$\widetilde{P}_i(\alpha, s) \;=\; P^{eq}(\alpha)\frac{\cosh\left[\frac{\xi}{2}(M + 1 - 2i)\right]}{s\cosh\left[\frac{\xi}{2}(m+1)\right]} \tag{4.14}$$

$$+\sum_{j=1}^{M} P_j(\alpha, t=0)\frac{\sinh\left[\xi \min(i,j)\right]\sinh\left[\xi\,(M+1-\max(i,j))\right]}{k\sinh\xi\sinh\left[\xi(M+1)\right]}$$

with

$$\cosh\xi = 1 + \frac{s}{2k}. \tag{4.15}$$

This result describes how the orientation of the segment i evolves in time, given an initial configuration $P_j(\alpha, t=0)$ for every segment $j = 1, \ldots, M$. Note that the equilibrium distribution appears in a simple way as the coefficient of the second term in the r.h.s. of Eq. (4.14). Furthermore, we see that correlations do not enter at this level. A convenient check of the calculation so far is provided by the verification of the short and long time limits.
For $s \to \infty$ (the short time limit) we find

$$\tilde{P}_i(\alpha, s) \underset{s\to\infty}{\sim} \frac{1}{s} P_i(\alpha, t=0), \tag{4.16}$$

and for $s \to 0$ (the long time limit)

$$\tilde{P}_i(\alpha, s) \underset{s\to 0}{\sim} \frac{1}{s} P^{eq}(\alpha). \tag{4.17}$$

These are obviously the correct results.

For orientational relaxation in three dimensions, α is a solid angle characterized by the angles (θ, ϕ). For simplicity, we will assume from now on that P^{eq} is a function of θ only, i.e. $P^{eq} = P^{eq}(\theta)$. Eq. (4.14) thus reduces to

$$\widetilde{P}_i(\theta,s) = P^{eq}(\theta)\frac{\cosh\left[\frac{\xi}{2}(M+1-2i)\right]}{s\cosh\left[\frac{\xi}{2}(M+1)\right]} \tag{4.18}$$

$$+\sum_{j=1}^{M} P_j(\theta,t=0)\frac{\sinh\left[\xi\min(i,j)\right]\sinh\left[\xi\left(M+1-\max(i,j)\right)\right]}{k\sinh\xi\sinh\left[\xi(M+1)\right]}.$$

This exact result will be used in the next section to calculate the stationary anisotropy and related measures of orientational relaxation.

Before proceeding, we note the following interesting property. For equilibrium orientation of all the segments at time $t = 0$, $P_j(\theta,t=0) \equiv P^{eq}(\theta)$, it is clear that the probability distribution of the i th segment at time t will also be of the equilibrium form, i.e. $\widetilde{P}_i(\theta,s) = P^{eq}(\theta)/s$. This implies the following summation property

$$\sum_{j=1}^{M}\frac{\sinh\left[\xi\min(i,j)\right]\sinh\left[\xi\left(M+1-\max(i,j)\right)\right]}{k\sinh\xi\sinh\left[\xi(M+1)\right]}$$

$$=\frac{\cosh\left[\frac{\xi}{2}(M+1)\right]-\cosh\left[\frac{\xi}{2}(M+1-2i)\right]}{s\cosh\left[\frac{\xi}{2}(M+1)\right]}, \tag{4.19}$$

as can also be verified by performing explicitly the sum in the l.h.s.

The dependence of Eq. (4.18) on the Laplace variable s is rather complicated, but the inverse Laplace transformation can be performed provided we consider the continuum limit where (a is the length of the chain segments)

$$\begin{aligned} M &\to \infty \\ a &\to 0 \\ k &\to \infty \end{aligned} \tag{4.20}$$

with

$$L = Ma \tag{4.21}$$

the length of the chain and

$$D = a^2 k \tag{4.22}$$

the diffusion coefficient both kept constant. In this limit Eq. (4.18) becomes

$$\widetilde{P}_x(\theta, s) = \int_0^L \frac{\sinh\left[\sqrt{\frac{s}{D}}\min(x,y)\right]}{\sqrt{sD}\sinh\left[\sqrt{\frac{s}{D}}L\right]} \sinh\left[\sqrt{\frac{s}{D}}(L - \max(x,y))\right]$$

$$\times P_y(\theta, t=0)dy + \frac{\cosh\left[\sqrt{\frac{s}{D}}(\frac{L}{2} - x)\right]}{s\cosh\left[\sqrt{\frac{s}{D}}\frac{L}{2}\right]} P^{eq}(\theta). \tag{4.23}$$

Using the identities [58]

$$\frac{\cosh[b(\pi - \omega)]}{\sinh[b\pi]} = \frac{1}{\pi\omega} + \frac{2b}{\pi}\sum_{q=1}^{\infty}\frac{\cos(q\omega)}{q^2 + b^2} \tag{4.24}$$

and

$$\frac{\cosh[b(\frac{\pi}{2} - \omega)]}{\cosh[b\frac{\pi}{2}]} = \frac{4}{\pi}\sum_{q\ odd}\frac{q\sin(q\omega)}{q^2 + b^2}, \tag{4.25}$$

the two terms on the left hand side of Eq. (4.23) can be expanded into infinite

sums. This leads to :

$$\tilde{P}_x(\theta,s) = \sum_{q=1}^{\infty} \sin(\frac{\pi q x}{L}) \frac{1}{(\frac{q^2}{\tau_c}+s)} \frac{2}{L} \int_0^L \sin(\frac{\pi q y}{L}) P_y(\theta,t=0) dy$$

$$+ P^{eq}(\theta) \sum_{q\ odd} \frac{4}{\pi} \frac{q}{s(\frac{q^2}{\tau_c}+s)} \sin(\frac{\pi x q}{L}) \qquad (4.26)$$

with

$$\tau_c = \frac{L^2}{\pi^2 D}. \qquad (4.27)$$

In this way, the dependence of the probability distribution (4.26) on the Laplace variable s has become very simple and Laplace inversion is easy to perform :

$$P_x(\theta,t) = \sum_{q=1}^{\infty} \sin(\frac{\pi q x}{L}) \frac{2}{L} \int_0^L \sin(\frac{\pi q y}{L}) P_y(\theta,t=0) dy \ e^{-\frac{tq^2}{\tau_c}}$$

$$+P^{eq}(\theta) \sum_{q\ odd} \frac{4}{q\pi} \sin(\frac{\pi x q}{L}) \left(1 - e^{-\frac{tq^2}{\tau_c}}\right). \qquad (4.28)$$

This expression can be further simplified if we take the initial condition $P_y(\theta,t=0)$ identical for all the segments, i.e. independent of y,

$$P_y(\theta,t=0) = P(\theta,t=0). \qquad (4.29)$$

Combining Eqs. (4.28) and (4.29) and integrating over y, we get

$$P_x(\theta,t) = P(\theta,t=0)\sum_{q\ odd}\frac{4}{\pi q}\sin(\frac{\pi x q}{L})e^{-\frac{tq^2}{\tau_c}}$$

$$+P^{eq}(\theta)\sum_{q\ odd}\frac{4}{\pi q}\sin(\frac{\pi x q}{L})\left(1-e^{-\frac{tq^2}{\tau_c}}\right). \qquad (4.30)$$

For the isotropic case ($P^{eq}(\theta)=\frac{\sin\theta}{2}$), this result is in agreement with the one obtained by Doi & Edwards [49] and Curtiss & Bird [59].

4.2 Time dependent order parameters and stationary anisotropy

A classical measure of orientational order is provided by the average of the second Legendre polynomial $< P_2(\cos\theta) >= \frac{1}{2}(3 < \cos^2\theta > -1)$. It can vary from zero, in the case of random orientations, to one, for complete alignment. The result (4.18) allows us to calculate the time dependence of this quantity for every segment i, in terms of its Laplace transform :

$$< \tilde{P}_2(\cos\theta_i,s) >= \int_0^\pi d\theta P_2(\cos\theta)\tilde{P}_i(\theta,s)$$

$$=\sum_{j=1}^{M}\frac{\sinh\left[\xi\min(i,j)\right]\sinh\left[\xi\left(M+1-\max(i,j)\right)\right]}{k\sinh\xi\sinh\left[\xi(M+1)\right]} < P_2(\cos\theta_j,t=0) >$$

$$+\frac{\cosh\left[\frac{\xi}{2}(M+1-2i)\right]}{s\cosh\left[\frac{\xi}{2}(M+1)\right]} < P_2(\cos\theta) >^{eq} . \qquad (4.31)$$

Let us now consider Eq. (4.31) for some special initial conditions. If we start from the steady state distribution

$$P_i(\theta, t=0) = P^{eq}(\theta), \tag{4.32}$$

we get, as should be expected, that $< P_2 >$ is independent of time (cf. Eq. (4.19)) :

$$< P_2(\cos\theta_i, t) >=< P_2(\cos\theta) >^{eq} . \tag{4.33}$$

For an initial state with all the segments aligned along a preferential direction $\theta = 0$, one finds (using again Eq. (4.19))

$$< \widetilde{P}_2(\cos\theta_i, s) >= \frac{1}{s} + \frac{\cosh\left[\frac{\xi}{2}(M+1-2i)\right]}{s\cosh\left[\frac{\xi}{2}(M+1)\right]} [< P_2(\cos\theta) >^{eq} -1], \tag{4.34}$$

while for random initial orientations of all segments, one has

$$< \widetilde{P}_2(\cos\theta_i, s) >=< P_2(\cos\theta) >^{eq} \frac{\cosh\left[\frac{\xi}{2}(M+1-2i)\right]}{s\cosh\left[\frac{\xi}{2}(M+1)\right]}. \tag{4.35}$$

The dependence on the Laplace variable s is still complicated, but again we can invert the transformation if we take the appropriate continuum limit. Following the same procedure as before (cf. Eqs. (4.20) - (4.25)), or alternatively, using Eq. (4.28) to calculate the average $< P_2(\cos\theta_x, t) >$, we get

$$< P_2(\cos\theta_x, t) > = \sum_{q=1}^{\infty} \sin(\frac{\pi x q}{L})\ e^{-\frac{tq^2}{\tau_c}}$$

$$\frac{2}{L}\int_0^L \sin(\frac{q\pi y}{L}) < P_2(\cos\theta_y, t=0) > dy \qquad (4.36)$$

$$+ < P_2(\cos\theta) >^{eq} \sum_{q\ odd} \frac{4}{q\pi} \sin(\frac{\pi x q}{L}) \left(1 - e^{-\frac{tq^2}{\tau_c}}\right).$$

In the isotropic case ($< P_2(\cos\theta) >^{eq}$ vanishes) and with the same initial conditions for all segments, the average orientation (Eq. (4.36)) reduces to

$$< P_2(\cos\theta_x, t) >=< P_2(\cos\theta, t=0) > \sum_{q\ odd} \frac{4}{\pi q} \sin(\frac{\pi x q}{L}) e^{-\frac{tq^2}{\tau_c}}, \qquad (4.37)$$

a result also calculated by Tassin et al [60] and Lawrey et al [61].

Let us now turn our attention to the stationary anisotropy given by Eq. (4.2). In this case (for probes with an exponentially distributed lifetime) the Laplace transform is precisely what we need. To calculate r_s^i for segment i, we have to evaluate the following expression :

$$C^i(s) = \int_0^{\infty} \ll P_2(\cos\theta_0) P_2(\cos\theta) \gg e^{-st} dt$$

$$= \int_0^{\pi} d\theta \int_0^{\pi} d\theta_0 \widetilde{P}_i(\theta, s \mid \theta_0, t=0) P^{eq}(\theta_0) P_2(\cos\theta_0) P_2(\cos\theta). \quad (4.38)$$

Here, $\widetilde{P}_i(\theta, s \mid \theta_0, t=0)$ is the Laplace transform of the probability distribution that segment i has orientation θ at time t, starting from the orientation θ_0 at $t=0$. All the other segments j have orientations sampled independently

from the equilibrium distribution at $t = 0$. Filling in these initial conditions in Eq. (4.18), we obtain for $\widetilde{P}_i(\theta, s \mid, \theta_0, t = 0)$

$$\widetilde{P}_i(\theta, s \mid \theta_0, t = 0) = P^{eq}(\theta) \frac{\cosh\left[\frac{\xi}{2}(M + 1 - 2i)\right]}{s \cosh\left[\frac{\xi}{2}(M + 1)\right]}$$

$$+ \sum_{J=1}^{M} \frac{\sinh\left[\xi \min(i, j)\right] \sinh\left[\xi\,(M + 1 - \max(i, j))\right]}{k \sinh \xi \sinh\left[\xi(M + 1)\right]} \qquad (4.39)$$

$$\times \left[P^{eq}(\theta) - \delta_{ij}[P^{eq}(\theta) - \delta(\theta - \theta_0)]\right].$$

Note that, here again, the Laplace inversion can be performed in the continuum limit we discussed in the previous section.
The expression Eq. (4.39) can be further simplified by using Eq. (4.19), and the following result is obtained for the orientation autocorrelation function $C^i(s)$ for segment i :

$$C^i(s) = \frac{1}{s}[< P_2(\cos\theta) >^{eq}]^2 \qquad (4.40)$$

$$- \frac{\sinh\left[\xi i\right] \sinh\left[\xi(M + 1 - i)\right]}{k \sinh \xi \sinh\left[\xi(M + 1)\right]} \left[[< P_2(\cos\theta) >^{eq}]^2 - < [P_2(\cos\theta)]^2 >^{eq}\right].$$

Combining the result Eq. (4.40) with Eq. (4.2), we finally obtain the following compact result for the stationary anisotropy :

$$r_s^i = < P_2(\cos\theta) >^{eq} \qquad (4.41)$$

$$+ \frac{\sinh\left[\xi i\right] \sinh\left[\xi(M + 1 - i)\right]}{\tau k \sinh \xi \sinh\left[\xi(M + 1)\right]} \left(\frac{< [P_2(\cos\theta)]^2 >^{eq} - [< P_2(\cos\theta) >^{eq}]^2}{1 + 2 < P_2(\cos\theta) >^{eq}} \right)$$

with

$$\cosh \xi = 1 + \frac{1}{2k\tau}, \tag{4.42}$$

and τ the average lifetime of the fluorescent probes.
In particular, for an isotropic system, Eq. (4.41) reduces to

$$r_s^i = \frac{2 \sinh [\xi i] \sinh [\xi(M+1-i)]}{5\tau k \sinh \xi \sinh [\xi(M+1)]}. \tag{4.43}$$

As was expected, the stationary anisotropy depends on the position i of the probe inside the chain. Indeed, orientational relaxation will take place faster for a probe close to one of the endpoints of the chain. Consequently, the stationary anisotropy is smaller. The limiting values of r_s^i for $\tau \ll k^{-1}$ and $\tau \gg k^{-1}$ however are independent of i :

$$\lim_{\tau \ll k^{-1}} r_s^i = \frac{< P_2(\cos\theta) >^{eq} + 2 < [P_2(\cos\theta)]^2 >^{eq}}{1 + 2 < P_2(\cos\theta) >^{eq}} \tag{4.44}$$

and

$$\lim_{\tau \gg k^{-1}} r_s^i = < P_2(\cos\theta) >^{eq} . \tag{4.45}$$

Indeed, for very short lifetimes, the probe is not exploring neighbouring segments, while, for very long lifetimes, relaxation to equilibrium has taken place. To get an idea of the i dependence at intermediate values of τ, we have calculated r_s^i for a simple one parameter anisotropic model in which one specific direction (chosen along the z axis) is preferred. This corresponds to a "potential landscape" which is flat, except for a delta function well centered at the privileged direction. The equilibrium distribution for this specific example is given by

$$P^{eq}(\theta) = (1-p)\frac{\sin\theta}{2} + p\ \delta(\theta), \tag{4.46}$$

in which p is a measure of the strength of the delta function well. It stands for the fraction of segments that have the preferential direction $\theta = 0$. It is also a measure of orientational order in the equilibrium state since $< P_2(\cos\theta) >^{eq} = p$. For $p = 0$, one recovers the isotropic case.

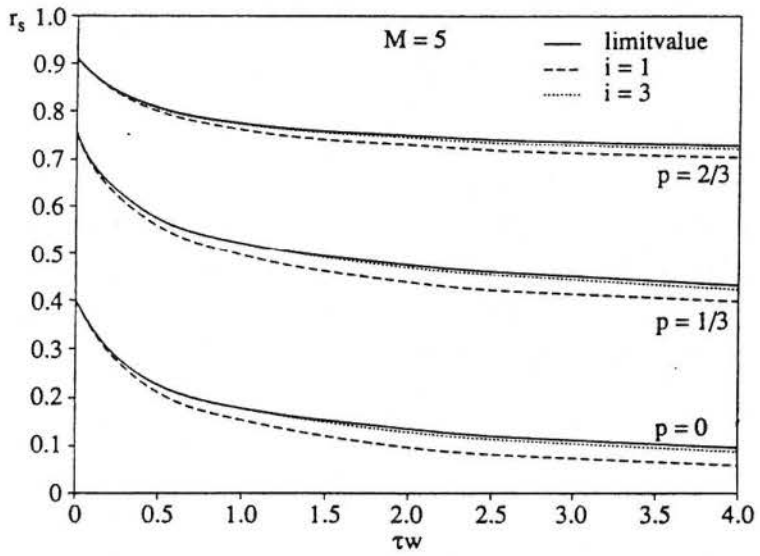

Figure 4.2: The stationary anisotropy r_s^i for different positions i along the chain, as a function of the dimensionless lifetime τk, compared to the limit value r_s for large M and i.

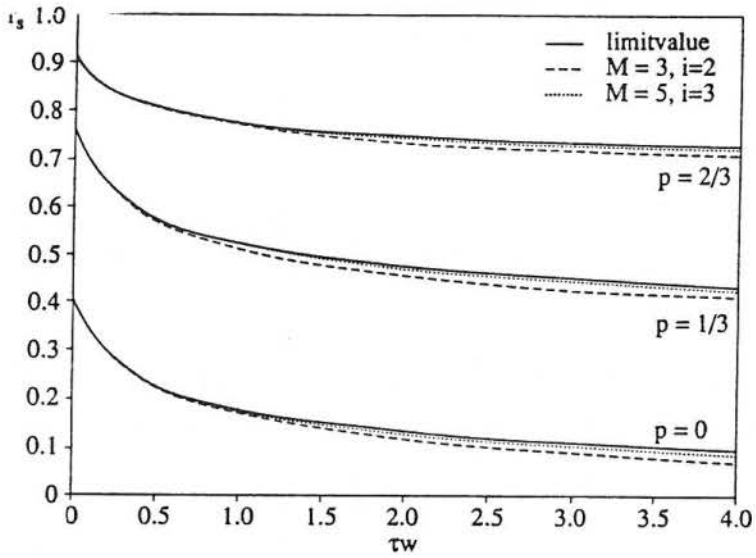

Figure 4.3: The stationary anisotropy r_s^i for the middle part of the chain, for different values of M, compared to the limit value r_s for large M and i.

In Fig. 4.2 and Fig. 4.3 we plotted r_s^i for various positions i of the probe, and various values of M, in function of the lifetime $k\tau$, measured in units k^{-1}. It turns out that the dependence on i, as well as on M is extremely weak. In fact, for $M \geq 10$, r_s^i is very well approximated by the limiting expression obtained for $M \to \infty$:

$$r_s^i \underset{M \to \infty}{=} < P_2(\cos\theta) >^{eq} + \frac{\sinh[\xi i]\, e^{-\xi i}}{\tau k} \left(\frac{< [P_2(\cos\theta)]^2 >^{eq} - [< P_2(\cos\theta) >^{eq}]^2}{1 + 2 < P_2(\cos\theta) >^{eq}} \right). \tag{4.47}$$

Moreover, the dependence on i is rather weak. For $i \geq 5$, r_s^i is almost independent of i, and we can write

$$r_s = \lim_{\substack{i \to \infty \\ M \to \infty}} r_s^i = < P_2(\cos\theta) >^{eq} \tag{4.48}$$

$$+\frac{1}{\sqrt{1+4\tau k}}\left(\frac{< [P_2(\cos\theta)]^2 >^{eq} - [< P_2(\cos\theta) >^{eq}]^2}{1+2 < P_2(\cos\theta) >^{eq}}\right).$$

In this limiting form, the dependence of r_s on the dynamic parameter $k\tau$ is extremely simple. For an isotropic system Eq. (4.48) reduces to

$$r_s = \frac{2}{5\sqrt{1+4k\tau}}, \tag{4.49}$$

and a log-log plot or r_s versus $1+4k\tau$ should yield a straight line with slope $-\frac{1}{2}$.

This has to be contrasted with the result for the case of one segment (just the probe) obtained from Eq. (4.41) by putting $M = 1$:

$$r_s = < P_2(\cos\theta) >^{eq} \tag{4.50}$$

$$+\frac{2}{1+2\tau k}\left(\frac{< [P_2(\cos\theta)]^2 >^{eq} - [< P_2(\cos\theta) >^{eq}]^2}{1+2 < P_2(\cos\theta) >^{eq}}\right).$$

In the isotropic case, this has a form identical to the result obtained by Perrin [62] for rotational Brownian motion :

$$r_s = \frac{2}{5}\frac{1}{1+\frac{\tau}{\tau_R}}, \tag{4.51}$$

in which $2k$ (the jump frequency) plays the role of the rotational relaxation time τ_R.

4.3 Conclusion

We have shown that, through the use of the Green's function, orientational relaxation in the reptation model can be discussed analytically, without going to a continuum limit for the chain. A somewhat surprising result is that the stationary anisotropy r_s^i, as measured in fluorescence depolarization experiments, is found to be almost independent of chain size and positioning of the probe. The exact dependence of r_s^i on these parameters is rather complicated, cf. Eq. (4.41), but a numerical evaluation for a specific anisotropic case (cf. Fig. 4.2 and Fig. 4.3) shows that this dependence is rather weak, and that r_s^i is very well approximated by the simple (limiting) form given in Eq. (4.48). This is true for all values of τk, i.e. independently of whether the fluorescent probes have a long, short, or intermediate lifetime (in units of the inverse k^{-1} of the jump frequency) and the resulting dependence on the parameter τk itself is extremely simple. Furthermore, we have investigated the effect of anisotropy, characterized by an equilibrium orientation distribution function P^{eq}, which need not be isotropic. As can be seen from the exact results (4.18) and (4.41), this anisotropy does not affect in an essential way the dependence on the position, chain length or the dynamic variable τk : the dependence on P^{eq} shows up in a different proportionality factor and in an additional term, both of which are such that the correct short and long time limits ($k\tau \to 0$, $k\tau \to \infty$) are reproduced.

Finally, we are aware of the limitations of a reptation type of description for polymer dynamics. Nevertheless, it would be interesting to compare the analytic results derived here for a discrete chain with computer experiments for more realistic discrete chain models.

Chapter 5

Dispersion of particles in spatially periodic flows

The transport or dispersion of neutrally buoyant particles in fluids is governed by two mechanisms : molecular diffusion and flow convection. Diffusion plays an important role in a wide variety of physical and chemical processes, such as chemical reactions, mixing of fluids, spreading of pollutants, chromatography and electrophoresis. It is therefore of fundamental and practical importance to understand the interaction between these two mechanisms, i.e. how does the flow pattern affect the dispersion of passive particles, and what is the resulting concentration profile of the particles.

Although the enhancement of dispersion by turbulence is well known, the fact that even laminar flow can increase the dispersion is far less well known. In 1953 Taylor [63] showed that the longitudinal dispersion in a Poiseuille flow in a cylindrical tube of radius R is described by an effective diffusion coefficient D^* (D^* is a measure for the width of the concentration profile of the particles) which is given by

$$D^* = D_m + \frac{< v >^2 R^2}{48 D_m}, \tag{5.1}$$

where D_m is the molecular diffusion coefficient and $< v >$ is the average flow velocity. The molecular diffusion coefficient being typically of the order of $10^{-5} - 10^{-8} cm^2/s$ in liquids, we see that the contribution of the flow to the effective dispersion of particles is by far the dominant effect.

The study of convection induced dispersion in a general velocity field is very complicated. However, analytic results can be obtained for an important subclass of flows, namely the ones with a periodic velocity field. Examples are flow profiles arising as a consequence of hydrodynamic instabilities, such as the Rayleigh-Benard system and the circular Couette system, or flow profiles in periodic media [64,65]. In these cases, the mean velocity $< v >$ of the flow is zero, and the dispersion of the particles occurs through the combination of convection along the streamlines and molecular diffusion between the streamlines. In particular, for the Rayleigh-Benard instability, Sagues and Horsthemke [66] found (using a perturbative method) an effective transport coefficient D^* equal to :

$$D^* = D_m + \frac{< v^2 > d^2}{(a^2 + \pi^2)\, D_m}. \tag{5.2}$$

The convection-induced contribution is again dominant, and has a form similar to that encountered in the original Taylor problem cf. Eq. (5.1).

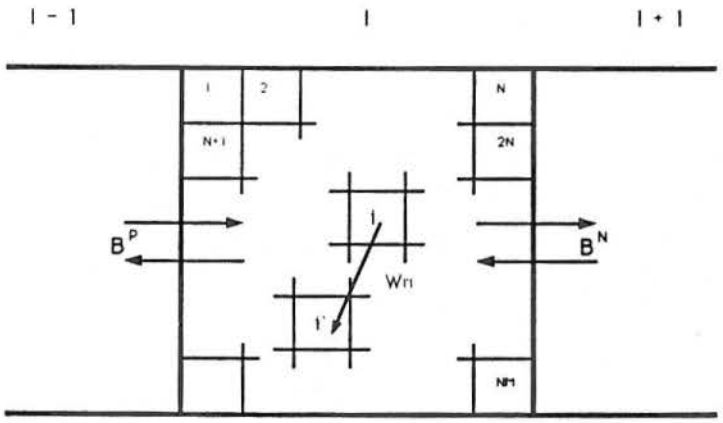

Figure 5.1: Periodically repeated unit cell consisting of $N \times M$ internal states.

Different ways to approach the description of such systems have been used (see e.g. [64]-[69]) among which perturbative methods and Monte Carlo simulation. The procedure we propose to follow is based on a study of the problem using the random walk formalism. The motion of the particles in the periodic fluid velocity field can be described as a random walk across a system consisting of a periodically repeated unit cell (see Fig. 5.1). The unit cell contains a number of internal states between which the particles can jump according to prescribed jump rates. The internal states can be interpreted in two different ways. They can represent possible spatial locations at which the particles reside, and jumping from one state to another thus constitutes a physical displacement of the particle. This is the way in which processes mentioned earlier can be modelled, e.g. Taylor dispersion or the dispersion of particles in Rayleigh-Benard instabilities. Another possibility is that they represent different states of the system, e.g. configuration states of a molecule. The random walk over the internal states then reflects changes in the state of the system. This description can be used to model processes such as chromatography, electrophoresis, NMR, molecular rotational dynamics, etc.

In section 5.1 we will first derive an expression for the average velocity v and the effective diffusion coefficient D^* in terms of the detailed structure of the unit cell, more precisely, in terms of the Green's function characterizing the walk inside each unit cell. Using the results obtained for the Green's function in section 2.1, we will apply the formalism to calculate the diffusion coefficient for several specific cases of interest in section 5.2.

5.1 General description

The periodically repeated unit cell consists of $M \times N$ internal states (see Fig. 5.1). The position of a particle is labelled by a number $i = n + l\,N(\ n \in [1, N]$ and $l \in [0, M-1])$ specifying the location inside each cell, and by the number I of the unit cell. The global horizontal position $x = n + NI$ of the particle is determined by both the number of the internal state and that of the unit cell in which the particle is located. As the particles move through the system, they jump from one state to another. The jump rate to go from a

state i to another state i' (not necessarily nearest neighbours) inside the same unit cell is given by the matrix element $W_{i'i}$, while the transitions to states in the previous or next unit cell are denoted by the elements of resp. the matrices $\mathbf{B^{N(ext)}}$ and $\mathbf{B^{P(revious)}}$. The probability to find a particle in state i in unit cell I at time t is the solution of the following Master equation :

$$\begin{aligned}
\partial_t\, P(i,I,t) &= \sum_{i'\neq i}(W_{ii'}\, P(i',I,t) - W_{i'i}\, P(i,I,t)) \\
&+ \sum_{i'\neq i}(B^N_{ii'}\, P(i',I+1,t) - B^N_{i'i}\, P(i,I,t)) \qquad (5.3) \\
&+ \sum_{i'\neq i}(B^P_{ii'}\, P(i',I-1,t) - B^P_{i'i}\, P(i,I,t))
\end{aligned}$$

with the sum over i' extending over the whole range of the internal states except i : $W_{ii} = 0$. We expect that the displacement of the particles will, in the long time regime, obey a Gaussian law [70] and thus only the first $< x(t) >$ and the second moments $< x^2(t) >$ are needed to characterize the process. Since $x = n + lN$, we have that

$$< x(t) > = < n(t) > + N < I(t) > \qquad (5.4)$$

$$= \sum_{l=0}^{M-1}\sum_{n=1}^{N} n\, \mu^0_{n+lN}(t) + N \sum_{l=0}^{M-1}\sum_{n=1}^{N} \mu^1_{n+lN}(t) \qquad (5.5)$$

$$< x^2(t) > = < n^2(t) > + 2N < n(t)\, I(t) > + N^2 < I^2(t) > \qquad (5.6)$$

$$= \sum_{l=0}^{M-1}\sum_{n=1}^{N} n^2\, \mu^0_{n+lN}(t) + 2N \sum_{l=0}^{M-1}\sum_{n=1}^{N} n\, \mu^1_{n+lN}(t)$$

$$+ N^2 \sum_{l=0}^{M-1}\sum_{n=1}^{N} \mu^2_{n+lN}(t) \qquad (5.7)$$

were $\mu^0_j(t)$, $\mu^1_j(t)$ and $\mu^2_j(t)$ are the reduced moments of the distribution $P(j,I,t)$

$$\mu^0_j(t) = \sum_I P(j,I,t) \qquad (5.8)$$

$$\mu_j^1(t) = \sum_I IP(j,I,t) \tag{5.9}$$

$$\mu_j^2(t) = \sum_I I^2 P(j,I,t). \tag{5.10}$$

The equations governing the reduced moments can be derived from Eq. (5.3) by multiplying with the appropriate power of I and then carrying out the sum over I. As explained in detail in appendix 7.C, these equations are solved by Laplace transformation. Using the long time limit expressions for the moments $< x(t) >$ (Eq. (7.C.20)) and $< x^2(t) >$ (Eq. (7.C.21)), we find for the average velocity v

$$v = \lim_{t\to\infty} \frac{< x(t) >}{t} = N \sum_j \sum_m (B_{jm}^N - B_{jm}^P)\ P_m^{st}. \tag{5.11}$$

Only the stationary distribution P_m^{st} of states m from which the particles can leave or enter a unit cell and the jump rates between these boundary states determine the average velocity v.

In a similar way the expression for the effective diffusion coefficient D^* is obtained

$$\begin{aligned} D^* &= \lim_{t\to\infty} \frac{< x^2(t) > - < x(t) >^2}{2\,t} \\ &= N^2 \left(\frac{1}{2} \sum_l \sum_m (B_{lm}^N + B_{lm}^P)\ P_m^{st} \right. \\ &\quad \left. - \sum_l \sum_m \sum_n \sum_r (B_{lm}^N - B_{lm}^P)\ G_{mn}^{*1}\ (B_{nr}^N - B_{nr}^P)\ P_r^{st} \right), \end{aligned} \tag{5.12}$$

with G_{mn}^{*1} the second term in the expansion of the Green's function $\mathbf{G}(s)$ (for the random walk inside the unit cell with periodic boundary conditions) around $s = 0$ (cf. Eqs. (2.58) and (7.C.22)). The factors $(B_{lm}^N + B_{lm}^P)$ and $(B_{lm}^N - B_{lm}^P)$ in D^* indicate the influence on the diffusion coefficient of the particles passing from one unit cell to another, while G_{mn}^{*1}, which depends explicitly on the specific structure of the unit cell, reflects the motion of the

particles inside the unit cell. We conclude that the average velocity v and the effective diffusion coefficient D^* can be expressed in terms of $\mathbf{P}^{st}$ and $\mathbf{G}^{*1}$, thus only the small s behaviour of the Green's function of the random walk on the unit cell with periodic boundary conditions is needed. In the next section we will apply the results we obtained for the Green's function (or its expansion) in section 2.1 to calculate the diffusion coefficient D^* for some specific cases of interest.

5.2 Applications

To check and illustrate the method introduced in the previous section, we will first calculate the diffusion coefficient for a very simple case : a one-dimensional symmetric random walk with periodic boundary conditions.
The unit cell consists of a strip of N internal states (see Fig. 5.2).

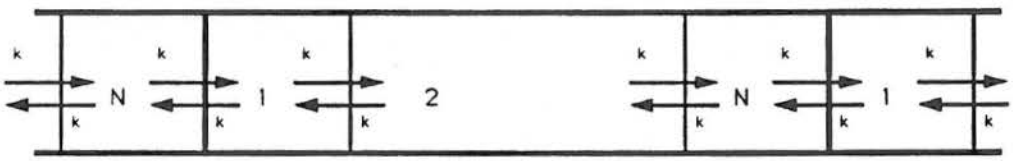

Figure 5.2: Unit cell consisting of a strip of N internal states.

There are only transitions possible between nearest neighbour states, with equal jump rates k to go from state i to state $i+1$ or from $i+1$ to i. The transition matrix $\mathbf{W}$ has thus the very simple tridiagonal form

$$\mathbf{W} = \begin{pmatrix} -2k & k & 0 & \cdots & & & 0 \\ k & -2k & k & 0 & \cdots & & 0 \\ 0 & k & -2k & k & 0 & \cdots & 0 \\ \vdots & & & \ddots & & & \vdots \\ 0 & \cdots & 0 & k & -2k & k & 0 \\ 0 & & \cdots & 0 & k & -2k & k \\ 0 & 0 & & \cdots & 0 & k & -2k \end{pmatrix}. \qquad (5.13)$$

The only transitions that occur through the boundaries are the ones from state 1 to state N and vice versa. The matrices $\mathbf{B^N}$ and $\mathbf{B^P}$ have but one element different from zero

$$B^N_{ij} = \delta_{i1}\,\delta_{jN}\,k \tag{5.14}$$

$$B^P_{ij} = \delta_{iN}\,\delta_{j1}\,k. \tag{5.15}$$

The Green's function for this periodic random walk was given in section 2.1.2 :

$$\begin{aligned} G_{mn} &= (s\mathbf{1} - (\mathbf{W} + \mathbf{B}^P + \mathbf{B}^N))^{-1}_{mn} \\ &= \frac{\cosh\xi(|m-n| - \frac{N}{2})}{2k\,\sinh\xi\,\sinh\frac{N\xi}{2}} \end{aligned} \tag{5.16}$$

with

$$\cosh\xi = 1 + \frac{s}{2k}. \tag{5.17}$$

To calculate the diffusion coefficient, we need the first two terms in the expansion around $s = 0$ of the Green's function

$$\begin{aligned} G_{mn}(s) &\underset{s\to 0}{=} \frac{P^{st}_m}{s} - G^{*1}_{mn} + O(s) \\ &= \frac{1}{s}\frac{1}{N} + \frac{N^2 - 6\,|m-n|\,N + 6\,(m-n)^2 - 1}{12Nk} + O(s^1). \end{aligned} \tag{5.18}$$

Filling in the appropriate values of m and m_0 we find

$$P^{st}_1 = P^{st}_N = \frac{1}{N} \tag{5.19}$$

$$G^{*1}_{11} = G^{*1}_{NN} = -\frac{N^2-1}{12kN} \tag{5.20}$$

$$G^{*1}_{1N} = G^{*1}_{N1} = -\frac{N^2 - 6N + 5}{12kN} \tag{5.21}$$

Combining Eq. (5.11) with Eqs. (5.19), (5.20) and (5.21), we find that the average velocity v equals zero, as was to be expected, because the random walk is symmetric. For the diffusion coefficient D^* (Eq. (5.12)) we also find the correct result, namely k.

5.2.1 Taylor dispersion phenomena

We now turn to the description of the dispersion of particles in a flow consisting of N layers, on which a transverse random walk is superimposed (see Fig. 5.3).

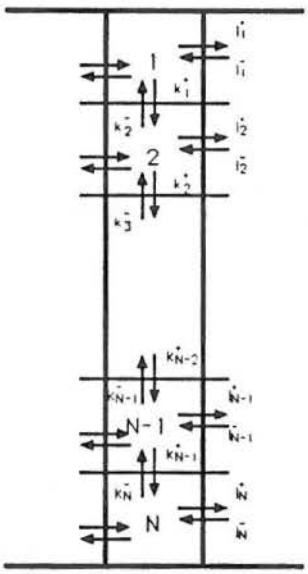

Figure 5.3: Unit cell used to describe Taylor dispersion phenomena.

The unit cell contains N internal states. Inside the unit cell, the particle can jump from state i to its nearest neighbours $i-1$ and $i+1$ with transition probabilities k_i^- and k_i^+ resp. Because the particles can not leave the system through the upper or the lower boundaries, the jump rates k_1^- and k_N^+ are

equal to zero. The transition matrix $\mathbf{W}$ is given by

$$\mathrm{W} = \begin{pmatrix} -k_1^+ & k_2^- & 0 & \cdots & 0 & 0 \\ k_1^+ & -(k_2^+ + k_2^-) & k_3^- & 0 & \cdots & 0 \\ 0 & k_2^+ & & \ddots & & \vdots \\ \vdots & & & & k_{N-1}^- & 0 \\ 0 & \cdots & 0 & k_{N-2}^+ & -(k_{N-1}^+ + k_{N-1}^-) & k_N^- \\ 0 & 0 & \cdots & 0 & k_{N-1}^+ & -k_N^- \end{pmatrix}. \quad (5.22)$$

From each internal state i, the particles can move to the previous or the next unit cell with jump rates l_i^- or l_i^+ resp. The matrices $\mathbf{B^N}$ and $\mathbf{B^P}$ are thus diagonal

$$B_{ij}^N = \delta_{ij} l_i^+ \quad (5.23)$$

$$B_{ij}^P = \delta_{ij} l_i^- . \quad (5.24)$$

When the particles leave unit cell I through the boundaries, they jump to the same internal state i they left. Consequently, the transitions rates $l_i^\pm$ do not enter in the calculation of the Green's function

$$\mathbf{G} = \frac{1}{s\mathbf{1} - \mathbf{W}}. \quad (5.25)$$

We calculated the stationary distribution P_i^{st} and G_{ij}^{*1} for this particular random walk in chapter 2, Eqs. (2.62) and (2.75) :

$$P_i^{st} = \frac{1}{\mathcal{N}} \, k_1^+ \cdots k_{i-1}^+ \, k_{i+1}^- \cdots k_N^- \quad (5.26)$$

with $\mathcal{N}$

$$\mathcal{N}^{-1} = k_2^- \cdots k_N^- + k_1^+ \, k_3^- \cdots k_N^- + \cdots + k_1^+ \cdots k_{N-1}^+, \quad (5.27)$$

and

$$G_{ij}^{*1} = -\sum_{r=1}^{N-1}\sum_{l=1}^{r}\sum_{k=1}^{r} P_i^{st}\frac{(\delta_{ik}-P_k^{st})(\delta_{jl}-P_l^{st})}{k_r^+ P_r^{st}}. \tag{5.28}$$

From Eq. (5.11) we obtain for the average velocity v

$$v = \sum_{i=1}^{N}(l_i^+ - l_i^-)P_i^{st} \tag{5.29}$$

and the effective diffusion coefficient D^* (Eq. (5.12)) equals

$$\begin{aligned} D^* &= \frac{1}{2}\sum_{i=1}^{N}(l_i^+ + l_i^-)P_i^{st} + \sum_{i=1}^{N}\sum_{j=1}^{N}\sum_{r=1}^{N-1}\sum_{l=1}^{r}\sum_{n=1}^{r}(l_i^+ - l_i^-)P_i^{st} \\ &\quad \times (l_j^+ - l_j^-)P_j^{st}\frac{(\delta_{in}-P_n^{st})(\delta_{jl}-P_l^{st})}{k_r^+ P_r^{st}}. \end{aligned} \tag{5.30}$$

As already mentioned in the introduction, we see that the particles are more effectively dispersed due to the presence of the flow in the horizontal direction. In the case of two layers with $l_1^+ = l_2^- = l_1$ and $l_1^- = l_2^+ = l_2$, Eqs. (5.29) and (5.30) reduce to the well known results ($k_1^+ = k_1$ and $k_2^- = k_2$)

$$v = \frac{(k_1 - k_2)(l_1 - l_2)}{k_1 + k_2} \tag{5.31}$$

and

$$D^* = \frac{l_1 + l_2}{2} + 4k_1k_2\frac{(l_1 - l_2)^2}{(k_1 + k_2)^3}. \tag{5.32}$$

From the general expressions Eqs. (5.29) and (5.30) for the discrete system, we can derive several other results by taking the appropriate continuum limits (see appendix 7.A). To obtain a continuum of states in the horizontal x-direction, we take the following limits (introducing the parameter a, being

the width of the unit cell) :

$$\begin{cases} a \to 0 \\ I \to \infty \\ l_i^{\pm} \to \infty \end{cases} \quad \text{with} \quad \begin{cases} x = Ia \\ a^2 \dfrac{(l_i^+ - l_i^-)}{2} = D_i \\ a(l_i^+ + l_i^-) = v_i \end{cases} \quad \text{fixed.} \quad (5.33)$$

We recover in this case the results previously obtained by Van den Broeck and Mazo [71]

$$v = \sum_{i=1}^{N} v_i P_i^{st} \quad (5.34)$$

$$D^* = \sum_{i=1}^{N} D_i P_i^{st} + \sum_{r=1}^{N} \frac{(\sum_{l=1}^{r}(v_l - v)p_l^{st})^2}{k_r^+ P_r^{st}}. \quad (5.35)$$

An example of a process that can be described in this continuum limit, is the dispersion of particles in a chromatographic column. Here, the layers (two in this case) do not represent physical locations of the particles, but possible internal states (see also chapter 6 and [101]). The particles can either be in the adsorbed state ($v_1 = 0$) or in the mobile phase ($v_2 = v$). They switch between these two states with jump rates $k_1^+ = k_1$ and $k_2^- = k_2$. The effective diffusion coefficient D^* is given by (if the diffusion in the horizontal direction is neglected)

$$D^* = v^2 \frac{k_1 k_2}{(k_1 + k_2)^3}. \quad (5.36)$$

The dispersion of particles suspended in a fluid flowing through a tube or between plates has been extensively investigated : see e.g. [63], [72]-[75]. We can describe this phenomenon with our formalism (for systems in which there occurs no interaction between the suspended particles and the boundaries such as adsorption, i.e. we only consider reflecting boundaries in the layers 1 and N) in the limit that the number of layers N of the fluid goes to infinity. The random walk across the system then becomes a diffusive process. Using the

limit procedure described in appendix 7.A we get from Eqs. (5.34) and (5.35) (the variable y describes the vertical position of the particles) :

$$v = \int_0^L v(y)P^{st}(y)dy \tag{5.37}$$

$$D^* = \int_0^L D(y)P^{st}(y)dy + \int_0^L \frac{(\int_0^y (v(y') - v)P^{st}(y')dy')^2}{D(y)P^{st}(y)}dy, \tag{5.38}$$

with L the total thickness of the system, $v(y)$ the velocity profile of the flow and $D(y)$ the diffusion coefficient in the transverse direction, which in general can depend on the vertical location of the particles in the fluid. Here again, we see that the transport of the particles is enhanced due to the interplay between convection and molecular diffusion.

As an example, we will consider the analog of Taylor diffusion (the disperion of particles in a laminar flow through a tube of radius R) for a system with planar symmetry. The Poisseuille velocity field $v(y)$ for a laminar flow between plane parallel plates at a distance L from each other is given by :

$$v(y) = 6v\frac{y}{L}(1 - \frac{y}{L}) \qquad \forall\ y\epsilon\ [0, L] \tag{5.39}$$

with v the average solvent velocity, which is also equal to the average velocity of the dispersed particles. We have in this case :

$$D(y) = D \tag{5.40}$$

$$P^{st}(y) = \frac{1}{L} \tag{5.41}$$

and thus we find for D^* (Eq. (5.38)) :

$$D^* = D + \frac{v^2L^2}{210D}, \tag{5.42}$$

a result simular to the one obtained by Taylor (cf. Eq. (5.1)).

5.2.2 Dispersion of particles in a system of rotating fluid rolls

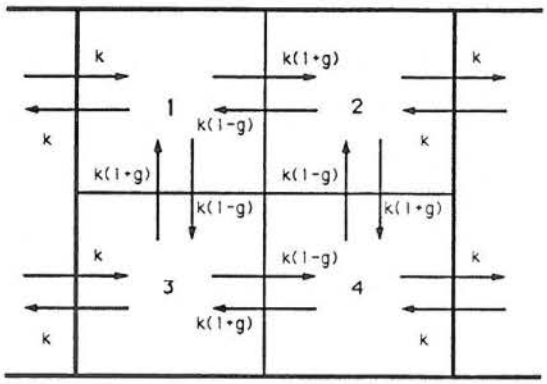

Figure 5.4: Unit cell with four internal states for a periodic system consisting of clockwise rotating rolls.

As a next example, we turn to the transport of particles moving through a system of rotating rolls. The unit cell we use to model this situation has four internal states (see Fig. 5.4) with transition rates $k(1-g)$ between nearest neighbours in the counter clockwise direction and $k(1+g)$ in the clockwise direction. The particles can move through the boundaries to the next or previous cells with jump rates k. The matrices $\mathbf{T}$ (with periodic boundary conditions), $\mathbf{B^N}$ and $\mathbf{B^P}$ are given by :

$$T = \begin{pmatrix} -3k & k(2-g) & k(1+g) & 0 \\ k(2+g) & -3k & 0 & k(1-g) \\ k(1-g) & 0 & -3k & k(2+g) \\ 0 & k(1+g) & k(2-g) & -3k \end{pmatrix} \tag{5.43}$$

$$\mathbf{B^N} = \begin{pmatrix} 0 & k & 0 & 0 \\ 0 & 0 & 0 & 0 \\ 0 & 0 & 0 & k \\ 0 & 0 & 0 & 0 \end{pmatrix} \tag{5.44}$$

$$\mathbf{B^P} = \begin{pmatrix} 0 & 0 & 0 & 0 \\ k & 0 & 0 & 0 \\ 0 & 0 & 0 & 0 \\ 0 & 0 & k & 0 \end{pmatrix}. \tag{5.45}$$

The Green's function for this random walk can be obtained by simple matrix inversion. Expanding it around $s = 0$, we obtain for P_i^{st} and G_{ij}^{*1}

$$P_i^{st} = \frac{1}{4} \tag{5.46}$$

$$\begin{aligned}
G_{11}^{*1} = G_{22}^{*1} = G_{33}^{*1} = G_{44}^{*1} &= -\frac{(g^2-7)^2}{144k^2(g^2+2)^2} \\
G_{12}^{*1} = G_{43}^{*1} &= \frac{g^4+4g^2+54g-23}{144k^2(g^2+2)^2} \\
G_{13}^{*1} = G_{42}^{*1} &= \frac{g^4+4g^2-54g+31}{144k^2(g^2+2)^2} \\
G_{14}^{*1} = G_{23}^{*1} = G_{32}^{*1} = G_{41}^{*1} &= -\frac{g^4+22g^2-41}{144k^2(g^2+2)^2} \\
G_{24}^{*1} = G_{31}^{*1} &= \frac{g^4+4g^2+54g+31}{144k^2(g^2+2)^2} \\
G_{21}^{*1} = G_{34}^{*1} &= \frac{g^4+4g^2-54g-23}{144k^2(g^2+2)^2}.
\end{aligned} \tag{5.47}$$

The average velocity v equals zero and D^* (Eq. (5.12)) can be expressed as

$$D^* = k\left(1 + \frac{g^2}{g^2+2}\right). \tag{5.48}$$

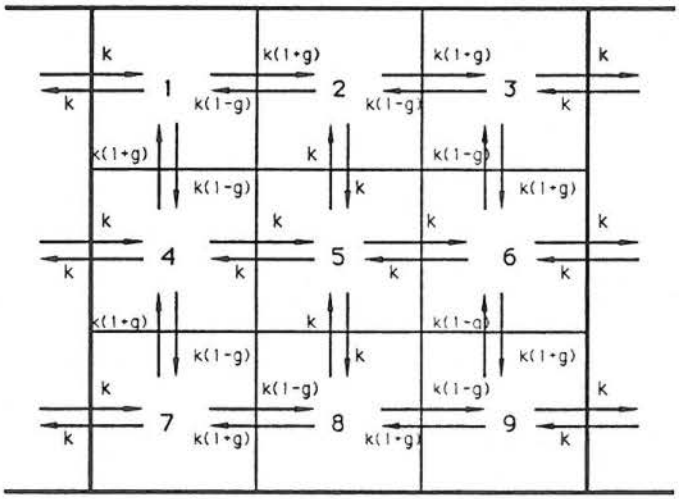

Figure 5.5: Unit cell with nine internal states for a periodic system consisting of clockwise rotating rolls.

In an analogous way we obtain the result for D^* when the unit cell contains nine internal states (see Fig. 5.5)

$$D^* = k\left(1 + \frac{2g^2(g^2+11)}{g^4+13g^2+18}\right). \tag{5.49}$$

We see that the dependence on g becomes more complicated as the number of internal states increases. Note that if the bias g tends to zero we recover the result for normal diffusion. Note also that D^* is even in g and thus not sensitive to the direction of the flow.

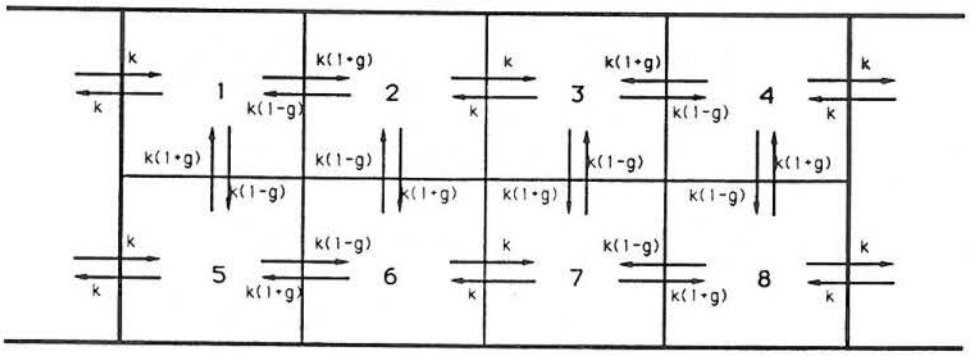

Figure 5.6: Unit cell for a periodic system consisting of counter rotating rolls.

In the Rayleigh-Benard system counter rotating fluid rolls arise. To model this situation, we considered a very simple system in which the unit cell contains eight internal states (see Fig. 5.6). We find for the matrices $\mathbf{T}$, $\mathbf{B^N}$ and $\mathbf{B^P}$:

$$\mathbf{T} = \begin{pmatrix} -3k & k(1+g) & 0 & k & k(1-g) & 0 & 0 & 0 \\ k(1-g) & -3k & k & 0 & 0 & k(1+g) & 0 & 0 \\ 0 & k & -3k & k(1-g) & 0 & 0 & k(1+g) & 0 \\ k & 0 & k(1+g) & -3k & 0 & 0 & 0 & k(1-g) \\ k(1+g) & 0 & 0 & 0 & -3k & k(1-g) & 0 & k \\ 0 & k(1-g) & 0 & 0 & k(1+g) & -3k & k & 0 \\ 0 & 0 & k(1-g) & 0 & 0 & k & -3k & k(1+g) \\ 0 & 0 & 0 & k(1+g) & k & 0 & k(1-g) & -3k \end{pmatrix} \tag{5.50}$$

$$\begin{aligned} B^N_{14} &= k \\ B^N_{85} &= k \qquad (5.51) \\ B^P_{41} &= k \\ B^P_{58} &= k, \qquad (5.52) \end{aligned}$$

with the other elements of $\mathbf{B^N}$ and $\mathbf{B^P}$ equal to zero. The Green's function is found by direct inversion of the matrix $(s\mathbf{1} - \mathbf{T})$. After expanding it around $s = 0$, we get for P^{st}_i and G^{*1}_{ij} (we only list here the elements of $\mathbf{G^{*1}}$ that we

need the calculation of D^*)

$$P_i^{st} = \frac{1}{8} \tag{5.53}$$

$$\begin{aligned}
G_{11}^{*1} = G_{44}^{*1} = G_{55}^{*1} = G_{88}^{*1} &= -\frac{11g^4 + 91g^2 + 116}{k(96g^4 + 480g^2 + 384)} \\
G_{14}^{*1} = G_{41}^{*1} = G_{85}^{*1} = G_{58}^{*1} &= \frac{5g^4 + 37g^2 - 4}{k(96g^4 + 480g^2 + 384)} \\
G_{15}^{*1} = G_{48}^{*1} &= -\frac{g^4 - 24g^3 + 5g^2 - 60g + 4}{k(96g^4 + 480g^2 + 384)} \\
G_{18}^{*1} = G_{45}^{*1} &= \frac{7g^4 + 35g^2 + 36g + 28}{k(96g^4 + 480g^2 + 384)} \\
G_{51}^{*1} = G_{84}^{*1} &= -\frac{g^4 + 24g^3 + 5g^2 + 60g + 4}{k(96g^4 + 480g^2 + 384)} \\
G_{81}^{*1} = G_{54}^{*1} &= \frac{7g^4 + 35g^2 - 36g + 28}{k(96g^4 + 480g^2 + 384)}.
\end{aligned} \tag{5.54}$$

The average velocity v of the dispersed particles is again zero and D^* equals

$$D^* = k\left(1 + \frac{g^2}{g^2 + 4}\right). \tag{5.55}$$

A comparison of this result with Eq. (5.48) shows that the particles are more effectively dispersed in the case where the fluid rolls have the same direction than in the case of alternating rolls.

5.3 Conclusion

In this chapter we have shown that the calculation of the effective diffusion coefficient for the dispersion of particles in spatially periodic systems can be reduced to the calculation of the Green's function for the random walk in the periodically repeated unit cell. In the case of small unit cells, as in the last example, the Green's function can be calculated explicitly (possibly with the use of symbolic manipulators like Macsyma). In other cases, such as a random walk in a one-dimensional unit cell with general transition rates, the small s expansion of the Green's function is known analytically (cf. section 2.1.3). In all these models, the enhancement of the effective diffusion coefficient due to the interplay between convection and molecular diffusion can be calculated.

In principle, similar calculations can be performed for two-dimensional systems where we have periodical boundary conditions in both the horizontal and vertical direction. The expressions for the diffusion coefficients D^*_{xx} and D^*_{yy} are thus the same, because the influence of the additional periodic boundaries will only prevail in the Green's function.

Chapter 6

Stochastic resonance for dispersion in oscillatory flows

In 1955, Giddings and Eyring [76] proposed the following simple model for chromatography. A particle in a chromatographic column can be in two different states. Either it is in the mobile phase, and it moves along the chromatographic column with a velocity equal to the fluid velocity v, or it is immobile, while it is adsorbed in the stationary phase. The rates of change from mobile to stationary phase, and vice versa, will be denoted by k_1 and k_2 respectively. The average fraction of time spent by a particle in the mobile phase, is equal to $k_2/(k_1 + k_2)$. Therefore, the particles move, on the average, with a speed equal to $u\ k_2/(k_1 + k_2)$, leading at time t, to a concentration peak at a location

$$< x(t) >= v\ t\ \frac{k_2}{k_1 + k_2} \tag{6.1}$$

downstream of the injection point. The idea behind flow chromatography is that different types of particles will be characterized by different values of the exchange rates, which will lead to separated peaks in the chromatographic column. However, due to the stochastic nature of the adsorption-desorption process, these peaks will not be infinitely sharp. The form and width of these

peaks will determine the separating power of the set up. For their simple model, Giddings and Eyring were able to calculate explicitly the shape of the peaks. In particular, they showed that the probability density $P(x,t)$, describing the distribution of identical particles along the x axis, approaches a Gaussian form in the limit $t \rightarrow \infty$, with an average value given by Eq. (6.1) and with a mean-square deviation increasing proportional to time ($\delta x = x - < x >$)

$$< \delta x^2(t) >= 2\ K_o\ t + O(t). \tag{6.2}$$

The proportionality constant K_o describes the dispersion of the particles in the direction of the flow, and is therefore called the longitudinal dispersion coefficient. In the present problem, it is given by

$$K_o = v^2\ \frac{k_1\ k_2}{(k_1 + k_2)^3}. \tag{6.3}$$

Note that the average position $< x(t) >$ of the chromatographic peak only depends on the ratio of the rate constants, cf. Eq. (6.1), while its width depends on the actual time scales involved, cf. Eq. (6.3). In particular, for the simple case of equal transition rates $k_1 = k_2 = k$, we find that $K_o \sim k^{-1}$, i.e. the dispersion rate decreases as the exchange rate between the layers increases. This can be understood as a result of the law of large numbers : as the frequency of exchanges between the layers increases, the fluctuations in the total time spent in each layer are suppressed.

The above-described dispersion process is a simple example of what is called Taylor dispersion [20]. In many problems of this type (e.g., dispersion of particles suspended in blood vessels or estuary flows), the velocity field under consideration is oscillating in time. In these cases, the corresponding longitudinal dispersion coefficient becomes a function of the oscillation frequency ω. This function has been calculated in the literature for several cases of interest [77] - [101]. In particular, Mysels [101] studied the dispersion for the above-described two-layer model, with the additional feature that the flow velocity

of the mobile phase is equal to $v\cos(\omega t)$. The correct result for K reads :

$$K = \lim_{t\to\infty} \frac{<\delta x^2(t)>}{2\,t} = \frac{v^2}{2}\frac{k_1\,k_2}{(k_1+k_2)(\omega^2+(k_1+k_2)^2)}. \qquad (6.4)$$

Note that K reduces, in the limit $\omega \to 0$, to half the value of the dispersion coefficient K_o for the non oscillatory flow. Note also that K decreases monotonously as ω increases. These properties are well known and understood, and are also found in other Taylor dispersion problems (see e.g. [98]).

A feature which seems to have escaped attention, is that the coupling between the oscillatory flow field and the stochastic jump process leads to a phenomenon of stochastic resonance [102]. To illustrate this, we consider the simple case of equal transition rates $k_1 = k_2 = k$, for which Eq. (6.4) becomes :

$$K = v^2\,\frac{k}{4(\omega^2+(2k)^2)}. \qquad (6.5)$$

For $k >> \omega$, the coefficient K behaves as in the non oscillatory case, namely $K \sim k^{-1}$. For $k << \omega$ however, we have that $K \sim k$, to be contrasted with the divergence of K_o for $k \to 0$. Moreover, K reaches a maximum for $k = \omega/2$. This maximum is the result of a resonance effect between the stochastic hopping process between the two states and the oscillatory velocity field. For $k = \omega/2$, the hopping of the particles between the two states with rate equal to k is, "as much as possible", in phase with the oscillation of the flow with frequency ω.

The jump process between the stationary and mobile phase is the so-called random telegraph signal. The spectrum $S(\omega)$ of this stationary stochastic process is a Lorentzian, and is, in fact, equal to K times $4/\pi$. This is not a coincidence. It turns out that the longitudinal dispersion coefficient is equal to the spectrum of the amplitude fluctuations of the velocity field. The measurement of K in function of ω thus corresponds to an indirect measurement of the power spectrum of this stochastic process.

The outline of this chapter is as follows. In section 6.1, we derive the relation between K and the spectrum of the underlying stochastic process. In section 6.2, we present the generalization of the Giddings-Eyring model for a

time-periodic flow where the transitions between the two states are described by a non-Markovian process. In section 6.3, we discuss some cases that have been studied previously in the literature. Finally, in section 6.4, we consider the problem of field flow fractionation with an oscillatory velocity field. In all these examples, the phenomenon of stochastic resonance is put to evidence.

6.1 The frequency dependent dispersion coefficient K

We are monitoring the motion of particles along the x axis. The rate of change, or velocity, along this axis, is supposed to be of the following form

$$\partial_t x = A(t)\cos\omega t, \tag{6.6}$$

where A stands for the amplitude of the time-periodic motion. This amplitude undergoes an independent stochastic process, which we will assume to be stationary. In the Giddings-Eyring model for chromatography, $A(t)$ is a random telegraph signal, switching between the two possible values $A = u$ and $A = 0$.

As a result of the stochastic properties of A, the particles do not follow identical trajectories, and will be dispersed in the course of time around an average position $< x(t) >$. By integration of Eq. (6.6), one finds for this dispersion (using the notation $\delta f = f - < f >$, and assuming that $< \delta x^2(t=0) >= 0$) :

$$< \delta x^2(t) >= \int_0^t d\tau \int_0^t d\tau' < \delta A(\tau)\delta A(\tau') > \cos\omega\tau \ \cos\omega\tau'. \tag{6.7}$$

By introducing the time auto-correlation function of the amplitude

$$C(\tau - \tau') =< \delta A(\tau)\delta A(\tau') >, \tag{6.8}$$

one can rewrite Eq. (6.7) as follows

$$< \delta x^2(t) > \;=\; t \int_0^t du\; C(u)\; \cos\omega u$$
$$+ \int_0^t du\; C(u) \left[\frac{\sin\omega(2t-u) - \sin\omega u}{2\omega} - u\cos\omega u \right]. \quad (6.9)$$

In the long-time limit, the following expression for the longitudinal diffusion coefficient K is obtained :

$$K = \lim_{t\to\infty} \frac{< \delta x^2(t) >}{2\,t} = \frac{1}{2} \int_0^\infty d\tau\; C(\tau) \cos\omega\tau = \frac{\pi}{4} S(\omega). \quad (6.10)$$

We conclude that K is (apart form a factor $\pi/4$) identical to the spectrum of the amplitude fluctuations. Note that positivity of K is guaranteed by the Wiener-Khintchin theorem [103].

In the general case of Taylor dispersion, the flow velocity along the x axis depends on the transverse location y of the particles, but not on the position along the flow axis x. This location y changes in a stochastic manner in the course of time, due to the intrinsic random motion, e.g. diffusion, of the particles. Hence A is a stochastic process through its dependence on y : $A(t) = A(y(t))$. The time-dependent dispersion and the longitudinal dispersion coefficient K can then be obtained from the Green's function of the stochastic process $y(t)$. To show this, we start by writing explicitly in Eq. (6.7) the average that now refers to an average over the y-coordinate

$$< \delta x^2(t) > \;=\; 2 \int_0^t d\tau \int_0^\tau d\tau' \int dy \int dy' \delta A(y) \delta A(y')$$
$$P(y'|y;\tau'-\tau) p^{st}(y) \cos\omega\tau \cos\omega\tau'. \quad (6.11)$$

Here $P(y'|y;\tau)$ stands for the conditional probability to go from y to y' during a time interval equal to τ, and $p^{st}(y') = \lim_{\tau\to\infty} P(y'|y;\tau)$ is the corresponding steady state density. For simplicity, we assume that the particles are initially distributed according to the steady state density $p^{st}(y)$, an assumption that does not influence the long-time behaviour of the particles. The

integral over the $\boldsymbol{y}$ variable is over the total state-space of this variable and has to be replaced by a summation in the case of a discrete valued variable. By introducing Laplace transforms

$$\tilde{f}(s) = \int_0^\infty f(t) e^{-st} dt, \tag{6.12}$$

one obtains the following result :

$$< \delta\tilde{x}^2(s) > \;=\; 2 \int d\boldsymbol{y} \int d\boldsymbol{y}' \delta A(\boldsymbol{y}) \delta A(\boldsymbol{y}') \left[\frac{2\omega^2 + s^2}{s^2\,(s^2 + 4\omega^2)}\; Re\tilde{P}(\boldsymbol{y}'|\boldsymbol{y}; s + i\omega) \right.$$

$$\left. + \frac{\omega}{s\,(s^2 + 4\omega^2)}\; Im\tilde{P}(\boldsymbol{y}'|\boldsymbol{y}; s + i\omega) \right] p^{st}(\boldsymbol{y}). \tag{6.13}$$

$Re(z)$ and $Im(z)$ stand for the real and imaginary part of z, respectively. In the limit $s \to 0$, corresponding to the long-time behaviour, the following expression is obtained for the longitudinal dispersion coefficient K (this is another way of writing Eq. (6.10), for $A(t) = A(\boldsymbol{y}(t))$)

$$K = \lim_{s \to 0} \frac{s^2}{2} < \delta\tilde{x}^2(s) >= \frac{1}{2} \int d\boldsymbol{y} \int d\boldsymbol{y}'\; \delta A(\boldsymbol{y}) \delta A(\boldsymbol{y}')\; Re\tilde{P}(\boldsymbol{y}'|\boldsymbol{y}; i\,\omega)\; p^{st}(\boldsymbol{y}). \tag{6.14}$$

The Laplace transform $\tilde{P}(\boldsymbol{y}'|\boldsymbol{y}; s)$ of $P(\boldsymbol{y}'|\boldsymbol{y}; t)$ is the so-called Green's function of the stochastic process $\boldsymbol{y}(t)$. Its explicit form is known in several cases of interest as we saw in chapter 2. Eqs. (6.13) and (6.14) are the basis for the results derived in the next sections.

Finally, we mention that the calculation of the long-time dispersion coefficient K can also be related to the time-dependent dispersion for the same problem in a non oscillatory flow. The Laplace transform of Eq. (6.7) in the absence of the time periodic term in the velocity field reads

$$< \delta\tilde{x}^2(s) >_{N.O.} = \int_0^\infty e^{-st}\; < \delta x^2(t) >_{N.O.}\; dt = \frac{2}{s^2} \int_0^\infty e^{-st}\; C(t)\; dt. \tag{6.15}$$

By comparison with Eq. (6.10), one easily verifies that

$$K = -\frac{\omega^2}{4}\; Re < \delta\tilde{x}^2(i\omega) >_{N.O.} \tag{6.16}$$

where the subscript $N.O.$ is an abbreviation for non-oscillatory. The calculation of the frequency - dependent dispersion rate is thus of the same level of difficulty as that of calculating the dispersion at all times for the non-oscillatory problem.

6.2 Non-Markovian two-layer system

As a first illustration of the above results, we consider the non-Markovian generalization of the Giddings-Eyring model of chromatography. In this case, the time τ between the changes in state, from velocity $A_1 \cos\omega t$ to velocity $A_2 \cos\omega t$ or vice versa, is a random variable with probability density $\psi(\tau)$. For simplicity, we consider the symmetric case for which this waiting time density is the same in both phases. In order to apply the results of the preceding section, we need to consider a stationary jump process, for which the waiting time density for the first jump, $\psi_o(t)$ is of the following form [27,37] :

$$\psi_o(t) = \frac{\int_t^\infty \psi(\tau)d\tau}{\int_0^\infty \tau\ \psi(\tau)d\tau}. \tag{6.17}$$

We assume here that the average waiting time $< \tau >$, appearing in the denominator of Eq. (6.17), is finite (if this is not the case, there exists no stationary jump process with $\psi(t)$ as waiting time density).
Let $P(i|j;t)$ denote the probability to go from state j at time zero to state i at time t (i, $j = 1$ or 2). Its Laplace transform, the Green's function $\tilde{P}(i|j;s)$ is given by (cf. section 2.1.4, Eqs. (2.81) and (2.82))

$$\begin{aligned} \tilde{P}(1|1;s) = \tilde{P}(2|2;s) &= \frac{1}{s} - \frac{\tilde{\psi}_o(s)}{s\ (1+\tilde{\psi}(s))} \\ \tilde{P}(1|2;s) = \tilde{P}(2|1;s) &= \frac{\tilde{\psi}_o(s)}{s\ (1+\tilde{\psi}(s))}, \end{aligned} \tag{6.18}$$

while the dispersion reads (cf. Eqs. (6.13), (6.17) and (6.18))

$$< \delta\tilde{x}^2(s) >= \frac{(A_1 - A_2)^2}{2} \left[\frac{s^2 + 2\omega^2}{s^2\,(s^2 + 4\omega^2)} \right.$$

$$\times Re \left[\frac{1}{s + i\omega} - \frac{2\,(1 - \tilde{\psi}(s + i\omega))}{(s + i\omega)^2 < \tau > (1 + \tilde{\psi}(s + i\omega))} \right] \tag{6.19}$$

$$\left. + \frac{\omega}{s\,(s^2 + 4\omega^2)} Im \left[\frac{1}{s + i\omega} - \frac{2\,(1 - \tilde{\psi}(s + i\omega))}{(s + i\omega)^2 < \tau > (1 + \tilde{\psi}(s + i\omega))} \right] \right].$$

The diffusion coefficient K is found from Eqs. (6.14), (6.17) and (6.18)

$$K = \frac{(A_1 - A_2)^2}{4} \frac{1 - a^2 - b^2}{< \tau >\ \omega^2\,[(a + 1)^2 + b^2]} \tag{6.20}$$

where

$$\begin{aligned} < \tau > &= \int_0^\infty \tau\ \psi(\tau)\ d\tau \\ a &= \int_0^\infty \cos\omega\tau\ \psi(\tau)\ d\tau \\ b &= \int_0^\infty \sin\omega\tau\ \psi(\tau)\ d\tau. \end{aligned} \tag{6.21}$$

In the limit $\omega \to \infty$, Eq. (6.20) reduces to the simple result

$$K \underset{\omega \to \infty}{\sim} \frac{(A_1 - A_2)^2}{4} \frac{1}{< \tau >\ \omega^2}, \tag{6.22}$$

so that only $< \tau >$ enters in the determination of the dispersion rate. On the other hand, for $\omega \to 0$, one finds

$$K \underset{\omega \to 0}{\sim} \frac{K_o}{2} = \frac{(A_1 - A_2)^2}{4} \frac{(< \tau^2 > - < \tau >^2)}{4 < \tau >}, \tag{6.23}$$

which depends both on the first and the second moment of the waiting time density $\psi(\tau)$.

For the particular case of an exponential waiting time

$$\psi(\tau) = k\ e^{-k\tau}, \tag{6.24}$$

we recover the result given in Eq. (6.5). This waiting time density corresponds to transitions that occur at completely random time points, with an average waiting time equal to

$$< \tau >= \frac{1}{k}. \tag{6.25}$$

At the other extreme, we consider the case of transitions occurring in a perfectly regular manner

$$\psi(\tau) = \delta(\tau - k^{-1}). \tag{6.26}$$

In this case, instead of calculating the diffusion coefficient K, we need the result for the complete time dependence of the mean square displacement given by Eq. (6.20) (the fluctuations in jump times arise from the fact that, under stationary conditions, the first jump takes place at a random time $\tau \in [0, k^{-1}]$)

$$\begin{aligned} < \delta\tilde{x}^2(s) >= & \frac{(A_1 - A_2)^2}{2\ s^2\ (s^2+\omega^2)(s^2+4\omega^2)(e^{2\frac{s}{k}} + 2\ e^{\frac{s}{k}}\ \cos\frac{\omega}{k} + 1)} \\ \times & \left[s\ (s^2+\omega^2)(e^{2\frac{s}{k}}+1) - 2k\ (s^2-2\omega^2)(e^{2\frac{s}{k}}-1) \right. \\ & \left. + 2\ s\ e^{\frac{s}{k}} \left(s^2 \cos\frac{\omega}{k} + \omega^2\ \cos\frac{\omega}{k} - 6\ k\ \omega\ \sin\frac{\omega}{k} \right) \right]. \end{aligned} \tag{6.27}$$

In the limit $s \to 0$, corresponding to the long-time behaviour, one has to make the distinction between the following resonant and non resonant regimes.

For $\omega/k = (2\ n + 1)\pi$, $(n = 0, 1, 2, 3, ...)$, Eq. (6.28) reduces to

$$< \delta\tilde{x}^2(s) > \underset{s \to 0}{\sim} (A_1 - A_2)^2 \frac{k^2}{\omega^2\ s^3}. \tag{6.28}$$

In the other cases $(\omega/k \neq (2n + 1)\pi)$, one has

$$< \delta\tilde{x}^2(s) > \underset{s \to 0}{\sim} \frac{1}{s} (A_1 - A_2)^2 \left(\frac{\omega\ \cos\frac{\omega}{k} + 5\ \omega - 6\ k\ \sin\frac{\omega}{k}}{8\ \omega^3\ (\cos\frac{\omega}{k} + 1)} \right). \tag{6.29}$$

In the first case, the transverse jumps are in resonance with the oscillatory velocity field, leading to a ballistic separation ($< \delta x^2(t) > \sim t^2$). The diffusion coefficient K is thus divergent. When the two processes are not in resonance, the dispersion tends to a constant in the long-time limit, and the diffusion constant K is equal to zero.

The so-called Erlang waiting time density includes both previous situations as particular cases :

$$\psi_n(\tau) = nk \frac{(nk\tau)^{n-1}}{(n-1)!} e^{-nk\tau} \tag{6.30}$$

or

$$\tilde{\psi}_n(s) = \frac{(nk)^n}{(s + nk)^n}. \tag{6.31}$$

For $n = 1$, one recovers the exponential waiting time density (cf. Eq. (6.24)). The fluctuations around the average jump time $< \tau >= k^{-1}$ become smaller as one considers larger n. In the limit $n \to \infty$, the distribution given in Eq. (6.26) is recovered. For general n, K can be obtained from Eq. (6.20), with

$$\begin{aligned} < \tau > &= \frac{1}{k} \\ a &= Re\left[1 + i\frac{\omega}{nk}\right]^{-n} \end{aligned} \tag{6.32}$$

$$b \;=\; Im\left[1+i\frac{\omega}{nk}\right]^{-n}.$$

In Fig. 6.1, we have plotted $K/(A_1 - A_2)^2$ as a function of k for $\omega = 1$ and different values of n. All these plots exhibit the phenomenon of stochastic resonance, discussed in the introduction. As $n \to \infty$, the structure of the resonances approaches that of the equally spaced jump process, cf. Eq. (6.26). In particular, the number of resonances increases as n becomes larger, while at the same time, the resonance peaks become sharper. We conclude that the resonance structure can be quite complicated if the jump process deviates markedly from a Markov process. On the other hand, the existence of sharp resonance peaks may be useful to separate particles. Only particles corresponding to a k value close to a resonant value will be dispersed.

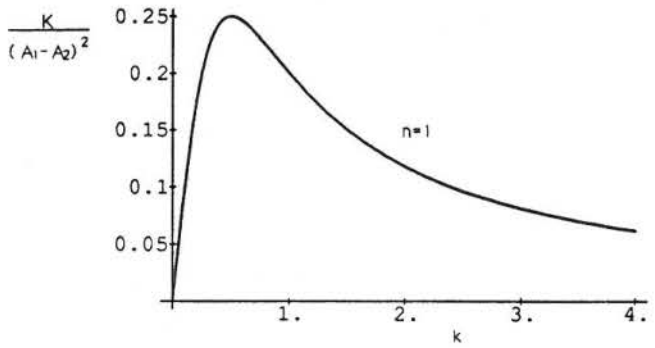

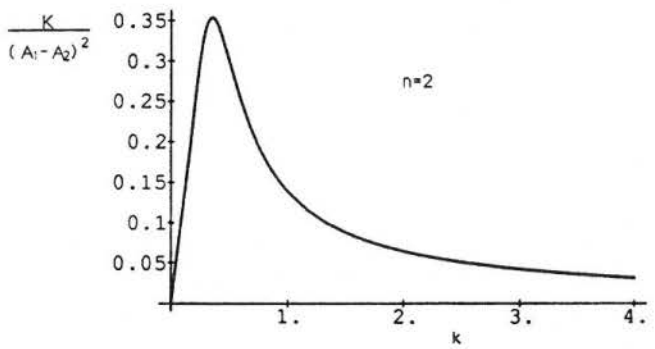

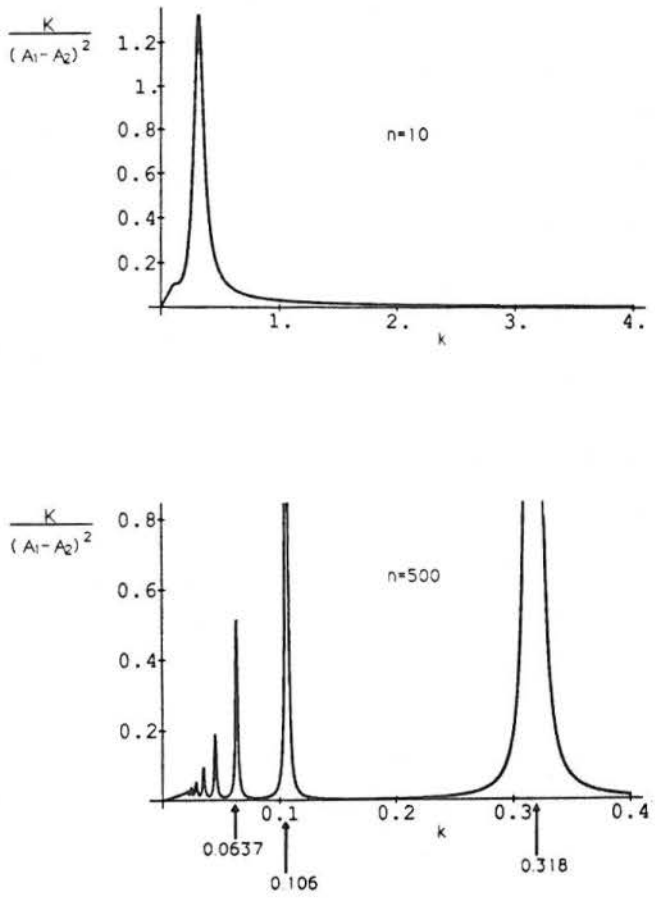

Figure 6.1: $\frac{K}{(A_1-A_2)^2}$ as a function of k with $\omega = 1$ for the two layer non-Markovian model with the Erlang-distribution as waiting time density, for different values of $n = 1, 2, 10, 500$. The arrows indicate the position of the resonant peaks for the case of equally spaced hoppings.

6.3 Comparison with some results from the literature

Consider the dispersion of particles, suspended in a time-periodic flow between two plane parallel plates (cf. Fig. 6.2).

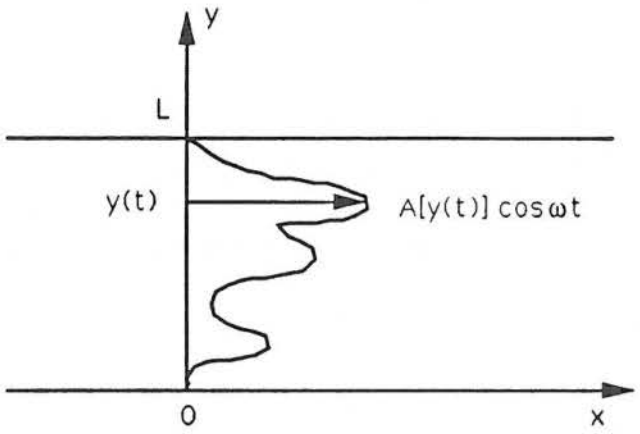

Figure 6.2: Time periodic flow between plane parallel plates.

The equation of motion of the particles along the x axis reads

$$\partial_t x = A\left[y(t)\right]\ \cos\omega t, \tag{6.33}$$

where $y(t)$ stands for the transverse location of the particle. We will suppose that the particles undergo, in this direction, a diffusive motion with a diffusion coefficient D between reflecting boundaries located at $y = 0$ and $y = L$. We neglect the diffusion in the x direction. The Green's function for this situation can be found in the table in chapter 2 (pages 17-20) :

$$\tilde{P}(y'|y;s) = \frac{\cosh\left[\sqrt{\frac{s}{D}}\left[L - \max(y,y')\right]\right]\ \cosh\left[\sqrt{\frac{s}{D}}\min(y,y')\right]}{\sqrt{sD}\ \sinh\left(L\sqrt{\frac{s}{D}}\right)} \tag{6.34}$$

and the dispersion coefficient K reads :

$$K = \frac{L^2}{2\,D}\int_0^1 dv \int_0^1 dw\ \left(A(vL) - \overline{A}\right)\ \left(A(wL) - \overline{A}\right) \tag{6.35}$$

$$\times Re\left[\frac{\cosh\left[(i+1)\sqrt{\Omega}\,[1-\max(v,w)]\right]\ \cosh\left[(i+1)\sqrt{\Omega}\min(v,w)\right]}{(i+1)\sqrt{\Omega}\ \sinh\left[(i+1)\sqrt{\Omega}\right]}\right].$$

The ratio

$$\Omega = \frac{\omega\ L^2}{2\ D} \tag{6.36}$$

measures the relative importance of the characteristic time for diffusion across the system over the characteristic oscillation time.

For an oscillating Poiseuille flow between plane parallel plates at a distance L from each other, the velocity field reads (for $y\ \in [0, L]$)

$$A(y)\cos\omega t = 6\ \overline{A}\ \frac{y}{L}\left(1 - \frac{y}{L}\right)\cos\omega t \tag{6.37}$$

and one finds

$$K = \frac{\overline{A}^2\ L^2}{D}\frac{3}{2\ \Omega^2}\ \left(1 - \frac{3}{\sqrt{\Omega}}\frac{\sinh\sqrt{\Omega} - \sin\sqrt{\Omega}}{\cosh\sqrt{\Omega} - \cos\sqrt{\Omega}}\right). \tag{6.38}$$

For a linear shear flow with velocity field (for $y\ \in [0, L]$)

$$A(y)\cos\omega t = 2\ \overline{A}\ \frac{y}{L}\cos\omega t, \tag{6.39}$$

one has

$$K = \frac{\overline{A}^2\ L^2}{D}\frac{1}{2\ \Omega^2}\ \left(1 - \frac{1}{\sqrt{\Omega}}\frac{\sinh\sqrt{\Omega} + \sin\sqrt{\Omega}}{\cosh\sqrt{\Omega} + \cos\sqrt{\Omega}}\right). \tag{6.40}$$

These results agree with those given previously in the literature [89,98], see also [99].

The following velocity profile simulates the presence of an immobile layer :

$$A(y)\ \cos\omega t = \begin{cases} 0 & for\ 0 \leq y \leq l \\ A\cos\omega t & for\ l \leq y \leq L \end{cases} . \tag{6.41}$$

The flow has a uniform oscillating velocity $A\cos\omega t$ in the top-layer of width $L - l$, while the bottom-layer of thickness l is at rest. After a lengthy but straightforward calculation, one obtains from Eq. (6.36)

$$K = \frac{\overline{A}^2\ L^2}{D}\ g(\Omega) \tag{6.42}$$

with

$$g(\Omega) = \left[\cos\left(2q\sqrt{\Omega}\right)\ \sinh\left(2\,(q-1)\,\sqrt{\Omega}\right) + \cosh\left(2q\sqrt{\Omega}\right)\ \sin\left(2\,(q-1)\,\sqrt{\Omega}\right)\right.$$

$$- \sin\left(2q\sqrt{\Omega}\right)\ \cosh\left(2\,(q-1)\,\sqrt{\Omega}\right) - \sinh\left(2q\sqrt{\Omega}\right)\ \cos\left(2\,(q-1)\,\sqrt{\Omega}\right)$$

$$\left. + \sinh 2\sqrt{\Omega} + \sin 2\sqrt{\Omega}\right] / \left[16\ \Omega^{3/2}\ \left(\cosh 2\sqrt{\Omega} - \cos 2\sqrt{\Omega}\right)\right] \tag{6.43}$$

and $q = \frac{l}{L}$. This result is equivalent to (but more convenient than) the series expansion obtained by Yasuda [100].

In the limit $\Omega \rightarrow \infty$, the following asymptotic result is obtained :

$$K = \frac{\overline{A}^2\ L^2}{D}\ \frac{1}{16\ \Omega^{3/2}}. \tag{6.44}$$

Note that, in this limit, K is independent of l, and decreases asymptotically as $\omega^{3/2}$. This somewhat surprising result can be understood from the fact that the large frequency behaviour of K is determined by the crossings of the $y = l$ border by the particles close to this border. These crossings occur in a self-similar manner with a fractal dimension equal to 1/2 [104].

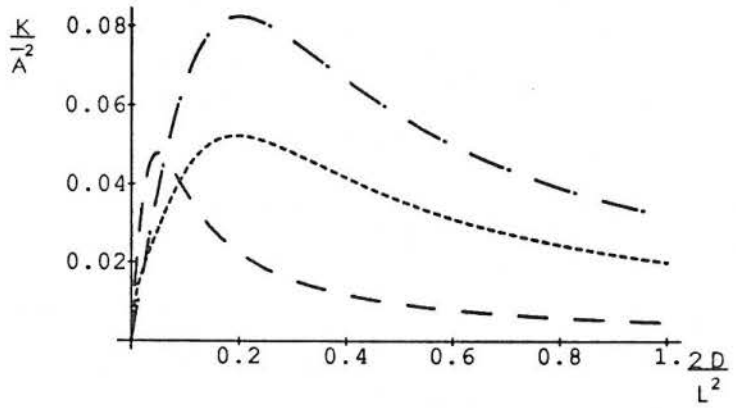

Figure 6.3: $\frac{K}{\overline{A}^2}$ with $\omega = 1$ as a function of $\frac{2D}{L^2}$ for a Poisseuille flow between plane parallel plates (– – –), for a linear shear flow (–.–) and for the velocity field given by Eq. (6.41) (- - -).

To discuss the above results in the context of stochastic resonance, we note that 2 D/L^2 is equal to the inverse of the typical time for diffusion between the boundaries. In Fig. 6.3, we have plotted $K/\overline{A}^2$ as a function of $2D/L^2$ for the three cases discussed above (with $\omega = 1$). In all these cases, one observes that K goes through a maximum at a specific resonant value of 2 D/L^2.

6.4 Field flow fractionation with an oscillatory velocity field

Field flow fractionation is a chromatographic method first proposed by Giddings [105] and independently by Berg and Purcell [106]. Particles are suspended in a non uniform flow and are subject to a transverse (e.g. electric or gravitational) external field. Under the influence of this field, particles of a different type will move to different regions of the velocity field, leading to separated peaks in the dispersion. Again, it is of interest to calculate the width

of these peaks, since they reflect properties of the random motion of the suspended particles, and determine the separating power of the chromatographic technique. Here, we present results for the case of field flow fractionation in a time-periodic Poiseuille flow.

The velocity field for an oscillatory Poiseuille flow between plane parallel plates (located at the positions $y = 0$ and $y = L$) is given by (cf. Eq. (6.37)) :

$$A(y)\cos\omega t = 6\,\overline{A}\,\frac{y}{L}\left(1-\frac{y}{L}\right)\cos\omega t, \tag{6.45}$$

with $\overline{A}$ the average solvent velocity. An external field is applied perpendicular to the plates (i.e. along the y direction). The particles undergo Brownian motion with diffusion coefficient D, on which is superimposed a sedimentation process with sedimentation velocity v_s proportional to the strength of the external field. The competition between these two processes leads to the establishment of a barometric equilibrium distribution

$$p^{st}(y) = \frac{\alpha\, e^{\alpha}}{L\,(e^{\alpha}-1)}\, e^{-\frac{\alpha y}{L}}, \tag{6.46}$$

where

$$\alpha = \frac{v_s\, L}{D} \tag{6.47}$$

measures the relative importance of the sedimentation versus diffusion. The Green's function for the combined diffusion-sedimentation process, with reflecting boundaries at the walls located at 0 and L was given in section 2.1.2 :

$$\begin{aligned}\tilde{P}(y|y_o;s) &= \frac{L\, e^{-(y-y_o)\frac{\alpha}{2L}}}{2DQ_o\sinh Q_o} \\ &\times\left[\left(1+\frac{\alpha^2 D}{2sL^2}\right)\cosh\left[Q_o\left(1-\frac{y_>}{L}-\frac{y_<}{L}\right)\right]\right. \\ &\left.+\cosh\left[Q_o\left(1-\frac{y_>}{L}+\frac{y_<}{L}\right)\right]+\frac{\alpha DQ_o}{sL}\sinh\left[Q_o\left(1-\frac{y_>}{L}-\frac{y_<}{L}\right)\right]\right]\end{aligned} \tag{6.48}$$

with

$$Q_o = \frac{1}{2}\sqrt{\alpha^2 + \frac{4sL^2}{D}} \tag{6.49}$$

and

$$\begin{aligned} y_> &= \max(y, y_o) \\ y_< &= \min(y, y_o). \end{aligned} \tag{6.50}$$

The average velocity of the dispersed particles $< A >$ is now different from the average solvent velocity $\overline{A}$

$$< A >= \int_0^L A(y)\, p^{st}(y)\, dy = \frac{6\,\overline{A}}{\alpha}\left(\coth\frac{\alpha}{2} - \frac{2}{\alpha}\right). \tag{6.51}$$

Inserting the results Eqs. (6.48) and (6.51) in Eq. (6.14) leads to the following expression for the frequency dependent dispersion rate K :

$$\begin{aligned} K \;=\; & \frac{L^2}{2\,D}\, Re\left[\frac{1}{Q\sinh Q}\int_0^1 dv \int_0^v dw\; e^{-(v+w)\frac{\alpha}{2}}\right. \\ & \times (A(vL) - < A >)\;(A(wL) - < A >) \\ & \times \left(\left(1 + \frac{\alpha^2}{4i\Omega}\right)\cosh(Q(1-v-w)) + \cosh(Q(1-v+w))\right. \\ & \left.\left. + \frac{\alpha Q}{2i\Omega}\sinh(Q(1-v-w))\right)\right] \end{aligned} \tag{6.52}$$

with

$$Q = \frac{1}{2}\sqrt{\alpha^2 + 8i\Omega}. \tag{6.53}$$

The calculation of the integrals in Eq. (6.52) is quite straightforward, but the final result is extremely lengthy. The complete expression for the dispersion rate, as well as some limiting results are given in appendix 7.D.

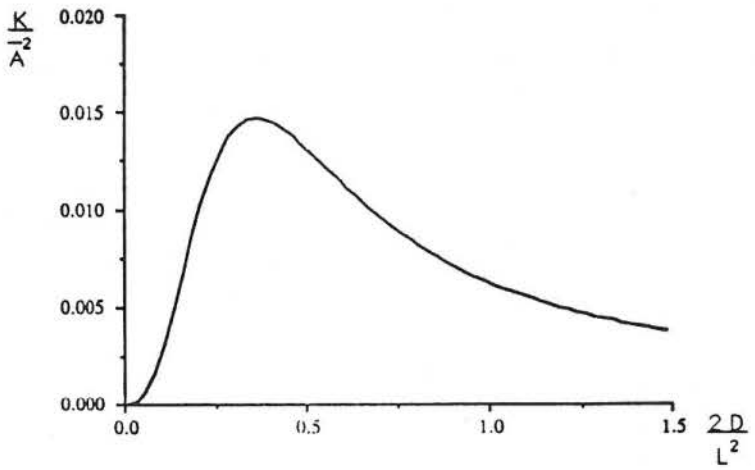

Figure 6.4: $\frac{K}{A^2}$ with $\omega = v_s = 1$ as a function of $\frac{2D}{L^2}$ for field flow fractionation in an oscillating velocity field.

In Fig. 6.4, we have plotted the result obtained for K from Eq. (6.52) for $\omega = 1$ and $v_s = 1$ as a function of $2\ D/L^2$. One again observes the phenomenon of stochastic resonance.

6.5 Conclusion

We have studied the dispersion of particles in time-periodic inhomogeneous flows. We saw that the diffusion coefficient can be expressed in terms of the Green's function for the transverse stochastic motion of the particles. One of the central results is that the dispersion rate K possesses one or more maxima, when plotted as a function of the characteristic time for the intrinsic stochastic motion of the particles. These maxima can be explained by a phenomenon of stochastic resonance between this stochastic motion and the periodic flow. On the other hand, we proved that the longitudinal dispersion coefficient K is directly proportional to the power spectrum of this stochastic process, which can thus in principle be obtained from the measurement of the

dispersion in time periodic flows. Finally, we expect that the measurement of the dispersion will be easier for time oscillatory flows, since much shorter tubes can be used in the experiments.

Chapter 7

Appendices

7.A Relation between discrete time and continuous time random walks and diffusion

In this appendix, we illustrate by a formal calculation how the results obtained for the case of a discrete time random walk can be used for the continuous time random walk and the diffusion process by taking the appropriate limits. We would like to stress that the derivation given here, merely constitutes a "recepy" to make these transitions and for a more rigorous treatment of this problem, we refer the reader to the literature (see e.g. [38,103]).

Consider a discrete time random walk where the particles can jump to their nearest neighbours $m-1$ and $m+1$ with transition probabilities α^+ and α^- resp. We assume that the time interval Δt between each jump is fixed. The probability to find the walker in site m after n steps, starting its trajectory in m_0, is governed by the following Master equation :

$$\begin{aligned} P(m,m_0;n) &= \alpha^+ P(m-1,m_0;n-1) \\ &\quad +(1-\alpha^+-\alpha^-)P(m,m_0;n)+\alpha^- P(m+1,m_0;n-1) \\ P(m,m_0;n) &= \sum_{m'} M_{mm'} P(m',m_0;n-1) \qquad \forall\ n>1 \end{aligned} \tag{7.A.1}$$

where we introduced the transition matrix $\mathbf{M}$ with elements

$$M_{mm'} = \alpha^+ \delta_{m',m-1} + (1 - \alpha^- - \alpha^+)\delta_{m',m} + \alpha^- \delta_{m',m+1}. \qquad (7.A.2)$$

The solution of Eq. (7.A.1) is equal to

$$P(m, m_0; n) = \sum_{m'} (M^n)_{mm'} P(m', m_0; 0) = (M^n)_{mm_0}. \qquad (7.A.3)$$

Multiplying both sides with z^n and summing over n we get

$$\tilde{P}(m, m_0; z) = \sum_{m'} \left(\frac{1}{\mathbf{1} - z\mathbf{M}} \right)_{mm'} P(m', m_0; 0) = G^D_{mm_0}(z), \qquad (7.A.4)$$

with $\mathbf{G}^D(z)$ the Green's function or generating function of the discrete time random walk. To relate this result to the continuous time random walk we let the time interval Δt between successive jumps tend to zero

$$\begin{cases} \Delta t \to 0 \\ n \to \infty \\ \alpha^\pm \to 0 \end{cases} \quad \text{with} \quad \begin{cases} t = n\Delta t \\ k^\pm = \dfrac{\alpha^\pm}{\Delta t} \end{cases} \quad \text{fixed.} \qquad (7.A.5)$$

In this limit, Eq. (7.A.1) is transformed into

$$\begin{aligned} \partial_t P(m, m_0; t) &= k^+ P(m-1, m_0; t) - (k^+ + k^-) P(m, m_0; t) \\ &\quad + k^- P(m+1, m_0; t) \\ \partial_t P(m, m_0; t) &= \sum_{m'} T_{mm'} P(m', m_0; t). \end{aligned} \qquad (7.A.6)$$

Here, $\mathbf{T}$ is the transition matrix for the continuous time random walk, which is related to the matrix $\mathbf{M}$ in the following way :

$$\mathbf{T} = \lim_{\Delta t \to 0} \frac{\mathbf{M} - \mathbf{1}}{\Delta t}. \qquad (7.A.7)$$

The Master equation (7.A.6) is usually solved by taking the Laplace transform. Rearranging the terms we get

$$G^C_{mm_0}(s) = \sum_{m'} \left(\frac{1}{s\mathbf{1} - \mathbf{T}} \right)_{mm'} P(m', m_0; 0) \tag{7.A.8}$$

with

$$G^C_{mm_0}(s) = \int_0^\infty e^{-st} P(m, m_0; t) dt. \tag{7.A.9}$$

This limiting procedure can be carried out not only on the equations describing the random walks, but also on results derived from them, in particular on the Green's function itself. Substituting $\frac{1}{1+s\Delta t}$ for z and taking the limit $\Delta t \to 0$, the following relation between $\mathbf{G}^C(s)$ and $\mathbf{G}^D(z)$ can be derived [38] :

$$\mathbf{G}^C(s) = \lim_{\Delta t \to 0} \Delta t \; \mathbf{G}^D \left(z = \frac{1}{1 + s\Delta t} \right). \tag{7.A.10}$$

Multiplying $P(m, m_0; n)$ with z^n and summing over n thus constitutes the discrete equivalent of taking the Laplace transform of $P(m, m_0; t)$. If one is interested in the long time behaviour of the probability distribution $P(t)$, such as e.g. in the calculation of the diffusion coefficient, it is not always necessary to know the complete s dependence of the Laplace transform $\widetilde{P}(s)$. Using Tauberian theorems, one can establish that the long time behaviour of some functions $P(t)$ is given by the leading terms of $\widetilde{P}(s)$ as s goed to zero

$$\lim_{t \to \infty} P(t) \qquad \longleftrightarrow \qquad \lim_{s \to 0} \widetilde{P}(s), \tag{7.A.11}$$

and its analog for discrete time steps

$$\lim_{n \to \infty} P(n) \qquad \longleftrightarrow \qquad \lim_{z \to 1} \widetilde{P}(z). \tag{7.A.12}$$

Finally we decribe the limiting procedure transforming the random walk into a diffusive process. We will represent the position of the particles by a continuous variable $x = am$ with a the length of site which will tend to zero. The transition rates $k^{\pm}$ will diverge, but combinations of the rates scaled with

factors of a can be related to the drift velocity and the diffusion constant. Using the Taylor expansion of $P(x \pm a, x_0; t)$ around x, one can see that Eq. (7.A.6) goes over into the Focker-Planck equation

$$\partial_t P(x, x_0; t) = -v\partial_x P(x, x_0; t) + D\partial_x^2 P(x, x_0; t), \tag{7.A.13}$$

provided we define $P(x, x_0; t)$, D and v in the limit $a \longrightarrow 0$ as

$$\begin{aligned} P(x, x_0; t) &= \lim_{a \to 0} \frac{1}{a} P(ma, m_0 a; t) \\ D &= \lim_{a \to 0} a^2 \frac{(k^+ + k^-)}{2} \\ v &= \lim_{a \to 0} a(k^+ - k^-). \end{aligned} \tag{7.A.14}$$

The Green's function is again the solution of the Laplace transform of Eq. (7.A.13)

$$(s - D\partial_x^2 + v\partial_x) G^C(x, x_0; s) = P(x, x_0; 0) = \delta(x - x_0). \tag{7.A.15}$$

7.B Moments of the end-to-end distance for a persistant random walk

In this appendix we show how the moments of the end-to-end distance for the persistent random walk can be obtained from the Fourier transform $F(k,z)$ of the Green's function.

A Taylor expansion is a standard procedure on a symbolic manipulator (we used MACSYMA) and thus the coefficients $A_{2\ell}(z)$ in Eq. (3.13) can easily be obtained. These coefficients all have the following form :

$$A_{2\ell}(z) = \frac{1}{(1-z)^{\ell+1}} \frac{1}{(1-pz)^{2\ell-1}} (C_{3\ell-1} z^{3\ell-1} + \ldots + C_1 z) \qquad (7.B.1)$$

where C_i are functions of p alone.
The inversion of Eq. (3.14), and thus of the expansion of Eq. (7.B.1), in order to get $< R^{2\ell}(n) >$, is made by using the relations

$$\begin{aligned} F(z) &= \sum_{n=0}^{\infty} z^n f(n) \\ \widetilde{F}(z) &= \sum_{n=0}^{\infty} z^n \widetilde{f}(n) \end{aligned} \qquad (7.B.2)$$

$\widetilde{F}(z)$	$\widetilde{f}(n)$
$\frac{1}{(1-pz)^k}$	$\frac{p^n}{n!}\frac{(k+n-1)!}{(k-1)!}$
$\frac{1}{(1-z)}F(z)$	$\sum_{i=0}^{n} f(i)$
$sF(z)$	$f(n-1)$ with $\widetilde{f}(0)=0$

As an example, we make the inversion for $< R^4(n) >$.
$< R^4(z) >$ is given by

$$\begin{aligned} < R^4(z) > &= \sum_{n=0}^{\infty} z^n < R^4(n) > \\ &= \frac{1}{(1-z)^3}\frac{1}{(1-pz)^3}\frac{b^4}{3}\Big[-3p^3z^5 - (7p^3+23p^2)z^4 \\ &\quad +(13p^2-13p)z^3 + (23p+7)z^2 + 3z\Big]. \end{aligned} \tag{7.B.3}$$

Using Eq. (7.B.2) we get

$$\frac{1}{(1-z)^3}\frac{1}{(1-pz)^3} = \sum_{n=0}^{\infty} z^n f(n) \tag{7.B.4}$$

with

$$f(n) = \frac{1}{2}\left[\frac{1}{(1-p)^3}(p^{n+5} - p^4 - (n-1)p^3(1-p) - (n+1)(n+2)\frac{(1-p)^2}{2})\right]. \tag{7.B.5}$$

And thus

$$\begin{aligned} < R^4(n) > &= \frac{b^4}{3}\Big[-3p^3 f(n-5) - (7p^3+23p^2)f(n-4) \\ &\quad +(13p^2-13p)f(n-3) + (23p+7)f(n-2) + 3f(n-1)\Big], \end{aligned} \tag{7.B.6}$$

which finally results in Eq. (3.16).

7.C Long time behaviour of the moments of the displacement for particles in a periodic system

In this appendix the reduced moments $\mu_j^0(t)$, $\mu_j^1(t)$ and $\mu_j^2(t)$, introduced in chapter 5, are calculated. They are subsequently used to derive the expression for the long time behaviour of the moments $< x(t) >$ and $< x^2(t) >$ of the displacement of particles in the periodic system under consideration.

Summing Eq. (5.3) over I we find for $\mu_j^0(t)$:

$$\begin{aligned} \partial_t\, \mu_j^0(t) \;=\; & \sum_{j' \neq j} \left(W_{jj'}\, \mu_{j'}^0(t) - W_{j'j}\, \mu_j^0(t) \right) \\ & + \sum_{j' \neq j} \left(B_{jj'}^N\, \mu_{j'}^0(t) - B_{j'j}^N\, \mu_j^0(t) \right) \\ & + \sum_{j' \neq j} \left(B_{jj'}^P\, \mu_{j'}^0(t) - B_{j'j}^P\, \mu_j^0(t) \right) \end{aligned} \tag{7.C.1}$$

or

$$\partial_t\, \mu_j^0(t) = \sum_{l=1}^{N \times M} T_{jl}\, \mu_l^0(t). \tag{7.C.2}$$

We introduced the matrix $\mathbf{T}$

$$\mathbf{T} = \mathbf{W} + \mathbf{B^N} + \mathbf{B^P}, \tag{7.C.3}$$

being the transition matrix for the random walk inside the same unit cell but with periodic boundaries. The diagonal matrix elements T_{jj} contain the contributions to the jump rate from the particles that leave state j

$$T_{jj} = -\sum_{j' \neq j} \left(W_{j'j} + B_{j'j}^N + B_{j'j}^P \right). \tag{7.C.4}$$

The equations for $\mu_j^1(t)$ and $\mu_j^2(t)$ are derived in the same way :

$$\partial_t\, \mu_j^1(t) = \sum_{j'} T_{jj'}\, \mu_{j'}^1(t) + \sum_{j'} \left(B_{jj'}^N - B_{jj'}^P\right)\, \mu_{j'}^0(t) \qquad (7.C.5)$$

$$\partial_t\, \mu_j^2(t) = \sum_{j'} T_{jj'}\, \mu_{j'}^2(t) + 2\sum_{j'} \left(B_{jj'}^N - B_{jj'}^P\right)\, \mu_{j'}^1(t) + \sum_{j'} \left(B_{jj'}^N + B_{jj'}^P\right)\, \mu_{j'}^0(t). \qquad (7.C.6)$$

The three equations (7.C.2), (7.C.5) and (7.C.6) can be solved successively : the solution for $\boldsymbol{\mu}^0(t)$ is inserted in the equation for $\boldsymbol{\mu}^1(t)$, which on its turn is needed to obtain $\boldsymbol{\mu}^2(t)$. To find the solutions of these equations, we will first take the Laplace transform and then solve for the Laplace transformed reduced moments $\tilde{\boldsymbol{\mu}}^0(s)$, $\tilde{\boldsymbol{\mu}}^1(s)$ and $\tilde{\boldsymbol{\mu}}^2(s)$:

$$\tilde{\boldsymbol{\mu}}^n(s) = \int_0^\infty \boldsymbol{\mu}^n(t) e^{-st} dt \qquad (7.C.7)$$

After the transformation Eq. (7.C.2) becomes

$$s\, \tilde{\mu}_j^0(s) - \mu_j^0(0) = \sum_{l=1}^{N\times M} T_{jl}\, \tilde{\mu}_l^0(s). \qquad (7.C.8)$$

By rearranging the terms can be written as

$$\tilde{\mu}_j^0(s) = \sum_{l=1}^{N\times M} G_{jl}(s)\, \mu_l^0, \qquad (7.C.9)$$

with $\mathbf{G}(s)$ the Green's function of the random walk in the unit cell with periodic boundary conditions :

$$G_{jl}(s) = (s\mathbf{1} - \mathbf{T})_{jl}^{-1} = \frac{P_j^{st}}{s} + \sum_{\alpha=1}^{N\times M-1} X_{j\alpha}\, \frac{1}{s-\lambda_\alpha}\, Y_{\alpha l}. \qquad (7.C.10)$$

The vector elements $X_{i\alpha}$ and $Y_{\alpha i}$ are the i th elements of the right, resp. left eigenvectors of the matrix $\mathbf{G}(s)$ matching the eigenvalue λ_α. The state $\alpha = 0$ is the stationary state with eigenvalue 0, $Y_{0i} = 1$ and $X_{i0} = P_i^{st}$ (cf. section 2.1.1). Substituting Eq. (7.C.10) in Eq. (7.C.9) gives for $\tilde{\mu}_j^0(s)$

$$\tilde{\mu}_j^0(s) = \frac{P_j^{st}}{s} + \sum_{l=1}^{N\times M} \sum_{\alpha=1}^{N\times M-1} X_{j\alpha} \frac{1}{s-\lambda_\alpha} Y_{\alpha l}\, \mu_l^0(0). \tag{7.C.11}$$

For simplicity, we will assume that the particles are initially located in unit cell $I = 0$ and are distributed according to the stationary distribution :

$$\begin{aligned} &\mu_k^0(0) = P_k^{st} \\ &< I(0) >= 0 \\ &< I^2(0) >= 0. \end{aligned} \tag{7.C.12}$$

We thus have for $\tilde{\mu}_j^0(s)$:

$$\tilde{\mu}_j^0(s) = \frac{P_j^{st}}{s} + \sum_{l=1}^{N\times M} \sum_{\alpha=1}^{N\times M-1} X_{j\alpha} \frac{1}{s-\lambda_\alpha} Y_{\alpha l}\, P_l^{st}. \tag{7.C.13}$$

In an analogous way the expressions for $\tilde{\mu}_j^1(s)$ and $\tilde{\mu}_j^2(s)$ are obtained :

$$\tilde{\mu}_j^1(s) = \sum_l G_{jl}(s)\mu_l^1(0) + \sum_l \sum_m \sum_n G_{jl}(s)(B_{lm}^N - B_{lm}^P)G_{mn}(s)P_n^{st} \tag{7.C.14}$$

$$\begin{aligned} \tilde{\mu}_j^2(s) = &\sum_l G_{jl}(s)\mu_l^2(0) + 2\sum_l \sum_m \sum_n G_{jl}(s)(B_{lm}^N - B_{lm}^P)G_{mn}(s)\mu_n^1(0) \\ &+2\sum_l \sum_m \sum_n \sum_r \sum_q G_{jl}(s)(B_{lm}^N - B_{lm}^P)G_{mn}(s)(B_{nr}^N - B_{nr}^P) \\ &\times G_{rq}(s)P_q^{st} + \sum_l \sum_m \sum_n G_{jl}(s)(B_{lm}^N + B_{lm}^P)G_{mn}(s)P_n^{st}. \end{aligned} \tag{7.C.15}$$

To simplify the notations, we have dropped the limits to which the summation indices extend.

The solutions Eqs. (7.C.13), (7.C.14) and (7.C.15) will now be transformed back to real time to compute the moments $< x(t) >$ and $< x^2(t) >$. The diffusion coefficient D^* reflects only the long time behaviour of the particles. It is therefore not necessary to calculate the complete time dependence of the moments, only the leading terms in the limit $t \to \infty$ will suffice. The terms containing $\frac{1}{s-\lambda_\alpha}$ for $\alpha \neq 0$ (cf. Eq. (7.C.10)) give rise to a factor of the order of $e^{\lambda_\alpha t}$ after inverse Laplace transformation. These contributions will vanish as t goes to infinity because all the eigenvalues of the matrix $\mathbf{G}(s)$ are negative (except for the maximum eigenvalue $\lambda_0 = 0$). In the long time limit, the expressions for $\mu_j^0(t)$, $\mu_j^1(t)$ and $\mu_j^2(t)$ thus reduce to :

$$\mu_j^0(t) \underset{t \to \infty}{\sim} P_j^{st} + O(t^{-1}) \tag{7.C.16}$$

$$\begin{aligned}\mu_j^1(t) \underset{t \to \infty}{\sim} & \; t\, P_j^{st} \sum_l \sum_m (B_{lm}^N - B_{lm}^P)\, P_m^{st} \\ & - \sum_{\alpha \neq 0} \sum_l \sum_m X_{j\alpha}\, \frac{1}{\lambda_\alpha}\, Y_{\alpha l}\, (B_{lm}^N - B_{lm}^P)\, P_m^{st} \\ & - \sum_{\alpha \neq 0} \sum_l \sum_m X_{j\alpha}\, \frac{1}{\lambda_\alpha}\, Y_{\alpha l}\, (B_{lm}^N - B_{lm}^P)\, \mu_m^1(0) + O(t^{-1})\end{aligned} \tag{7.C.17}$$

$$\begin{aligned}\mu_j^2(t) \underset{t \to \infty}{\sim} & \; t^2\, P_j^{st} \left[\sum_l \sum_m (B_{lm}^N - B_{lm}^P)\, P_m^{st} \right]^2 \\ & + t\, P_j^{st} \sum_l \sum_m (B_{lm}^N + B_{lm}^P)\, P_m^{st} \\ & - 2\, t \left[\sum_n \sum_r (B_{nr}^N - B_{nr}^P)\, P_r^{st} \right] \\ & \times \left[\sum_{\alpha \neq 0} \sum_l \sum_m X_{j\alpha}\, \frac{1}{\lambda_\alpha}\, Y_{\alpha l}\, (B_{lm}^N - B_{lm}^P)\, P_m^{st} \right]\end{aligned} \tag{7.C.18}$$

$$-2\,t\,P_j^{st}\sum_{\alpha\neq 0}\sum_{l}\sum_{m}\sum_{n}\sum_{r}(B_{lm}^N-B_{lm}^P)X_{m\alpha}\,\frac{1}{\lambda_\alpha}\,Y_{\alpha n}$$

$$\times(B_{nr}^N-B_{nr}^P)\,P_r^{st}+O(t^0).$$

With the above derived results, we can now calculate the the moments $< x(t) >$ (Eq. (5.5)) and $< x^2(t) >$ (Eq. (5.7)). Carrying out the sum over j, the second and the third term in $< \mu_j^1(t) >$ (Eq. (7.C.17)) and the third in $< \mu_j^2(t) >$ (Eq. (7.C.18)) vanish due to the orthogonality of the left and right eigenvectors

$$\sum_{j=1}^{N\times M} 1\;X_{j\alpha}=\sum_{j=1}^{N\times M} Y_{0j}\;X_{j\alpha}=\delta_{\alpha 0}. \tag{7.C.19}$$

We thus get for the leading terms in the long time limit of the first and the second moment :

$$< x(t) > \quad \underset{t\to\infty}{\sim} \quad Nt\sum_{l}\sum_{m}(B_{lm}^N-B_{lm}^P)\,P_m^{st}+\sum_{l=0}^{M-1}\sum_{n=1}^{N}nP_{n+lN}^{st}$$

$$+O(t^{-1}) \tag{7.C.20}$$

$$< x^2(t) > \quad \underset{t\to\infty}{\sim} \quad N^2t^2\left[\sum_{l}\sum_{m}(B_{lm}^N-B_{lm}^P)\,P_m^{st}\right]^2$$

$$+2Nt\sum_{l=0}^{M-1}\sum_{n=1}^{N}nP_{n+lN}^{st}\sum_{r}\sum_{m}(B_{rm}^N-B_{rm}^P)\,P_m^{st}$$

$$+N^2t\sum_{l}\sum_{m}(B_{lm}^N+B_{lm}^P)\,P_m^{st} \tag{7.C.21}$$

$$-2t\sum_{l}\sum_{m}\sum_{n}\sum_{r}(B_{lm}^N-B_{lm}^P)G_{mn}^{*1}$$

$$\times(B_{nr}^N-B_{nr}^P)\,P_r^{st}+O(t^0)$$

where we introduced G^{*1}_{mn} as

$$G^{*1}_{mn} = \sum_{\alpha \neq 0} X_{m\alpha} \frac{1}{\lambda_\alpha} Y_{\alpha n}. \qquad (7.C.22)$$

7.D Frequency dependent dispersion coefficient for field flow fractionation in an oscillating velocity field

After a straight forward calculation of the integrals in Eq. (6.52) we obtain for the frequency dependent diffusion coefficient K :

$$
\begin{aligned}
K \;=\; & 9\{-\alpha\Big[\cosh\frac{\alpha}{2}\sinh^2\frac{\alpha}{2}\,[\,16\Omega(10\alpha^2\Omega^4+8\Omega^4-\alpha^6\Omega^2-4\alpha^4\Omega^2+\alpha^8)P \\
& +8\alpha^2\Omega Q(\alpha^2\Omega^2-4\Omega^2-\alpha^4)P \qquad (7.D.1) \\
& -\alpha^2 R(84\alpha^2\Omega^4-240\Omega^4-\alpha^6\Omega^2-76\alpha^4\Omega^2+\alpha^8) \\
& -RQ(12\alpha^2\Omega^4+16\Omega^4-\alpha^6\Omega^2-4\alpha^4\Omega^2+\alpha^8)\Big] \\
& +2\alpha\sinh^3\frac{\alpha}{2}\Omega\Big[-(128\Omega^4+80\alpha^4\Omega^2-\alpha^8)P+\alpha^2(8\Omega^2-\alpha^4)QP \\
& +8R\Omega(2\Omega^2+\alpha^4)Q-16\alpha^2R\Omega(7\Omega^2-\alpha^4)\Big] \\
& +4\alpha\sinh\frac{\alpha}{2}\Omega^2\Big[4\alpha^2\Omega QP-4\Omega(8\Omega^2+3\alpha^4)P \\
& +R(4\Omega^2+\alpha^4)Q-\alpha^2R(28\Omega^2-\alpha^4)\Big] \\
& +4\alpha^2\cosh\frac{\alpha}{2}\Omega^4\Big[8\Omega P-RQ-\alpha^2R\Big]\Big]\cosh P\sinh P \\
& -\alpha\cos R\Big[\sinh^2\frac{\alpha}{2}\,[\,4\Omega(8\alpha^2\Omega^4-32\Omega^4-3\alpha^6\Omega^2+16\alpha^4\Omega^2-4\alpha^8)P \\
& +4\alpha^2\Omega Q(\alpha^2\Omega^2+8\Omega^2+2\alpha^4)P \\
& -\alpha^2R(36\alpha^2\Omega^4+240\Omega^4-\alpha^6\Omega^2+76\alpha^4\Omega^2-\alpha^8) \\
& +RQ(4\alpha^2\Omega^4+16\Omega^4+\alpha^6\Omega^2-4\alpha^4\Omega^2+\alpha^8)\,] \\
& -4\alpha\cosh\frac{\alpha}{2}\sinh\frac{\alpha}{2}\Omega^2\,[\,4\alpha^2\Omega QP-4\Omega(8\Omega^2+3\alpha^4)P
\end{aligned}
$$

$$+R(4\Omega^2+\alpha^4)Q-\alpha^2R(28\Omega^2-\alpha^4)\,]$$

$$-32\alpha^2\Omega^5P+4\alpha^2R\Omega^4Q+4\alpha^4R\Omega^4\Big]\sinh P$$

$$+8\sinh^2\frac{\alpha}{2}\Omega^3Q\left[2\sinh\frac{\alpha}{2}\left[\alpha^2\Omega^2+8\Omega^2-\alpha^4\right]\right.$$

$$\left.-\cosh\frac{\alpha}{2}\left[8\Omega^2+\alpha^4\right]\right]\cosh^2P$$

$$+\alpha\sin R\left[\sinh^2\frac{\alpha}{2}\left[\alpha^2(36\alpha^2\Omega^4+240\Omega^4-\alpha^6\Omega^2+76\alpha^4\Omega^2-\alpha^8)\,P\right.\right.$$

$$+Q(4\alpha^2\Omega^4+16\Omega^4+\alpha^6\Omega^2-4\alpha^4\Omega^2+\alpha^8)P$$

$$+4R\Omega(8\alpha^2\Omega^4-32\Omega^4-3\alpha^6\Omega^2+16\alpha^4\Omega^2-4\alpha^8)$$

$$\left.-4\alpha^2R\Omega Q(\alpha^2\Omega^2+8\Omega^2+2\alpha^4)\right]$$

$$-4\alpha\cosh\frac{\alpha}{2}\sinh\frac{\alpha}{2}\Omega^2\left[(4\Omega^2+\alpha^4)QP+\alpha^2(28\Omega^2-\alpha^4)P\right.$$

$$\left.-4\alpha^2R\Omega Q-4R\Omega(8\Omega^2+3\alpha^4)\right]$$

$$+4\alpha^2\Omega^4QP-4\alpha^4\Omega^4P-32\alpha^2R\Omega^5\Big]\cosh P$$

$$+\alpha\cos R\sin R\left[-\cosh\frac{\alpha}{2}\sinh^2\frac{\alpha}{2}\right.$$

$$\left[-\alpha^2(84\alpha^2\Omega^4-240\Omega^4-\alpha^6\Omega^2-76\alpha^4\Omega^2+\alpha^8)P\right.$$

$$+Q(12\alpha^2\Omega^4+16\Omega^4-\alpha^6\Omega^2-4\alpha^4\Omega^2+\alpha^8)P$$

$$-16R\Omega(10\alpha^2\Omega^4+8\Omega^4-\alpha^6\Omega^2-4\alpha^4\Omega^2+\alpha^8)$$

$$\left.+8\alpha^2R\Omega Q(\alpha^2\Omega^2-4\Omega^2-\alpha^4)\right]$$

$$+4\sinh\frac{\alpha}{2}\Omega^2\left[(4\Omega^2+\alpha^4)QP+\alpha^2(28\Omega^2-\alpha^4)P\right.$$

$$\left.-4\alpha^2R\Omega Q-4R\Omega(8\Omega^2+3\alpha^4)\right]$$

$$+2\alpha \sinh^3 \frac{\alpha}{2}\Omega \left[8\Omega(2\Omega^2+\alpha^4)QP + 16\alpha^2\Omega(7\Omega^2-\alpha^4)P\right.$$

$$\left. -R(128\Omega^4+80\alpha^4\Omega^2-\alpha^8) - \alpha^2 R(8\Omega^2-\alpha^4)Q\right]$$

$$\left. -4\alpha^2 \cosh\frac{\alpha}{2}\Omega^4\left[QP-\alpha^2 P - 8R\Omega\right]\right]$$

$$-8\sinh^2\frac{\alpha}{2}\cos^2 R\ \Omega^3 Q$$

$$\times\left[2\sinh\frac{\alpha}{2}\left[\alpha^2\Omega^2+8\Omega^2-\alpha^4\right] - \cosh\frac{\alpha}{2}\left[8\Omega^2+\alpha^4\right]\right]\}$$

$$/\{16\alpha^2\sinh^3\frac{\alpha}{2}\Omega^7 Q\,[\cosh(2P)-\cos(2R)]\}$$

with

$$\begin{aligned} Q &= \sqrt{64\Omega^2+\alpha^4} \\ P &= \frac{\sqrt{Q+\alpha^2}}{2\sqrt{2}} \\ R &= \frac{\sqrt{Q-\alpha^2}}{2\sqrt{2}}. \end{aligned} \qquad (7.D.2)$$

For small ω this reduces to :

$$K = \frac{L^2\,\overline{A}^2}{D}\left\{\frac{3}{\alpha^6\,\sinh^3\frac{\alpha}{2}}\left[3\,(\alpha^2+28)\,\sinh\frac{3\alpha}{2} - 30\alpha\,\cosh\frac{3\alpha}{2}\right.\right.$$

$$\left. + (\alpha^4+21\alpha^2-252)\,\sinh\frac{\alpha}{2} - 6\alpha\,(\alpha^2-5)\,\cosh\frac{\alpha}{2}\right]$$

$$-\frac{\Omega^2}{40\alpha^{10}\,\sinh^5\frac{\alpha}{2}}\left[20\,(126\alpha^2+475)\,\sinh\frac{5\alpha}{2} - 30240\alpha\,\cosh\frac{5\alpha}{2}\right.$$

$$+2\,(29\alpha^6-600\alpha^4-9180\alpha^2-237600)\,\sinh\frac{3\alpha}{2} + 5\,(-\alpha^7+36\alpha^5$$

$$\left.\left. -1152\alpha^3+18144\alpha)\,\cosh\frac{3\alpha}{2}\right.\right.$$

$$+2\,(153\alpha^6 - 3960\alpha^4 + 21240\alpha^2 + 475200)\,\sinh\frac{\alpha}{2}$$

$$+5\,(\alpha^7 - 612\alpha^5 + 1152\alpha^3 - 12096\alpha)\,\cosh\frac{\alpha}{2}\Big] + O(\Omega^4)\Big\}. \quad (7.D.3)$$

The first term in the series has been obtained previously by Giddings et al. [107]. The leading behaviour for large ω is given by :

$$K = \frac{L^2\,\overline{A}^2}{D}\frac{9}{\Omega^2\;16\alpha^2\;\sinh^3\frac{3\alpha}{2}}\Big[(\alpha^2+8)\,\sinh\frac{3\alpha}{2} - 4\alpha\,\cosh\frac{3\alpha}{2}$$

$$-\,(3\alpha^2+24)\,\sinh\frac{\alpha}{2} + 4\alpha\,\cosh\frac{\alpha}{2}\Big] + O(\Omega^{-5/2}). \quad (7.D.4)$$

Bibliography

[1] E. W. Montroll and M. F. Shlesinger, *The wonderful world of random walks* in *Nonequilibrium phenomena II. From statistics to hydrodynamics*, eds. J. L. Lebowitz and E. W. Montroll (North-Holland, Amsterdam, 1984).

[2] K. Pearson, *The problem of random walk*, Nature **72**, 294 (1905).

[3] Lord Rayleigh, *On the resultant of a large number of vibrations of the same pitch and arbitrary phase*, Phil. Mag. **10**, 73 (1880).

[4] L. Bachelier, *La théory de la spéculation*, Ann. Sci. École Norm. Sup. **17**, 21 (1905) ; **19**, 371 (1906).

[5] A. Einstein, Ann. d. Physik **17**, 549 (1905) ; **19**, 371 (1906).

[6] J. C. Kluyver, *A local probability problem*, Proc. Section of Sci., K. Akad. van Wet. te Amsterdam **8**, 341 (1906).

[7] A. A. Markov, *Wahrscheinlichkeitsrechnung* (Leipzig-Berlin, 1912).

[8] M. V. Smoluchowski, *Drei Vorträge über Diffusion, Brownsche Bewegung und Koagulation von Kolloidteilchen*, Physik. Zeits. **17**, 557 (1916) ; **17**, 588 (1916).

[9] N. Wiener, Acta Math. **55**, 117 (1930).

[10] G. E. Uhlenbeck and L. S. Ornstein, *On the theory of the Brownian motion*, Phys. Rev. **36**, 823–841 (1930).

[11] G. Pólya, *Über eine Aufgabe der Wahrscheinlichkeitsrechnung betreffend die Irrfarht in Stratzennetz*, Math. Ann. **84**, 149 (1921).

[12] W. Kuhn, Kolloid Z. **68**, 2 (1934).

[13] W. Kuhn and F. Grün, Kolloid Z. **101**, 248 (1942).

[14] E. W. Montroll, *Random walks in multidimensional spaces, especially on lattices*, J. Soc. Industr. Appl. Math. **4**(4), 241–260 (1956).

[15] M. N. Barber and B. W. Ninham, *Random and restricted walks. Theory and selected applications* (Gordon and Breach, New York, 1970).

[16] G. H. Weiss and R. J. Rubin, *Random walks : theory and selected applications*, Adv. Chem. Phys. **52**, 363–505 (1983).

[17] J. W. Haus and K. W. Kehr, *Diffusion in regular and disordered lattices*, Phys. Reports **150**(5-6), 263–406 (1987).

[18] I. Claes and C. Van den Broeck, *Random walk with persistence*, J. Stat. Phys. **49**(1-2), 383–392 (1987).

[19] I. Claes and C. Van den Broeck, *Orientational relaxation in the reptation model*, Chem. Phys. Research, **1**, 7 (1990).

[20] C. Van den Broeck, *Taylor dispersion revisited*, Physica **A168**, 677–696 (1990) ;
H. Brenner, *A general theory of Taylor dispersion phenomena*, Phys. Chem. Hydrodyn. **1**, 91–123 (1980).

[21] I. Claes and C. Van den Broeck, *Stochastic resonance for dispersion in oscillatory flows*, accepted for publication in Phys. Rev. A15.

[22] P. Lancaster and M. Tismenetsky, *The theory of matrices*, (Academic press, Orlando, 1985).

[23] E. R. Hansen, *A table of series and products* (Prentice Hall, Englewood Cliffs, New Yersey, 1975).

[24] M. Khantha and V. Balakrishnan, *Hopping conductivity of a one-dimesional bond-percolation model in a constant field : Exact solution*, Phys. Rev. B **29**(8), 4679–4690 (1984).

[25] R. M. Mazo, *On the Green's function for a one dimensional random walk*, Cell Biophysics **11**, 19–24 (1987).

[26] H. Margeneau and G. Murphy, *The mathematics of Physics and chemistry*, (Van Nostrand, New York, 1943).

[27] W. Feller, *An introduction to probability theory and its applications* (Wiley, New York, 1967), vols. 1 and 2.

[28] S. Chandrasekhar, *Stochastic problems in physics and astronomy*, Rev. Mod. Phys. **15**(1), 1–89 (1943).

[29] M. Khantha and V. Balakrishnan, *Reflection principles for biased random walks and application to escape time distributions*, J. Stat. Phys. **41**(5/6), 811–824 (1985).

[30] M. Khantha and V. Balakrishnan, *First passage times distributions for finite one-dimensional random walks*, Pramana **21**(2), 111–122 (1983).

[31] M. Khantha and V. Balakrishnan, *Diffusion with drift on line*, J. Phys. C : Solid State Phys. **16**, 6291–6302 (1983).

[32] K. Lakatos-Lindenberg and K. E. Shuler, J. Math. Phys. **12**, 633 (1971).

[33] K. Lindenberg, *Random walks with nonnearest neighbour transitions II : Analytic one-dimensional theory for exponentially distributed steps in systems with boundaries*, J. Stat. Phys. **10**(6), 485–503 (1974).

[34] E. W. Montroll and G. H. Weiss, *Random walks on lattices II*, J. Math. Phys. **6**(2), 167–181 (1965).

[35] V. M. Kenkre, E. W. Montroll and M. F. Shlesinger, *Generalized Master equations for continuous time random walks*, J. Stat. Phys. **9**(1), 45–50 (1973).

[36] E. W. Montroll and H. Scher, *Random walks on lattices IV : continuous-time random walks and the influence of absorbing boundaries*, J. Stat. Phys. **9**(2), 101–135 (1973).

[37] D. R. Cox, *Renewal theory* (Methuen, London, 1962).

[38] D. Bedeaux, K. Lakatos-Lindenberg and K. E. Shuler, *On the relation between Master equations and random walks and their solutions*, J. Math.Phys. **12**(10), 2116–2123 (1971).

[39] V. Balakrishnan and M. Khantha, *First passage times and escape time distributions for continuous time random walks*, Pramana **21**(3), 187–200 (1983).

[40] D. A. Darlin and J. F. Siegert, *The first passage time problem for a continuous Markov process*, Ann. Math. Stat. **24**, 624–638 (1953).

[41] E. W. Montroll and B. J. West, in *Fluctuation phenonena*, Eds. E. W. Montroll and J. L. Lebowitz (North-Holland, Amsterdam, 1979).

[42] E. W. Montroll, *Random walks on lattices* in *Stochastic processes in mathematical physics and engineering*, Proc. Symp. Appl. Math. XVI (American Mathematical Society, Providence, 1964) 193–200.

[43] P. J. Flory, *Statistical Mechanics of Chain Molecules* (Interscience Publishers, New York, 1969).

[44] H. Yamakawa, *Modern Theory of Polymer Solutions* (Harper and Row, New York, 1971).

[45] C. M. Tchen, *Random flight with multiple partial correlations*, J. Chem. Phys. **20**, 214 (1952).

[46] J. J. G. Molina and J. C. de la Torre, *Randomly broken chain as a semiflexible macromolecular model. Computer simulation of statistical properties*, J. Chem. Phys. **84**, 4026–4030 (1986).

[47] P. G. de Gennes, *Reptation of a polymer chain in the presence of fixed obstacles*, J. Chem. Phys. **55**(2), 572–579 (1971).

[48] S. F. Edwards, Proc. Phys. Soc. London **92**, 9 (1967).

[49] M. Doi and S. F. Edwards, *Dynamics of concentrated polymer chains part 1 : Brownian motion in the equilibrium state*, J. Chem. Soc., Far. Trans II **74**, 1789–1801 (1978) ;
M. Doi and S. F. Edwards, *Dynamics of concentrated polymer chains part 2 : Molecular motion under flow*, J. Chem. Soc., Far. Trans II **74**, 1802–1817 (1978) ;
M. Doi and S. F. Edwards, *Dynamics of concentrated polymer chains part 3 : The constitutive equation*, J. Chem. Soc., Far. Trans II **74**, 1818–1832 (1978) ;
M. Doi and S. F. Edwards, *Dynamics of concentrated polymer chains part 4 : Rheological properties*, J. Chem. Soc., Far. Trans II **75**, 38–54 (1979).

[50] S. A. Allison, *Brownian dynamics simulation of wormlike chains. Fluorescence depolarized light scattering*, Macromolecules **19**, 118–124 (1986).

[51] J. M. Deutch, *Simulation of entangled polymer chains*, J. Pol. Sci. : Pol. Symp. **73**, 161–173 (1985).

[52] L. L. Chapoy and D. B. DuPré, *Polarized fluorescence measurements of orientational order in a uniaxial liquid crystal*, J. Chem. Phys. **70**(05), 2550–2553 (1979).

[53] L. Monnerie and J. L. Viovy, *Local molecular dynamics studies of polymer chains - in solution and in bulk - using the fluorescence anisotropy decay technique* in *Photophysical and Photochemical Tools in Polymer Science*, Ed. M. A. Winnik (D. Reidel Publishing Company, 1986) 193–224.

[54] L. Monnerie, *The fluorescence depolarization technique as a tool to investigate chain orientation and relaxation in bulk polymers* in *Photophysical and Photochemical Tools in Polymer Science*, Ed. M. A. Winnik (D. Reidel Publishing Company, 1986) 371–396 .

[55] A. Szabo, *Theory of polarized fluorescent emission in uniaxial liquid crystals*, J. Chem. Phys. **72**(8), 4620–4626 (1980).

[56] G. W. Slater, J. Noolandi, *On the repation theory of gel electrophoresis*, Biopolymers **25**, 431–454 (1986).

[57] A. Ben-Shaul, Y. Rabin and W. M. Gelbart, *On the stretching of alkyl chains by nematics*, J. Chem. Phys. **78**(6), 4303–4308 (1983).

[58] L. B. W. Jolley, *Summation of series*, (Dover, New York, 1961).

[59] C. F. Curtis and R. B. Bird, *A kinetic theory for polymer melts. I. The equation for the single-link orientation distribution function*, J. Chem. Phys. **74**(3), 2016–2025 (1981).

[60] J. F. Tassin, L. Monnerie and L. J. Fetters, *Infrared dichroism study of the relaxation of selected segments along a stretched polymer chain and comparison with theoretical models*, Macromolecules **21**, 2404–2412 (1988).

[61] B. D. Lawrey, R. K. Prud'homme and J. T. Koberstein, *Polymer chain segment orientation during stress relaxation*, J. Polym. Sci. Polym. Phys. Ed. **24**, 203–208 (1986).

[62] F. Perrin, J. Phys. (Paris) **7**, 390 (1926).

[63] G. I. Taylor, *Dispersion of soluble matter in solvent flowing through a tube*, Proc. R. Soc. London **A219**, 186–203 (1953).

[64] H. Brenner, *Dispersion resulting from flow through spatially periodic porous media*, Phil. Trans. R. Soc. London **A297**, 81–133 (1980).

[65] H. Brenner and P. M. Adler, *Dispersion resulting from flow through spatially periodic porous media II. Surface and intraparticle transport*, Phil. Trans. R. Soc. London **A307**, 149–200 (1982).

[66] F. Sagues and W. Horsthemke, *Diffusive transport in spatially periodic hydrodynamic flows*, Phys. Rev. **A34**(5), 4136–4143 (1986).

[67] M. N. Rosenbluth, H. L. Berk, I. Doxas and W. Horton, *Effective diffusion in laminar convective flows*, Phys. Fluids **30**(9), 2636–2647 (1987).

[68] J. B. T. M. Roerdink and K. E. Shuler, *Asymptotic properties of multistate random walks I : Theory*, J. Stat. Phys. **40**(1/2), 205–240 (1985).

[69] V. Seshadri, K. Lindenberg and K. E. Shuler, *Random walks on periodic and random lattices II : Random walk properties via generating function techniques*, J. Stat. Phys. **21**, 517–548 (1979).

[70] M. Pinsky, *Differential equations with a small parameter and the central limit theorem for functions defined on a finite Markov chain*, Z. Wahr. Verw. Geb. **9**, 101–111 (1968).

[71] C. Van den Broeck and R. M. Mazo, *The asymptotic dispersion of particles in N-layer systems*, J. Chem. Phys. **81**(8), 3624–3634 (1984).

[72] R. Aris, *On the dispersion of a solute in a fluid flowing through a tube*, Proc. Roy. Soc. Lond. **A235**, 67–77 (1956).

[73] J. W. Westhaver, *Concentration of potassium by countercurrent electromigration : Some theoretical aspects of the operation*, J. Res. Natl. Bur. Stand. **38**, 169–183 (1947).

[74] K. F. Bowden, *Horizontal mixing in the sea due to a shearing current*, J. Fluid Mech. **21**, 83–95 (1964).

[75] H. Brenner and L. J. Gaydos, *The constraint Brownian movement of spherical particles in cylindrical pores of comparable radius. Models of the diffusive and convective transport of solute molecules in membranes and porous media*, J. Coll. Int. Sci. **58**(2), 312–356 (1977).

[76] J. C. Giddings and H. Eyring, *A molecular dynamic theory of chromatography*, J. Chem. Phys. **59**, 416–421 (1955) ;
see also : W. C. Thacker, *A solvable model for of "shear dispersion"*, J. Phys. Ocean. **6**, 66–75 (1976) ;
S. Goldstein, *On diffusion by discontinuous movements and on the telegraph equation*, Quart. Journ. Mech. and Applied Math. **4**(2), 129–156 (1951).

[77] R. Aris, *On the dispersion of a solute in a pulsating flow through a tube*, Proc. R. Soc. Lond. **A259**, 370–376 (1960).

[78] G. F. Carrier, *On diffusive convection in tubes*, Quart. J. Appl. Math. **14**(1), 108–112 (1956).

[79] P. C. Chatwin, *On the longitudinal dispersion of passive contaminant in oscillatory flows in tubes*, J. Fluid Mech. **71**, 513–527 (1975).

[80] G. T. Csanady, *Dispersal by randomly varying currents*, J. Fluid. Mech. **132**, 375–394 (1983).

[81] H. Dill and H. Brenner, *A general theory of Taylor dispersion phenomena V : Time-periodic convection*, Phys. Chem. Hydr. **3**(3/4), 267–292 (1982).

[82] H. B. Fisher, *The mechanics of dispersion in natural streams*, J. Hydr. Div. **6**, 187–216 (1967).

[83] H. W. Gill and R. Sankarasubramanian, *Dispersion of non-uniformly distributed time-variable continuous sources in time-dependent flow*, Proc. R. Soc. Lond. **A327**, 191–208 (1972).

[84] H. G. Harris and S. L. Goren, *Axial diffusion in a cylinder with pulsed flow*, Chem. Engn. Sci. **22**, 1571–1576 (1967).

[85] E. R. Holley, D. R. F. Harleman and H. B. Fisher, *Dispersion in homogeneous estuary flows*, J. Hydr. Div. **8**, 1691–1709 (1970).

[86] F. J. M. Horn and R. L. Kipp, *Induced transport in pulsating flow*, AIChE J. **17**(3), 621–626 (1971).

[87] F. J. M. Horn and R. L. Kipp, *Mass transport under oscillatory fluid flow conditions*, Chem. Engn. Sci. **22**, 1879–1880 (1967).

[88] M. J. Jaeger and U. H. Kurzweg, *Determination of the longitudinal dispersion coefficient in flows subjected to high frequency oscillations*, Phys. Fluid **26**(6), 1380–1382 (1983).

[89] C. Jimenez and P. J. Sullivan, *Contaminant dispersion in some time-dependent laminar flows*, J. Fluid Mech. **142**, 57–77 (1984).

[90] C. H. Joshi, R. D. Kamm, J. M. Drazen and A. S. Slutsky, *An experimental study of gas exchange in laminar oscillatory flow*, J. Fluid Mech. **133**, 245–254 (1983).

[91] A. Mukherjee and B. S. Mazumder, *Diffusion in an oscillatory channel flow* in *Proceedings of the Third Asian Congress of Fluid Mechanics*, Ed. T. Matsui, 252–255 (1986).

[92] J. R. Philip, *The theory of dispersal during laminar flows in tubes I*, Aust. J. Phys. **16**, 287–299 (1963) ;
J. R. Philip, *The theory of dispersal during laminar flows in tubes II*, Aust. J. Phys. **16**, 300–310 (1963).

[93] R. Sankarasubramanian and W. N. Gill, *Unsteady convective diffusion with interphase mass transfer*, Proc. R. Soc. Lond. **A333**, 115–132 (1973).

[94] R. Sankarasubramanian and W. N. Gill, *Correction to "Unsteady convective diffusion with interphase mass transfer"*, Proc. R. Soc. Lond. **A341**, 407–408 (1974).

[95] D. S. Scotter, G. W. Thurtell and P. A. C. Raats, *Dispersion resulting from sinusoidal gas flow in porous materials*, Soil Sci. **104**(4), 306–308 (1967).

[96] A. S. Slutsky, J. M. Drazen, R. H. Ingram, R. D. Kamm, A. H. Shapiro, J. F. Fredberg, S. H. Loring and J. Lehr, *Effective pulmonary ventilation with small-volume oscillations at high-frequency*, Science **209**, 609–610 (1980).

[97] C. Turfus, *Diffusion from a continuous source near a surface in steady reversing shear flow*, J. Fluid. Mech. **172**, 183–209 (1986).

[98] C. Van den Broeck, *A stochastic description of longitudinal dispersion in uniaxial flows*, Physica **A112**, 343–352 (1982).

[99] E. J. Watson, *Diffusion in oscillatory pipe flow*, J. Fluid Mech. **133**, 233–244 (1983).

[100] H. Yasuda, *Longitudinal dispersion of matter due to the shear effect of steady and oscillatory currents*, J. Fluid Mech. **148**, 383–403 (1984).

[101] K. Mysels, *Electrodiffusion : A fluctuation method for measuring reaction rates*, J. Chem. Phys. **24**(2), 371–375 (1956).

A correction to his $\omega = 0$ result is given in :
J. C. Giddings, *Kinetic model for chromatographic dispersion and electrodiffision*, J. Chem. Phys. **27**, 1755–1756 (1957).
The same mistake for $\omega \neq 0$ explains why Mysels obtained the wrong result for the frequency dependent dispersion.

[102] The term stochastic resonance has also been used in the different context of an increased hopping rate resulting from periodic forcing in nonlinear bistable systems, and an improved signal to noise ratio at the driving frequency in such systems. See e.g. :
P. Yung and P. Hänggi, *Stochastic nonlinear dynamics modulated by external periodic forces*, Europhys. Lett. **8**(6), 505–510 (1989) ;
H. Gang, G. Nicolis and C. Nicolis, *Periodically forced Focker-Planck equation and stochastic resonance*, Phys. Rev. **A42**(4), 2030–2041 (1990) ;
B. McNamara and K. Wiesenfeld, *Theory of stochastic resonance*, Phys. Rev. **A39**, 4854–4869 (1989).

[103] N. G. Van Kampen, *Stochastic Processes in Physics and Chemistry* (North-Holland, Amsterdam, 1981).

[104] B. B. Mandelbrot, *The Fractal Geometry of Nature* (Freeman, San Francisco, 1983).

[105] J. C. Giddings, *A new separation concept based on a coupling of concentration and flow nonuniformities*, Sep. Sci. **1**(1), 123–125 (1966).

[106] H. C. Berg and E. M. Purcell, *A method for separating according to mass a mixture of macromolecules on small particles suspended in a fluid I : Theory*, Proc. Natl. Acad. Sci. Am. **58**, 862–868 (1967) ;
H. C. Berg, E. M. Purcell and W. W. Stewart, *A method for separating according to mass a mixture of macromolecules on small particles suspended in a fluid II : Experiments in a gravitational field*, Proc. Natl. Acad. Sci. Am. **58**, 1286–1291 (1967) ;
H. C. Berg and E. M. Purcell, *A method for separating according to mass a mixture of macromolecules on small particles suspended in a fluid III : Experiments in a centrifugal field*, Proc. Natl. Acad. Sci. Am. **58**,1821–1828 (1967).

[107] J. C. Giddings, Y. H. Yoon, K. P. Caldwell, M. N. Myers and M. E. Hovingh, *Nonequilibrium plate height for field-flow fractionation in ideal parallel plate colums*, Sep. Sci. **10**, 447–460 (1975).